Journal of Medicinal Chemistry

Article

Synthesis, antiviral potency, in vitro ADMET and X-ray structure of potent CD4-mimics as entry inhibitors that target the Phe43 cavity of HIV-1 gp120

Francesca Curreli, Young Do Kwon, Dmitry S. Belov, Ranjith R. Ramesh, Alexander V. Kurkin, Andrea Altieri, Peter D. Kwong, and Asim Kumar Debnath

J. Med. Chem., **Just Accepted Manuscript** • DOI: 10.1021/acs.jmedchem.7b00179 • Publication Date (Web): 07 Mar 2017

Synthesis, antiviral potency, *in vitro* ADMET and X-ray structure of potent CD4-mimics as entry inhibitors that target the Phe43 cavity of HIV-1 gp120

Francesca Curreli[a], Young Do Kwon[b], Dmitry S. Belov[c], Ranjith R. Ramesh[a], Alexander V. Kurkin[c], Andrea Altieri[c], Peter D. Kwong[b] & Asim K. Debnath[a]*

[a]Laboratory of Molecular Modeling and Drug Design, Lindsey F. Kimball Research Institute, New York Blood Center, New York, NY 10065, USA.

[b]Structural Biology Section, Vaccine Research Center, National Institute of Allergy and Infectious Diseases, National Institutes of Health, Bethesda, MD 20892, USA.

[c]EDASA Scientific, Scientific Park, Moscow State University, Leninskie Gory, Bld.75, 77 – 101b; 119992 Moscow - Russia

*Corresponding author

Keywords

HIV-1, ENV-pseudovirus, virus entry antagonist, broad spectrum, structure-activity relationship (SAR), ADMET

ABSTRACT

In our attempt to optimize the lead HIV-1 entry antagonist, NBD-11021, we present in this study the rational design and synthesis of 60 new analogs, determination of their antiviral activity in a single-cycle and a multi-cycle infection assay to derive a comprehensive structure-activity relationship (SAR). Two of these compounds, NBD-14088 and NBD-14107, showed significant improvement in antiviral activity compared to the lead entry antagonist in a single-cycle assay against a large panel of Env-pseudotyped viruses. The X-ray structure of a similar compound, NBD-14010 confirmed the binding mode of the newly designed compounds. The *in vitro* ADMET profiles of these compounds are comparable to that of the most potent attachment inhibitor BMS-626529, a prodrug of which is currently undergoing Phase III clinical trials. The systematic study presented here is expected to pave the way for improving the potency, toxicity and ADMET profile of this series of compounds with the potential to be moved to the early preclinical development.

INTRODUCTION

Virus attachment and fusion to the host cell membrane are the critical steps for HIV-1 to enter the host cells and initiate its life-cycle by using host cell machinery[1]. Therefore, virus attachment and fusion (often collectively termed as "virus entry") have been the targets for new drug discovery for many years now[1-4]. There are only two drugs currently on the market that target the entry pathway, Fuzeone (Enfuvirtide), which targets the envelope glycoprotein gp41[5, 6] and Maraviroc, which targets the host cell receptor CCR5 to prevent the entry of the virus[7-9]. Despite the fact that HIV-1 gp120 is critical for virus entry and has been targeted to discover novel drugs there is no drug yet approved by the FDA against this target. The most advanced drug in this class, BMS-663068, which is a prodrug of **91** (1-(4-benzoylpiperazin-1-yl)-2-(4-methoxy-7-(3-methyl-1H-1,2,4-triazol-1-yl)-1H-pyrrolo[2,3-c]pyridin-3-yl)ethane-1,2-dione; BMS-626529[10]) and showed its safety and efficacy recently in a phase 2b clinical trials, is currently undergoing Phase III clinical trials[11]. BMS-663068 in 2015 received US FDA breakthrough therapy designation, implicating the importance of gp120 as a target to develop drugs in preventing virus entry into the host cells.

Our laboratory had focused on developing novel inhibitors targeted to the Phe43 cavity of gp120 since 2005 when we first reported the discovery of NBD-series CD4-mimic, NBD-556[12]. Unfortunately, NBD-556 was demonstrated to enhance HIV-1 infection in $CD4^{-}$-$CCR5^{+}$ cells, therefore, behaving as HIV-1 entry agonist[13, 14]. Since this finding we and others have striven to design CD4-mimics with not only higher potency and lower toxicity but also devoid of this undesirable trait, thereby representing as HIV-1 entry antagonists[14-24]. We recently reported our first success in converting NBD-556 to a full antagonist **89** (NBD-11021) [14]. However, we recognize that a concerted optimization effort is needed to improve the antiviral potency and toxicity of this NBD-series compounds to obtain clinically relevant entry inhibitors. Towards that

goal, we have co-crystallized the first antagonist, **89** with gp120, which provided us the structural details of the binding mode of this molecule in the Phe43 cavity of gp120[14]. We have utilized the structural information to design and synthesized a series of next generation gp120 antagonists as entry inhibitors. Here we report the details of the synthesis, antiviral evaluation, structure-activity relationship (SAR) analysis of 60 novel analogs. Also, we present the X-ray structure determination of one of this class of new generation compounds, **90** (NBD-14010), published recently[17]. Furthermore, we incorporated *in vitro* absorption, distribution, metabolism, excretion and toxicity (ADMET) study during the early phase of optimization effort which is recognized as a critical step to avoid high attrition rate during the late-stage drug development program[25, 26]. The optimization effort yielded valuable information on the key areas of the **89** type antagonist that can be targeted for further structural optimization to produce next-generation NBD-series antagonists suitable for further pre-clinical studies.

CHEMISTRY

Synthesis of CD4-mimics

We prepared the target compounds in a convergent manner from three fundamental building blocks: carboxylic acid, protected thiazole and enantiopure imine (**Schemes 1-5**). We described the synthesis of pyrrole-2-carboxylic acid 1 in our earlier work[14]. The details of the other carboxylic acid and their analogs (**23, 39, 40, 79, and 80**) will be published separately (in preparation).

A set of modified pyrrole-2-carboxylic acids including N-, 3- and 4-methylated and 4-MeO substituted compounds (**4, 8 and 12**) were prepared using known compounds (**5, 9 and 10**) as per the reported procedure[27-31] or from commercially available compounds. Aryl imidazole carboxylic

acids 20 and 22 were also prepared based on literature procedures[32, 33]. We synthesized thiazoles 36 and 73 using the method described previously[14, 17].

Previously we reported the development of a general route for the synthesis of NBD-compounds[17]. An appropriately protected aldehyde (34, 53 and 54) was prepared from readily available starting materials (see schemes 1-6 for details). Then aldehyde was treated with *R*- or *S*-Ellman auxiliary under dehydration conditions. The resulting enantiopure imines (**35, 55, 56, and 74**) were treated with an appropriate thiazolyl lithium derivative to give a 1,2-additon product (**Schemes 3, 4 and 5**). In all of the 1,2-addition reactions, only a single stereoisomer was isolated. In most cases no other products were observed; in some cases, minor products could not be isolated and characterized. Compounds derived from *S*-imines were marked as *f*S (from *S*-isomer). Compounds derived from *R*-imines were marked *f*R (from *R*-isomer). The absolute configuration of these compounds can be predicted using Felkin-Ahn model[17]. However, it was not unambiguously proved by any experiments.

Acidic cleavage of silyl and sulfinyl groups gave suitably protected diamines (**38, 59, 60, 77, and 78**). Preparation of amine **24** was described earlier[17]. HBTU-mediated peptide coupling with an appropriate acid, followed by Pd-catalyzed deprotection yielded the final compounds. Reductive amination with formalin was used to obtain two series of dimethylated compounds (**44-46, 67-69, Schemes 3 and 4**). It is important to note that all main building blocks (carboxylic acids, protected thiazoles, enantiopure imines and protected diamines) were accessible in decagram scale and bench-stable for an extended period (~one year). All of the synthetic procedures are easily scalable, and all NBD-compounds were prepared on at least 100 mg scale.

RESULTS

X-ray crystal structure of 90 in complex with HIV-1 gp120

The x-ray structure of **89** with gp120 reported earlier confirmed that the tetramethylpiperidine ring of the **89** benefited from enabling its nitrogen atom to hydrogen bond with Asp368 of gp120[14]. However, much of the hydrophobic portion of the piperidine ring was exposed to solvent, which may lead to an undesirable thermodynamic penalty. Therefore, we replaced the piperidine ring with a methylamine group to reduce solvent exposure of hydrophobic regions, while retaining the amine for a hydrogen bonding with Asp368 of gp120. We also replaced the phenyl ring of the molecule, which penetrates the Phe43 cavity, with a meta-fluoro substituted phenyl ring to enhance surface complementarity between the compound and the cavity[34, 35]. Furthermore, the piperidine ring in our earlier compound, **89**, introduced two chiral centers, which generated four isomers of this compound. Multiple isomers complicate the separation process after synthesis whereas the primary amine only has one chiral center and produces only two isomers. The new compound, **90**, showed much improved anti-HIV-1 activity, and more importantly, a substantially improved cytotoxicity profile compared to that of **89**[17].

To corroborate our rationale of designs and further understand the mechanism of improved antiviral activity, we determined the crystal structure of **90** in complex with HIV-1 gp120 at 2.1-Å resolution (**Figure 1a**). This structure revealed the meta-fluoro substituted phenyl ring to have improved surface complementarity with the Phe43 cavity. The surface complementarity by the fluorine atom has now been demonstrated in **Figure S1** using the structure of **90** with and without fluoro group at the meta position. When superimposed with **89**, **90** shared an almost identical mode of binding to that of **89**; the nitrogen in the amine group maintained the hydrogen bond with Asp368 as observed in the previous **89**-gp120 structure[14], but with much of the hydrophobic area present in the tetramethylpiperidine removed (**Figure 1b**). Notably, the **90** structure revealed five

ordered water molecules that mediate a hydrogen bonding network, which encompassed the nitrogen atom of the methylamine group of **90** and gp120 residues Asp368, Gly431, Asn432, Asn425, and Gly473 (**Figure 1c and 1d**). The finding of the water molecule networks is a novel finding and expected to help in guiding further optimization of this series of compounds.

Antiviral Screening and structure-activity relationship (SAR) analysis

We recently reported that our second generation compound **90**[17], besides maintaining the HIV-1 entry antagonist trait, first reported for **89**[14] also shown better cytotoxicity and improved antiviral activity compared to **89**. Here, we describe the design of a new series of 60 novel NBD-series compounds in an attempt to expand the series and derive a comprehensive structure-activity relationship (SAR). We evaluated the HIV-1 inhibitory activity and cytotoxicity (**Table 1**) of these molecules. The anti-HIV-1 activity was assessed in a single-cycle assay by infecting TZM-bl indicator cells with the pseudovirus HIV-1_{HXB2} and in a multi-cycle assay by infecting the human T-cell MT-2 with the full-length lab-adapted virus HIV-$1_{IIIB.}$ To derive systematic SAR of this series of NBD derivatives, initially, we concentrated in modifying only the Region I in the phenyl ring and a primary amine in Region III. When we replaced the chloro at R_2 with fluoro, which resulted in two compounds 25A and 25B, showed a reduction in cytotoxicity compared to **89** in both assays but the HIV-1 inhibitory activity dropped slightly in the pseudovirus assay but substantially against MT-2 cell-based assay. This decrease in activity in MT-2 cell-based assay was somewhat unusual, and we could not find that with other NBD compounds.

The x-ray structures of **89** and **90** with gp120 indicate that the methyl group in the thiazole ring does not contribute to any interactions with gp120 rather it is located at the solvent-exposed region outside the Phe43 cavity. Therefore, we decided to remove the methyl group from the

thiazole ring in Region III. We first synthesized this series with the primary amine (R_4= NH_2). The resulting compounds **81A and 81B** showed noticeable improvement in both antiviral activity and cytotoxicity against both single- and multi-cycle assays. Most significantly the selectivity index (SI) of **81B** improved from 10.7 to 49.4 (~5-fold improvement) in single-cycle assay compared to **89**. However, the SI value was slightly worse against multi-cycle assay. The reason for this discrepant result is not apparent at this time. When we added a fluoro at the R_1 position keeping chloro in the R_2 position (**82A and 82B**) we did not find any noticeable improvement in antiviral potency or SI compared to their parent molecules. But when we substituted chloro with a CH_3 group at R_2 and kept the fluoro at R_1, the antiviral activity of the resulting compounds [**83A** and **83B** (NBD-14088)] improved by about 2-fold and the SI values by ~3-4-fold in single-cycle assay but marginally enhanced in the multi-cycle assay. A further addition of a fluoro at the R_3 position resulted in **84A** (NBD-14107) and **84B** that showed similar activity as with 83A and **83B**. Although the antiviral activity and cytotoxicity did not improve significantly in these fluoro-containing molecules, the addition of fluoro is known to help in producing molecules with more metabolic stability than the unsubstituted ones. The introduction of OCH_3 in R_1 and R_2 resulted in compounds **85A and 85B** that had no anti-HIV-1 activity and cytotoxicity at the indicated doses. Most likely the reduction of antiviral activity was due to the steric effect of the bulky OCH_3 group. Then we modified R_4 by introducing a CH_3 in the primary amine moiety. Some of the resulting compounds (**86A -88B**) showed further improvement in antiviral potency. However, they all turn out to be more cytotoxic.

We then decided to retain 4-chloro and also use 4-CH_3 at the R_2 position and keep the 3-fluoro unchanged at the R_1 position and introduced a CH_3 in the primary amine group. The antiviral activity of all the resulting compounds (**41A - 43B**) was similar to **89**; however, they

showed slightly reduced cytotoxicity. The introduction of $N(CH_3)_2$ in the primary amine at R_4 yielded compounds **44A-46B** which were not cytotoxic at the doses we tested in both assays but had no antiviral activity at all. The introduction of CH_2NH_2 in R_4 produced compounds **61A-63B** which did not show improvement in anti-HIV-1 activity, but when we substituted Chloro with the methyl group in R_2, the cytotoxicity reduced slightly. Replacing the CH_2NH_2 group in R_4 with $CHN(CH_3)_2$ (**67A-69B**) did not provide any improvement in antiviral activity in both single-cycle and multi-cycle assays, but unlike in the previous series (**44A -63B**), compounds with 4-chloro and 3-fluoro retained similar activity as **89**.

In the above SAR study, it was evident that introduction of a fluorine atom, the most electronegative among halogens) at position R_1/R_3 (meta) and R_2 (para) in the phenyl ring reduced cytotoxicity (**25A, 25B**) considerably more than **82A and 82B** where chloro replaced the fluoro at R_2. However, the antiviral potency of compounds with chloro at the R_2 position was ~3-6-fold better. We also observed that when we introduced a methyl group at R_2, which is electron donating, the antiviral potency improved further. We also observed a marginal reduction of cytotoxicity. Analyzing this series it was evident that the antiviral potency of the compounds dependent more on the hydrophobic character of the R_2 substituent than its electronegativity. The hydrophobic parameter (Π) is very similar for chloro and methyl group. Therefore, the introduction of Cl/CH_3 at R_2 and fluoro at R_1/R_3 are critical for obtaining the best antiviral potency and lower cytotoxicity in this series of compounds.

We observed that in general, the modifications in region II in the pyrrole ring (**26A-31B**), especially in R_6 position, made the compounds inactive. This observation was not surprising because our earlier finding in the x-ray structure of **89** and also the structure reported here with gp120 led to the observation that the NH of pyrrole makes an H-bond with the residue Asn425,

which appears to be critical for the binding of this series of compounds in the Phe43 cavity. The methylation of this NH (compounds **26A, 26B**) may have two detrimental effects- loss of the H-bond donor atom and also possibly a steric effect that interferes with the binding. However, substituting H at R_7 and R_8 with methyl yielded compounds with somewhat better or similar activity as **89** (**27A, 27B, 28A and 28B**) in the single-cycle assay but slightly poorer activity in the multi-cycle assay. Noticeably, one of the isomers of 28 (**28B**) showed very high cytotoxicity. However, the underlying cause of cytotoxicity is not clear at this stage. When we introduced a methoxy group at the R_7 position (**29A and 29B**) the antiviral activity was completely lost most likely due to steric effect. Then, we moved to find out whether we could modify the pyrrole ring to imidazole by introducing one additional "N" in the R_9 or R_{10} position. These modifications resulted in compounds **30A-31B** which, although showing much-reduced cytotoxicity, had no antiviral activity. The SAR data obtained on pyrrole ring confirmed that modification in the pyrrole ring was detrimental to the antiviral activity.

Among the 60 new compounds that we tested **83B**, and **84A** showed the highest SI of ~86 and ~62, respectively in single cycle assay, which represents an enhancement of ~8- and ~6-fold, respectively, compared to **89**. However, in the multi-cycle assay, the SI of those two compounds were 50 and 38.5, respectively, which represent only ~2 and ~1.3-fold, respectively. Despite marginal enhancement in activity and selectivity in the multi-cycle assay, these nor-methyl analogs bring two distinct advantages over all other compounds reported earlier. **84A**/**84B** and **88A/88B** are expected to be more metabolically stable; and the deletion of the methyl group in the thiazole ring opened up the opportunity to introduce other groups, especially, solubilizing groups, which is expected to make these molecules more water soluble and more suitable for further preclinical studies. Therefore, we selected these two compounds for further research.

83B and 84A prevent cell-to-cell fusion and retain the HIV-1 entry antagonist trait

Two essential features for the HIV-1 entry inhibitors that target the Phe43 cavity of HIV-1 gp120 are the capability to inhibit HIV-1 Env-mediated cell-to-cell fusion and have HIV-1 entry antagonist property. First, we evaluated the inhibitory activity of the two best inhibitors, **83B** and **84A**, on the HIV-1 Env-mediated cell-to-cell fusion. To this end, we cocultured the indicator cells MAGI-CCR5 with the Env- and Tat-expressing HL2/3 cells in the presence of escalating doses of compounds. We used NBD-556 and **89** as a control. Our results (**Figure 2A**) indicate that both **83B** and **84A** prevent the HIV-1 Env-mediated cell-to-cell fusion, but the IC_{50} were ~2-3-fold higher than what we observed with NBD-556 and **89** (8.3±0.9 and 13.3±1.2 versus 2.9±0.1 and 6.1±0.4, respectively). As next step, we wanted to verify whether **83B** and **84A** maintained the HIV-1 entry antagonist property we previously reported for our lead compound **89**[14] and the second generation compounds N-{2-amino-1-[5-(hydroxymethyl)-4-methyl-1,3-thiazol-2-yl]ethyl}-5-(4-chlorophenyl)-1H-pyrrole-2-carboxamide (NBD-14009) and **90**[17]. To this end, we infected CD4-negative and CCR5-positive cells, Cf2Th-CCR5, with recombinant CD4-dependent HIV-1_{ADA} virus in the presence of the compounds. We used NBD-556 (HIV-1 entry agonist) and **89** (HIV-1 viral entry antagonist) as a negative and a positive control, respectively. As expected, NBD-556 enhanced the infection of the Cf2Th-CCR5 cells, and **83B** and **84A** did not enhance HIV-1 infectivity in these cells as was observed for **89**, indicating that the HIV-1 entry antagonist property is maintained in these compounds as well (**Figure 2B**).

Time-dependent HIV-1 inhibitory activity profiles of NBD compounds

To further understand the mechanism of action of the NBD compounds we performed a time of addition experiment. We used four known compounds as reference or control. As expected, we found that all the compounds inhibited HIV-1 when added to the cells at the time of infection (**Figure 3**). The co-receptor CXCR4 inhibitor, AMD3100, and the entry inhibitor BMS-378806 showed a decrease in efficacy when added to the culture 1 h post-infection (p.i.) and their effectiveness continued dropping to disappear at 2-4 h p.i completely. Moreover, the efficacy of the Reverse Transcriptase inhibitor, AZT decreased to about 50% when added 4 h p.i. while we only detected a slight decline in the efficiency of the Integrase inhibitor, Raltegravir when added 8 h p.i. Finally, the NBD compounds showed some efficacy when added to the culture 4 h p.i. and they gradually lost efficiency suggesting that **83B** and **84A** may also target the later phase of the HIV-1 life cycle. Earlier we reported that 89 inhibits HIV-1 reverse transcriptase (RT) enzyme but at much higher concentration. Based on that observation, we decided to test these compounds against HIV-1 RT.

NBD compounds also target HIV-1 Reverse Transcriptase (RT)

The time of addition experiment suggested that **83B** and **84A** may also have an additional mechanism of action. Consequently, we decide to evaluate the activity of **83B** and **84A** against HIV-1 RT. We used 89, NBD-556, and Nevirapine as controls. As expected, NBD-556 did not show any activity even at 300 μM and Nevirapine was extremely potent against HIV RT, with IC_{50} of 0.20 μM (**Table 2**). 89 inhibited HIV-1 RT with an IC_{50} of 47 μM while **83B** and **84A** had an IC_{50} of 7.2 and 8.4 μM, respectively. Comparing the IC_{50} values obtained with the NBD compounds for the entry inhibition assay and the RT-inhibition assay we found that the ratio IC_{50}-

RT/IC_{50}-HIV-1_{HXB2} was similar for the three compounds, i.e., 21, 16 and 13 for 89, **83B** and **84A**, respectively.

Antiviral activity of 83B and 84A against a large panel of HIV-1 Env-pseudotyped reference viruses.

The first and second generation NBD compounds 89 and **90** showed a broad range of antiviral activity against a large panel of clinical isolates of different subtype[14, 17]. In this study, we evaluated the HIV-1 inhibitory activity of our newly selected compounds, **83B** and **84A**, against a large panel of Env-pseudotyped viruses and we compared their activity with the **89** (**Table 3**). We selected fifty-five HIV-1 clones of clinical isolates from 9 subtypes including primary and transmitted/founder HIV-1 isolates and 12 recombinant HIV-1 clones. We found that both these compounds exhibited improved anti-HIV-1 activity compared to 89. For example, we observed that the overall mean of the IC_{50}s determined for 89 against the panel of pseudoviruses was 1.64 ± 0.12 μM (IC_{50}s in the range of 0.32-4.4 μM). On the contrary, we found that the overall means of the IC_{50}s determined for **83B** and **84A** were 0.41 ± 0.02 μM (IC_{50}s in the range of 0.2-0.75 μM) and 0.49 ± 0.02 μM (IC_{50s} in the range of 0.27-0.94 μM), respectively. Additionally, we found that although **84A** was equally active against all the pseudoviruses regardless of the subtype, 89 was slightly less active against the HIV-1 clones of subtype C (mean of 2.16 ± 0.18, n = 16). By contrast, **83B** was ~6-fold more active against subtype C viruses (mean of 0.35 ± 0.03, n = 16) compared to **89**. **83B** had similar activity against subtype D (mean of 0.36 ± 0.05, n = 5), subtype A (mean of 0.43 ± 0.04, n = 12) and subtype B (mean of 0.46 ± 0.04, n = 15) viruses. The data indicate that both **83B** and **84A** showed broad spectrum antiviral activity against a large number of HIV-1 Env-pseudotyped viruses representing clinical isolates of diverse subtypes. Finally, both

compounds **83B** and **84A** showed much poorer activity against the control pseudovirus VSV-G displaying an IC_{50} of ~42.9 μM and ~26 μM respectively versus the ~7.1 μM observed for **89**, suggesting that the inhibitory activity of these compounds is specific to HIV-1.

***In vitro* ADMET study of NBD-series compounds**

Early ADMET studies of drug molecules during discovery phase has been recognized as critical to reducing the attrition rate in late stage drug development[25, 26]. Therefore, we decided to initiate *in vitro* ADMET studies on **83B** and **84A** and compare the data with previously published inhibitor, **89** of this class. We also used **91** as a control, a highly potent attachment inhibitor, the pro-drug of which has been shown to be safe and efficacious and received "breakthrough therapy designation for investigational HIV-1 attachment inhibitor in 2015 by the US FDA. The *in vitro* ADMET data in **Table 4** show that the new molecules **83B**, **84A**, and our earlier reported compound **89**, as well as the control inhibitor **91**, have similar aqueous solubility profiles. However, in the bidirectional Caco-2 cell permeability assay, which predicts the human intestinal permeability potential of a molecule required for oral absorption, NBD compounds demonstrated to have relatively moderate permeability compared to **91**. The Caco-2 cell permeability in the basolateral to apical side (B2A) was measured principally to calculate the efflux ratio (Mean P_{app} B2A / Mean P_{app} A2B) of these molecules. A value greater than 2 indicates the possibility of these molecules to be removed out of the basolateral site most likely by the efflux transporter(s).

Since the liver is the major organ where drug metabolism occurs, we decided to study the metabolic stability of our molecules in human liver microsomes. The data in **Table 4** indicate that **83B** and **84A** showed improved stability compared to **91**, whereas **89** has similar stability to **91**.

We can classify all NBD molecules and **91** from their *in vitro* human intrinsic clearance data (CL_{int}) as low clearance compounds.

The NBD compounds were also tested for their human plasma protein binding potential and compared with the control **91**. The mean fraction unbound (fu) data in **Table 4** indicate that 96%, 90% and 88.6% of **83B**, **84A**, and **89**, respectively were bound to the plasma which is slightly higher than **91**, where 81.5% binding was observed.

We evaluated the NBD compounds and **91** against five CYP450 isoforms (CYP2C19, CYP3A4, CYP2D6, CYP2C9, and CYP1A), which metabolizes more than 80% of the drugs to identify any possible drug-drug interactions. All NBD compounds tested and the control **91** showed no inhibition of any of the isoforms tested. The only inhibition observed was for **83B** against CYP1A, with an IC_{50} of 8.01 μM, implicating a moderate inhibition potential of this particular molecule.

We also evaluated the potential of these molecules to inhibit hERG channel, known to be a predictor of the development of acquired long QT syndrome that may lead to fatal ventricular arrhythmia. All NBD compounds were tested along with the control **91**. **84A** and **91** showed weak or no inhibition of the hERG channel. However, **89** and **83B** showed moderate inhibition of hERG channel.

DISCUSSION

The HIV-1 gp120 binding site on the human primary cell receptor CD4 has been long recognized as one of the major sites for developing entry inhibitors[4, 36]. The major success came with the discovery of the first attachment inhibitor BMS-378806 with high potency, which, however, could

not proceed further for development due to a deficiency in its bioavailability that leads to the development of next generation BMS analogs with improved pharmacokinetics profiles. One such drug, BMS-663068 is currently in phase III clinical trials. We[14-17] and others[13, 18-20, 22-24, 34, 35, 37-40] have validated Phe43 cavity of HIV-1 gp120 as a target for discovering a new class of entry inhibitor drugs. Our success in converting a full agonist (NBD-556) to an antagonist (**89**) motivated us to optimize this molecule further to more potent and less toxic inhibitors that maintain the antagonist trait. Towards that goal, we recently reported the X-ray structure of **89** with HIV-1 gp120[14]. An in-depth analysis of the structure indicated that despite the introduction of a piperidine ring which enabled an H-bond interaction with Asp368 of gp120, the ring had a significant hydrophobic component which was located in the solvent exposed area, which may be undesirable for binding to gp120 due to high thermodynamic penalty. Therefore, to avoid such adverse effect, we recently reported the synthesis of a few new molecules by replacing piperidine ring with primary amines[17]. One of these molecules **90** showed improvement in antiviral potency against a large panel of Env-pseudotyped viruses. The x-ray structure of **90**, reported in this study, confirmed that this modification still could maintain the critical H-bond interaction with Asp368. This confirmation prompted us to synthesize a large number of analogs to derive a comprehensive SAR to guide in further optimization of this class of inhibitors. We have initially tested these molecules in a single-cycle and a multi-cycle HIV-1 inhibition assay and identified two molecules, **83B** and **84A** with improved antiviral activity and selectivity index. A further test with a large panel of Env-pseudotyped HIV-1 representing clinical isolates of different subtypes showed their broad-spectrum antiviral potency. The improvement of the mean IC_{50} values of **83B** and **84A** when compared with **89** among the same set of Env-pseudoviruses, was ~4-fold. Most significantly, these two molecules showed much improved antiviral potency across multiple subtypes (A-D)

tested unlike BMS-378806, which despite its low nM antiviral potency against subtype B, it showed relatively weak potency against A, C and D subtypes[41]. The cytotoxicity values of the NBD series molecules presented here showed an only marginal reduction in our best compounds. However, in the assay against a large panel of pseudoviruses containing the envelope from clinical isolates we see substantial improvement in antiviral activity, which leads to the belief that further modifications will result in compounds with higher potency, thereby, with higher selectivity index.

The time of addition data with **83B** and **84A** showed that there might be additional inhibitory activity besides inhibiting entry because these compounds show some activity even after adding beyond 2 h, indicative of some other target. Earlier we reported that some next generation NBD compounds, such as, **89** showed activity against HIV-1 RT enzyme. We also confirmed in this study that like **89**, **83B** and **84A** also target RT at higher doses. Despite the fact that the activity against HIV-1 RT of these two molecules was more potent than **89**, the relative ratio of IC_{50}-RT/IC_{50}-HIV-1_{HXB2} remained almost same, i.e., 21, 16 and 13 for **89**, **83B**, and **84A**, respectively. The data demonstrates that entry is the dominant mechanism of action of these inhibitors. It is worth noting that the new generation compounds, such as **83B** and **84A**, are several-fold more potent entry inhibitors against HIV-1 than **89**.

Poor physicochemical properties, pharmacokinetics, and toxicity are the principal cause of late-stage failure in drug development[25]. Use of *in vitro* evaluation of ADMET of drugs is especially attractive in this phase due to high cost with *in vivo* procedures involving an animal. We have decided to address this critical issue in our early optimization phase of developing these entry inhibitors as future clinical candidates. Published report demonstrated that addition of a fluoro group in the phenyl ring of NBD-556 series compounds enhances the antiviral potency[38] although

we observed mixed results in our study[17]. However, it is well-established that fluorine in medicinal chemistry has been used quite extensively to improve physicochemical properties and metabolic profiles of drugs[42-44]. We utilized that knowledge and added additional fluorine atom(s) in the most vulnerable positions in the phenyl ring of the NBD-series of compounds. Therefore, it was imperative for us to evaluate the effect on physicochemical and pharmacokinetic profiles of the two most active compounds in this study by *in vitro* ADMET studies. The *in vitro* ADMET data in **Table 4** indicate that NBD-series compounds have similar ADMET profiles to that of the clinical candidate, **91**, except Caco-2 permeability which is slightly lower. The Caco-2 permeability (expressed as P_{app}, 10-^{6} x cms^{-1}) of **83B**, **84A** and **89** have P_{aap} values of 2.56, 1.17 and 2.31 x 10^{-6} cms^{-1}, respectively compared to 7.62 x 10^{-6} cms^{-1} of **91**. However, the Caco-2 permeability value (P_{app} of >1 x 10^{-6} cms^{-1}) of a molecule is considered to have an acceptable permeability in drug development program[45]. The oral drug, atenolol, used as a control in our experiment, has a P_{app} of 0.220 x 10^{-6} cms^{-1}. The bi-directional Caco-2 cell permeability data also indicate that all the NBD compounds and **91** have high efflux ratio demonstrating that all these molecules may be subject to P-gp mediated efflux. However, the role of other transporters, such as BCRP, MRP2, etc could not be ruled out[46]. The results on metabolic stability in human microsomes indicate that all the NBD compounds are stable up to the 45 min limit of the experimental protocol. The intrinsic clearance data (CL_{int}, μL/min/mg protein) also indicate that these compounds have low clearance potential. It is worthwhile to mention that drugs with high clearance are considered unfavorable because they may be cleared rapidly *in vivo* and the drugs may have a short duration of action and require multiple/repeat dosing.

The protein binding data in **Table 4,** expressed as mean fraction unbound (fu), indicate that all NBD compounds and **91** bind strongly to plasma protein. However, Smith et al. from Pfizer Global Research, in 2010 convincingly illustrated that we need to be cautious in interpreting the plasma binding data and optimizing molecules based on those data because the efficacy of a drug is often dependent on the free drug concentration surrounding the drug target rather than the free drug fraction [47].

Cytochrome P450 enzymes (CYP450) are essential for the metabolism of many drugs[48]. However, inhibition of these enzymes may lead to drug-drug interaction when two or more drugs are co-administered through inhibition of CYP450 enzymes specific for one or other drugs. Inhibition of metabolism may lead to increased level of drug concentration in the system which may lead to toxicity. We have selected five isoforms (CYP2C19, CYP3A4, CYP2D6, CYP2C9 and CYP1A) responsible for the metabolism of the majority drugs. All NBD compounds and **91** showed a low level of inhibition of all five isoforms tested (IC_{50} >25 μM except **83B** has IC_{50} of 8.01 μM against CYP1A) indicating that these compounds are less likely to have toxicity due to drug-drug-interactions associated with drug metabolism[49].

Several drugs either had to be withdrawn or imposed restricted use due to cardiac toxicity. Many drugs are known to induce acquired long QT syndrome by prolonging QT interval and cardiac action potential due to inhibition of human ether-a-go-go-related gene (hERG) that encode the inward rectifying voltage-gated potassium channel[50]. Therefore, it was prudent for us to evaluate the inhibitory potential of the NBD compounds against hERG and compare that with the control, **91**. The data in **Table 4** demonstrate that all these compounds have μM IC_{50} values. **84A** inhibited hERG with similar potency as the **91** control. **89** showed the highest inhibition of hERG

but our next generation compounds **83B** and **84A** showed some improvement. It is worthwhile to mention that the drugs that had to be either taken out of the market or imposed restriction in use all had nM level inhibitory activity. It was evident from the above data that the best NBD compounds in this study have very similar ADMET profiles to that of the control **91**.

CONCLUSIONS

In our continuous effort to optimize the first HIV-1 entry antagonist, **89**, we have synthesized 60 new analogs, determined their antiviral potency and experimentally evaluated *in vitro* ADMET profile of two of the most active compounds. **83B** and **84A** showed measurable progress in improving the antiviral potency and the selectivity index compared to **89**. The x-ray structure confirms the binding mode of this class of molecules as well as provides structural details, which is expected to provide additional guidance in further optimizing these new molecules. The data presented here show that these molecules have the broad-spectrum potency against a large panel of Env-pseudotyped viruses representing clinical isolates of a wide variety of subtypes. These molecules also have comparable *in vitro* ADMET profiles to that of the clinical attachment inhibitor, **91**. The systematic study presented here is expected to pave the way for improving further the potency, toxicity and ADMET profile of this series of compounds with the potential to be moved to the early preclinical development.

EXPERIMENTAL SECTION

Cells and viruses

MT-2 cells[51], TZM-bl cells[52], `MAGI-CCR5 cells[53], U87CD4+CXCR4+ cells[54] and HL2/3 cells[55] were obtained through the NIH ARP. HEK 293T cells were purchased from ATCC. CD4-negative

Cf2Th-CCR5+ cells and Env expression vector pSVIIIenv-ADA were kindly provided by Dr. J. G. Sodroski[56]. HIV-1 Env molecular clone expression vector pHXB2-env (X4) DNA was also obtained through the NIH ARP[57]. HIV-1 Env molecular clones of gp160 genes for HIV-1 Env pseudovirus production were obtained as follows: clones representing the standard panels A, A/D, A2/D, D and C (QB099.391M.Env.B1) were obtained through the NIH ARP from Dr. J. Overbaugh[58, 59]. The HIV-1 Env molecular clones panel of subtype A/G and A/E (CRF01_AE clone 269) Env clones were obtained through the NIH ARP from Drs. D. Ellenberger, B. Li, M. Callahan and S. Butera[60]. The AE clone AA058 was kindly provided by Drs. R. J. McLinden and A. L. Chenine from US Military HIV Program, Henry M. Jackson Foundation (Silver Spring, MD). The HIV-1 Env panel of standard reference subtype B Env clones was obtained through the NIH ARP from Drs. D. Montefiori, F. Gao and M. Li (PVO, clone 4 (SVPB11); TRO, Clone 11 (SVPB12); AC10.0, clone 29 (SVPB13); QH0692, clone 42 (SVPB6); SC422661, clone B (SVPB8)); from Drs. B. H. Hahn and J. F. Salazar-Gonzalez (pREJO4541, clone 67 (SVPB16); pRHPA4259, clone 7 (SVPB14)); from Drs. B. H. Hahn and D. L. Kothe (pTHRO4156 clone 18 (SVPB15), pCAAN5342 clone A2 (SVPB19))[61, 62]. The subtype B clones pWEAUd15.410.5017, p1058_11.B11.1550, p1054.TC4.1499, p9014_01.TB1.4769 and p9021_14.B2.4571 were obtained through the NIH ARP from Drs. B. H. Hahn, B. F. Keele and G. M. Shaw[63]. The subtype C HIV-1 reference panel of Env clones were also obtained through the NIH ARP from Drs. D. Montefiori, F. Gao, S. A. Karim and G. Ramjee (Du 156.12; Du172.17); from Drs. D. Montefiori, F. Gao, C. Williamson and S. A. Karim (Du422.1), from Drs. B. H. Hahn, Y. Li and J. F. Salazar-Gonzalez (ZM197M.PB7; ZM249M.PL1); from Drs. E. Hunter and C. Derdeyn (ZM53M.PB12; ZM135M.PL10a; ZM109F.PB4); from Drs. L. Morris, K. Mlisana and D. Montefiori, (CAP45.2.00.G3; CAP210.2.00.E8)[64-66]. The HIV-1 Subtype C Panel of Indian gp160 Env Clones

HIV-16055-2 clone 3, HIV-16936-2 clone 21, HIV-25711-2 clone 4, HIV-225925-2 clone 22 and HIV-26191-2, clone 48 were obtained through the NIH ARP from Drs. R. Paranjape, S. Kulkarni and D. Montefiori[60]. HIV-1 Env molecular clones MF535.W0M.Env.C1 and BF535.W6M.Env.A1 of subtype D/A were obtained through the NIH ARP from Dr. J. Overbaugh[67]. The Env-pseudotyped genes of BG505.T332N, KNH1144 and B41 were kindly provided by Dr. J. P. Moore of the Weil Cornell Medical College, NY.

The Env-deleted pro-viral backbone plasmid and pSG3Δ^{env} DNA (Drs. J. C. Kappes and X. Wu)[52, 62] was obtained through the NIH ARP. MLV gag-pol-expressing vector pVPack-GP, Env-expressing vector pVPack-VSV-G and a pFB-luc vector were obtained from Stratagene (La Jolla, CA).

HIV-1_{IIIB} laboratory adapted strain was obtained through the NIH ARP. Full-length clinical isolates HIV-1 clones were obtained through the NIH ARP.

Pseudovirus preparation

Pseudoviruses capable of single cycle infection were prepared as previously described with a minor modification[15, 17]. Briefly, 5 x 10^6 HEK293T cells were transfected in a 15 ml volume of a solution containing 8 μg of an HIV-1 Env-deleted pro-viral backbone plasmid pSG3$^{\Delta env}$, and 8 μg of an HIV-1 Env-expression plasmid with FuGENE 6 (Roche). VSV-G pseudovirus was prepared by transfecting the HEK293T cells with a combination of the Env-expressing plasmid pVPack-VSV-G, the MLV gag-pol-expressing plasmid pVPack-GP, the pFB-luc plasmid and FuGENE 6. Pseudovirus-containing supernatants were collected two days after transfection, filtered, tittered and stored in aliquots at −80 °C.

Measurement of antiviral activity

Single-cycle infection assay in TZM-bl cells. The NBD compounds were tested against the pseudovirus HIV-1 expressing the Env from the lab-adapted HIV-1_{HXB-2} (X4) in a single-cycle infection assay. Moreover, the small molecules **89**, **83B**, and **84A** were also tested against a large group of HIV-1 pseudotyped viruses expressing the Env from the panel of clinical isolates as previously described[15, 17]. Briefly, TZM-bl cells were plated in a 96-well tissue culture plate at 1 x 10^4 / well and cultured at 37 °C. Following overnight incubation, aliquots of HIV-1 pseudovirus pre-treated with graded concentrations of the small molecules for 30 min were added to the cells and incubated for 3 days. Cells were washed and lysed with 50 µl of lysis buffer (Promega). 20 µl of the lysates were transferred to a white plate and mixed with the luciferase assay reagent (Promega). The luciferase activity was measured immediately with a Tecan Infinite M1000 reader, and the percent inhibition by the compounds and IC_{50} (the half maximal inhibitory concentration) values were calculated using the GraphPad Prism software.

Single-cycle infection assay in U87-CD4-CXCR4 cells. The small molecules **89**, **83B** and **84A** were also tested against control pseudovirus VSV-G, obtained as described above. Briefly, U87-CD4-CXCR4 cells were plated in a 96-well tissue culture plate at 1 x 10^4 / well and cultured overnight. The following day, aliquots of VSV-G pseudovirus pre-treated with graded concentrations of the small molecules for 30 min were added to the cells and incubated for three days. Cells were washed and lysed with 40 µl of lysis buffer. The lysates were then transferred to a white plate and mixed with the luciferase assay reagent. The luciferase activity was immediately measured to calculate the percent of inhibition and IC_{50} values by using the GraphPad Prism software.

Multi-cycle infection assay in MT-2 cells. The NBD small molecules were evaluated against the

full-length laboratory-adapted HIV-1_{IIIB} as previously described[68]. Briefly, MT-2 cells were infected with HIV-1_{IIIB} at 100 $TCID_{50}$ and pre-incubated with graded concentrations of compounds for 30 min. The following day, the culture supernatants were replaced with fresh media. Four days post-infection, the supernatants were collected and mixed with an equal volume of 5 % Triton X-100 and tested for p24 antigen by sandwich-ELISA. The percent inhibition of p24 production and IC_{50} values were calculated by the GraphPad Prism software.

Evaluation of cytotoxicity

TZM-bl cells. The cytotoxicity of the small molecules in TZM-bl cells was measured by the colorimetric XTT method as previously described[14]. Briefly, TZM-bl cells were plated in a 96-well tissue culture plate at 1 x 10^4 / well and cultured at 37 °C. Following overnight incubation, the cells were incubated with 100 µl of the compounds at graded concentrations and cultured for three days. The XTT solution was added to the cells and four h later the soluble intracellular formazan was quantitated at 450 nm. The percent of cytotoxicity and the CC_{50} (the concentration for 50 % cytotoxicity) values were calculated as above.

MT-2 cells. The **c**ytotoxicity of the small molecules in MT-2 cells which ran parallel to the neutralization assay was also measured with the colorimetrical XTT method as previously described[68]. Briefly, 100 µl of a small molecule at graded concentrations was added to an equal volume of cells (10^5 cells/ml) in 96-well plates. The following day, the culture supernatants were replaced with fresh media and incubated for four days. Four hours after the addition of XTT the soluble intracellular formazan was quantitated, and the percent of cytotoxicity and the CC_{50} values were calculated as above.

HIV-1 mediated cell-to-cell fusion inhibition assay.

The HIV-1 mediated cell-to-cell fusion assay was performed as previously described[14, 69, 70] with some minor modifications. We used the indicator cells MAGI-CCR5, a HeLa cell line expressing CD4, CXCR4, and CCR5, and HIV-LTR-β-gal under control of HIV-1 Tat as target cells. And HL2/3 cells, a HeLa cell line which expresses HIV-1_{HXB2} Env on the surface and Tat, Gag, Rev and Nef proteins in the cytoplasm but does not produce mature virions, as effector cells. Briefly, MAGI-CCR5 cells were plated in a 96-well 1.5×10^4 / well and cultured for four h at 37 °C. Then, the cells were incubated for one h with escalating concentrations of NBD-compounds. HL2/3 cells were then added to the culture at 7.5 x 10^3 cells/well and cultured for 24 h. β-gal expression was quantified with the Beta-Glo Assay system (Promega) following the manufacturer's instructions. The percent inhibition and the IC_{50} values were calculated using the GraphPad Prism software

Assay in Cf2Th-CCR5 cells

CD4-negative Cf2Th-CCR5 cells were plated at 6×10^3 cells/well in a 96-well tissue culture plate and incubated overnight. The cells were infected with the luciferase expressing recombinant CD4-dependent pseudovirus HIV-1_{ADA} as previously described[13]. Briefly, following overnight incubation, aliquots of HIV-1_{ADA} pseudovirus pre-treated with graded concentrations of the small molecules for 30 min were added to the cells and cultured for 48 h. Cells were washed with PBS and lysed with 40 µl of cell lysis reagent. Lysates were transferred to a white 96-well plate and mixed with 100 µl of luciferase assay reagent. The luciferase activity was immediately measured to obtain the relative infection compared to the untreated control. The Relative virus infectivity indicates the amount of infection detected in the presence of the compounds divided by the amount of infection detected in the absence of the compounds.

Time of addition assay

TZM-bl cells were plated in a 96-well tissue culture plate at 1 x 10^4 / well and cultured at 37 °C overnight. On the day of the infection, aliquots of the pseudovirus $HIV1_{HXB2}$ were added to the cells. The plates were immediately spun for 30 min at 2090 g at 4 ºC and subsequently incubated at 37 ºC for 90 min. Afterward, the medium was removed to eliminate unbound virus, and the cells were washed one time with PBS. Fresh medium was added to the cells. The cells were treated with 10-15 times their respective IC_{50} values as previously described Lin PF. Et al.[41] at the time of infection (Time "0") or 30 min, 1, 2, 4, 6 and 8 h postinfection (p.i.). As a control, cells were treated with AMD3100 (co-receptor CXCR4 inhibitor), BMS-378806 (entry inhibitor) Zidovudine (AZT, Nucleoside Reverse Transcriptase Inhibitor (NRTI)) and Raltegravir (Integrase inhibitor). Forty-eight hours post-infection, the cells were washed two times with PBS and lysed. The luciferase activity was immediately measured as described above. Two independent experiments were performed in triplicate, and the graph is representative of one experiment.

Quantitative determination of HIV-1 Reverse Transcriptase activity.

The inhibitory effect of the NBD compounds on the HIV-1 Reverse Transcriptase activity was determined by using the Colorimetric Reverse Transcriptase Assay (Roche) by following the manufacturer's instructions. NBD-556 and Nevirapine (Non-nucleoside Reverse Transcriptase Inhibitor (NNRTI)) were used as a control.

Crystallization, structure determination and refinement

Clade A/E gp120 $core_e$ H375S was produced by transient expression and purified as described previously[71]. The protein was concentrated to ~10 mg/ml in 5 mM Tris-HCl pH 7.5, 150 mM

NaCl, and 0.02% NaN_3 and mixed with 5 mM 90 in 50% DMSO in 10 to 1 ratio prior to crystallization. The protein and 90 mixture was then set up for crystallization by mixing 0.5 µl of the mixture and 0.5 µl of the reservoir solution containing 10-16% PEG 3350, 5% isopropanol, and 0.1M HEPES 7.5 by hanging drop vapor diffusion. Good diffracting quality crystals grew at 14% PEG3350, 5% isopropanol, and 0.1M HEPES 7.5. Crystals were flash-frozen with cryoprotectant containing 30% ethylene glycol, 14% PEG3350, 5% isopropanol, and 0.1M HEPES 7.5 for data collection at synchrotron beamline (SER-CAT ID22, Advanced Photon Source, Argonne National Laboratory). The diffraction data were processed and scaled with HKL2000[72] and the structure was determined by molecular replacement using Phaser[73]. The molecule was built with Coot[74] and refined with PHENIX[73]. The refinement statistics were summarized in Table S1. Figures were generated using PyMOL (The PyMOL Molecular Graphics System, Version 2.0, Schrödinger, LLC).

Turbidimetric Aqueous Solubility

Test compound (10 mM in DMSO) was serially diluted to give solutions of 0.1, 0.3, 1 and 3 mM in DMSO. Each test compound concentration was then further diluted 1 in 100 in buffer (typically 0.01 M phosphate buffered saline pH 7.4) so that the final DMSO concentration was 1 % and the final test compound concentrations were 1, 3, 10, 30 and 100 µM. The experiment was performed at 37 °C and each concentration was incubated in 7 replicate wells. The plates were incubated for 2 hr at 37 °C before the absorbance was measured at 620 nm. Nicardipine and pyrene were included as control compounds. The solubility of nicardipine is pH dependent whereas the solubility of pyrene is pH independent.

Data Analysis

The solubility was estimated from the concentration of test compound that produced an increase in absorbance above vehicle control (i.e., 1 % DMSO in the buffer).

Caco-2 Permeability (Bi-directional)

Caco-2 cells obtained from the ATCC were used between passage numbers 40 - 60. Cells were seeded onto Millipore Multiscreen Transwell plates at 1 x 10^5 cells/cm^2. The cells were cultured in DMEM and media was changed every two or three days. On day 20 the permeability study was performed. Cell culture and assay incubations were carried out at 37 ºC in an atmosphere of 5 % CO_2 with a relative humidity of 95 %. On the day of the assay, the monolayers were prepared by rinsing both basolateral and apical surfaces twice with Hanks Balanced Salt Solution (HBSS) at the desired pH warmed to 37 °C. Cells were then incubated with HBSS at the desired pH in both apical and basolateral compartments for 40 min to stabilize physiological parameters.

The dosing solutions were prepared by diluting test compound with assay buffer to give a final test compound concentration of 10 µM (final DMSO concentration of 1 % v/v). The fluorescent integrity marker lucifer yellow was also included in the dosing solution. Analytical standards were prepared from test compound DMSO dilutions and transferred to buffer, maintaining a 1 % v/v DMSO concentration.

Assay buffer was composed of supplemented HBSS pH 7.4.

For assessment of A-B permeability, HBSS was removed from the apical compartment and replaced with test compound dosing solution. The apical compartment insert was then placed into a companion plate containing a fresh buffer (containing 1 % v/v DMSO). For assessment of B-A permeability, HBSS was removed from the companion plate and replaced with test compound dosing solution. Fresh buffer (containing 1 % v/v DMSO) was added to the apical compartment insert, which is then placed into the companion plate.

At 120 min the apical compartment inserts and the companion plates were separated and apical and basolateral samples diluted for analysis. Test compound permeability was assessed in duplicate. Compounds of known permeability characteristics were run as controls on each assay plate.

Test and control compounds were quantified by LC-MS/MS cassette analysis using an 8-point calibration with an appropriate dilution of the samples. Cyprotex generic analytical conditions were used. The starting concentration (C_0) was determined from the dosing solution and the experimental recovery calculated from C_0 and both apical and basolateral compartment concentrations.

The integrity of the monolayer throughout the experiment was checked by monitoring lucifer yellow permeation using fluorimetric analysis. Lucifer yellow permeation is high if monolayers have been damaged.

Data Analysis

The permeability coefficient (P_{app}) for each compound was calculated from the following equation:

$$P_{app} = \left(\frac{dQ/dt}{C_0 \times A}\right)$$

Where dQ/dt is the rate of permeation of the drug across the cells, C_0 is the donor compartment concentration at time zero and A is the area of the cell monolayer. C_0 was obtained from analysis of the dosing solution.

For bi-directional experiments, an efflux ratio (ER) was calculated from mean A-B and B-A data. This is derived from:

$$ER = \frac{P_{app(B-A)}}{P_{app(A-B)}}$$

Three control compounds were screened alongside the test compounds, atenolol (human absorption 50 %), propranolol (human absorption 90 %) and talinolol (a substrate for P-gp).

Microsomal Metabolic Stability

Pooled liver microsomes were purchased from a reputable commercial supplier. Microsomes were stored at -80 °C prior to use. Microsomes (final protein concentration 0.5 mg/mL), 0.1 M phosphate buffer pH 7.4 and test compound (final substrate concentration 3 µM; final DMSO concentration 0.25 %) were pre-incubated at 37 °C before the addition of NADPH (final concentration 1 mM) to initiate the reaction. The final incubation volume was 50 µL. A minus cofactor control incubation was included for each compound tested where 0.1 M phosphate buffer pH 7.4 was added instead of NADPH (minus NADPH). Two control compounds were included with each species. All incubations were performed singularly for each test compound.

Each compound was incubated for 0, 5, 15, 30 and 45 min. The control (minus NADPH) was incubated for 45 min only. The reactions were stopped by transferring 20 µL of incubate to 60 µL methanol at the appropriate time points. The termination plates were centrifuged at 2,500 rpm for 20 min at 4 °C to precipitate the protein.

Quantitative Analysis

Following protein precipitation, the sample supernatants were combined in cassettes of up to 4 compounds, an internal standard was added, and samples analyzed using Cyprotex generic LC-MS/MS conditions.

Data Analysis

From a plot of ln peak area ratio (compound peak area/internal standard peak area) against time, the gradient of the line was determined. Subsequently, half-life and intrinsic clearance were calculated using the equations below:

Elimination rate constant (k) = (- gradient)

Half-life ($t_{½}$)(min) = $\frac{0.693}{k}$

Intrinsic clearance (CL_{int})(µL/min/mg protein) = $\frac{V \times 0.693}{t_{½}}$

where V = Incubation volume (µL)/Microsomal protein (mg)

Relevant control compounds were assessed, ensuring intrinsic clearance values fell within the specified limits (if available). Any failures were rejected and the experiment repeated.

Plasma Protein Binding (100 %)

Solutions of test compound (5 µM, 0.5 % final DMSO concentration) were prepared in buffer (pH 7.4) and 100 % species-specific plasma. The experiment was performed using equilibrium dialysis with the two compartments separated by a semi-permeable membrane. The buffer solution was added to one side of the membrane and the plasma solution to the other side. After equilibration, samples were taken from both sides of the membrane. Standards were prepared in plasma and buffer and were incubated at 37 °C. Test compound incubations were performed in duplicate. A control compound was included in each experiment.

The solutions for each batch of compounds were combined into two groups (protein free and protein containing), then cassette analyzed by LC-MS/MS using two sets of calibration standards for protein free (7 points) and protein containing solutions (6 points). Cyprotex generic LC-MS/MS conditions were used. Samples were quantified using standard curves prepared in the equivalent matrix.

Data Analysis

The fraction unbound in plasma (fu) was calculated using the following equation:

$$f_u^{corrected} = \frac{PF}{\{(PC - PF) \times V_{Correction}\} + PF}$$

PC = sample concentration in protein containing side

PF = sample concentration in protein free side

$V_{Correction}$ = correction factor for the volume shift i.e. ratio of the volume of the protein after dialysis to that before dialysis (1.166 for human, previously determined)

Cytochrome P450 Inhibition (IC_{50} Determination)

CYP1A Inhibition

Six test compound concentrations (0.1, 0.25, 1, 2.5, 10, 25 μM; final DMSO concentration 0.3 %) were incubated with human liver microsomes (0.25 mg/mL) and NADPH (1 mM) in the presence of the probe substrate ethoxyresorufin (0.5 μM) for 5 min at 37 °C. The selective CYP1A inhibitor, alpha-naphthoflavone, was screened alongside the test compound as a positive control. Formation of the metabolite resorufin was monitored.

CYP2C9 Inhibition

Six test compound concentrations (0.1, 0.25, 1, 2.5, 10, 25 μM; final DMSO concentration 0.25 %) were incubated with human liver microsomes (1 mg/mL) and NADPH (1 mM) in the presence of the probe substrate tolbutamide (120 μM) for 60 min at 37 °C. The selective CYP2C9 inhibitor, sulfaphenazole, was screened alongside the test compound as a positive control. Formation of the metabolite 4-hydroxytolbutamide was monitored.

CYP2C19 Inhibition

Six test compound concentrations (0.1, 0.25, 1, 2.5, 10, 25 μM; final DMSO concentration 0.25 %) were incubated with human liver microsomes (0.5 mg/mL) and NADPH (1 mM) in the presence of the probe substrate mephenytoin (25 μM) for 60 min at 37 °C. The selective CYP2C19 inhibitor, tranylcypromine, was screened alongside the test compound as a positive control. Formation of the metabolite 4-hydroxymephenytoin was monitored.

CYP2D6 Inhibition

Six test compound concentrations (0.1, 0.25, 1, 2.5, 10, 25 μM; final DMSO concentration 0.25 %) were incubated with human liver microsomes (0.5 mg/mL) and NADPH (1 mM) in the presence of the probe substrate dextromethorphan (5 μM) for 5 min at 37 °C. The selective CYP2D6 inhibitor, quinidine, was screened alongside the test compound as a positive control. Formation of the metabolite dextrorphan was monitored.

CYP3A4 Inhibition (Midazolam)

Six test compound concentrations (0.1, 0.25, 1, 2.5, 10, 25 μM; final DMSO concentration 0.26 %) were incubated with human liver microsomes (0.1 mg/mL) and NADPH (1 mM) in the presence of the probe substrate midazolam (2.5 μM) for 5 min at 37 °C. The selective CYP3A4 inhibitor, ketoconazole, was screened alongside the test compounds as a positive control. Formation of the metabolite 1-hydroxymidazolam was monitored.

Sample Analysis

The reactions were terminated by methanol. For CYP1A, aliquots of the termination solutions were transferred to the relevant wells of clear bottomed 96-well plates and the formation of the metabolite, resorufin, was monitored by fluorescence (excitation wavelength 535 nm, emission wavelength 595 nm). For all other substrates, the termination plates were centrifuged at 2500 rpm for 30 min at 4 °C and an aliquot of the supernatant was transferred to fresh 96-well plates.

Formic acid in deionised water (final concentration 0.1 %) containing internal standard was added to the supernatants prior to analysis by LC-MS/MS using Cyprotex generic methods.

Data Analysis

A decrease in the formation of the metabolite compared to vehicle control is used to calculate an IC_{50} value (test compound concentration which produces 50 % inhibition).

LC-MS/MS Analysis for CYP450 inhibition (CYP2C9, CYP2C19, CYP2D6 and CYP3A4 (Midazolam)

This system consisted of an Acquity™ Binary Solvent Manager (BSM), Acquity™ 4-position heated column manager, 2777 Ultra High-Pressure Autosampler and a Xevo-TQ MS Triple Quadrupole mass spectrometer (Waters Ltd, Herts, UK). The analysis was performed using the following solvent system and gradient:

Column: XBridge™ Phenyl-Hexyl (2.5 µm) 2.1 x 30 mm (Waters Ltd, Herts, UK)

Column Temp.: 70 °C

Injection Vol.: 8 µL

Mobile Phase A: 10 mM ammonium formate + 0.1 % v/v formic acid in water

Mobile Phase B: Methanol

Gradient Profile:

Time (min)	Flow Rate (µL/min)	% Mobile Phase A	% Mobile Phase B	Gradient Profile
0.00	700	90	10	6
1.20	700	5	95	6
1.60	700	90	10	11

1.90	700	90	10	6

hERG Channel Inhibition (IC_{50} Determination)

The experiments were performed on an IonWorks™ automated patch clamp instrument (Molecular Devices LLC), which simultaneously performs electrophysiology measurements for 48 single cells in a specialized 384-well plate (PatchPlate™). All cell suspensions, buffers, and test compound solutions were at room temperature during the experiment.

The cells used were Chinese hamster ovary (CHO) cells stably transfected with hERG (cell-line obtained from Cytomyx, UK). A single-cell suspension was prepared in extracellular solution (Dulbecco's phosphate buffered saline with calcium and magnesium pH 7.2) and aliquots added automatically to each well of a PatchPlate™. The cells were then positioned over a small hole at the bottom of each well by applying a vacuum beneath the plate to form an electrical seal. The vacuum was applied through a single compartment common to all wells which was filled with intracellular solution (buffered to pH 7.2 with HEPES). The resistance of each seal was measured via a common ground-electrode in the intracellular compartment and individual electrodes placed into each of the upper wells.

Electrical access to the cell was then achieved by circulating a perforating agent, amphotericin B, underneath the PatchPlate™. The pre-compound hERG current was then measured. An electrode was positioned in the extracellular compartment, and a holding potential of -80 mV applied for 15 sec. The hERG channels were then activated by applying a depolarizing step to +40 mV for 5 sec and then clamped at -50 mV for 4 sec to elicit the hERG tail current, before returning to -80 mV for 0.3 sec.

Compound dilutions were prepared by diluting a DMSO solution (default 10 mM) of the test compound using a factor 5 dilution scheme into DMSO, followed by dilution into extracellular buffer such that the final concentrations tested were typically 0.008, 0.04, 0.2, 1, 5, 25 μM (final DMSO concentration 0.25 %). The IonWorks™ instrument automatically adds test compound dilutions to the upper wells of the PatchPlate™. The test compound was left in contact with the cells for 300 sec before recording currents using the same voltage-step protocol as in the pre-compound scan. Quinidine, an established hERG inhibitor, was included as a positive control, and vehicle control (0.25 % DMSO) as a negative control.

Each concentration was tested in 4 replicate wells on the PatchPlate™ (maximum of 24 data points). Filters were applied to ensure only acceptable cells are used to assess hERG inhibition. The cell must maintain a seal resistance of greater than 50 MOhm and a pre-compound current of at least 0.1 nA, and ensure cell stability between pre-and post-compound measurements.

Data Analysis

For each replicate the hERG response was calculated using the following equation:

$$\%\ \text{hERG response} = \frac{\text{Post} - \text{compound current (nA)}}{\text{Pre} - \text{compound current (nA)}}\ \text{x}\ 100$$

The % hERG response was plotted against concentration for the test compound and, where concentration-dependent inhibition is observed, the data are fitted to the following equation and an IC_{50} value calculated:

$$y = \frac{y_{max} - y_{min}}{1 + \left(\frac{IC_{50}}{x}\right)^{s}} + y_{min}$$

Where:

y = hERG response

y_{max} = mean vehicle control response

x = concentration

IC_{50} = concentration required to inhibit current by 50 %

s = Hill slope

Chemistry

General. We used **c**ommercial reagents and solvents without further purification. We also performed all reactions in the air atmosphere unless otherwise stated. Reactions were monitored by thin-layer chromatography (TLC) carried out on Merck TLC Silica gel plates (60 F254), using UV light for visualization and basic aqueous potassium permanganate or iodine fumes as a developing agent. ^{1}**H** and ^{13}**C** NMR spectra were recorded on Bruker Avance 400 instrument with operating frequency of 400 and 100 MHz respectively and calibrated using residual undeuterated chloroform (δ**H** = 7.28 ppm) and $CDCl_3$ (δ**C** = 77.16 ppm), or undeuterated DMSO (δH = 2.50 ppm) and DMSO-d_6 (δC = 39.51 ppm) as internal references. The following abbreviations are used to set multiplicities: s = singlet, d = doublet, t = triplet, q =quartet, m = multiplet, br. = broad. The purity of the final compounds was checked by LCMS in a Shimadzu LCMS-2010A using three types of detection systems such as EDAD, ELSD, and UV and was found to be ≥95%.

methyl 5-(4-chlorophenyl)-1H-pyrrole-2-carboxylate (2)

The acid **1** (10.0 g, 45.1 mmol) was dissolved in DMF (45 mL) and finely grounded K_2CO_3 (6.20 g, 44.9 mmol) was added followed by MeI (3.10 mL, 49.8 mmol, 1.10 equiv). The reaction mixture was stirred for 1 day at rt and evaporated. The residue was suspended in DCM and dry loaded on silica. Elution with hexane\EtOAc (10:1, 1:1) provided the title compound as a yellow solid. M = 5.21 g. Yield = 49%.

^{1}H NMR ($CDCl_3$, 400 MHz): δ = 3.89 (s, 3 H), 6.54 (dd, *J*=3.9, 2.8 Hz, 1 H), 6.98 (dd, *J*=3.9, 2.4 Hz, 1 H), 7.38 (d, *J*=8.6 Hz, 2 H), 7.57 (d, *J*=8.7 Hz, 2 H), 9.93 (br. s, 1 H).

^{13}C NMR ($CDCl_3$, 100 MHz): δ = 51.8, 108.5, 117.2, 123.5, 126.2 (2C), 129.3 (2C), 130.0, 133.6, 136.1, 162.0.

methyl 5-(4-chlorophenyl)-1-methyl-1H-pyrrole-2-carboxylate (3)

The ester **2** (7.20 g, 30.6 mmol) was dissolved in DMF (31 mL) and NaH (60% suspension in mineral oil, 2.45 g, 61.3 mmol, 2 equiv) was added in several portions. MeI (5.70 mL, 91.6 mmol, 3 equiv) was added after 5 min . The reaction mixture was stirred for 1 day at rt. The excess NaH was quenched by dropwise addition of methanol (~5 mL) then the reaction mixture was evaporated. The residue was suspended in DCM and dry loaded on silica. Elution with hexane\EtOAc (10:1) yielded the title compound as a yellow solid. M = 7.11 g. Yield = 93%.

^{1}H NMR ($CDCl_3$, 400 MHz): δ = 3.86 (s, 3 H), 3.88 (s, 3 H), 6.20 (d, *J*=4.0 Hz, 1 H), 7.03 (d, *J*=4.0 Hz, 1 H), 7.33 (dt, *J* = 8.7, 2.2 Hz, 2H), 7.42 (dt, *J* = 8.7, 2.2 Hz, 2H).

^{13}C NMR ($CDCl_3$, 100 MHz): δ = 34.4, 51.1, 109.4, 117.7, 123.8, 128.8 (2C), 130.6 (2C), 134.2, 140.3, 161.9.

5-(4-chlorophenyl)-1-methyl-1H-pyrrole-2-carboxylic acid (4)

The ester **3** (1.51 g, 6.05 mmol) was suspended in ethanol (6 mL) and a solution of NaOH (0.48 g, 12 mmol, 2.0 equiv) in water (6 mL) was added. The resulting mixture was heated under reflux for 1 day, cooled to rt and acidified with conc. HCl (1.00 mL) and the precipitate was filtered. M = 1.21 g. Yield = 85%.

^{1}H NMR: (DMSO-d_6, 400 MHz) δ = 3.81 (s, 3 H), 6.25 (d, *J*=3.3 Hz, 1 H), 6.90 (d, *J*=3.3 Hz, 1 H), 7.51 (dd, *J*=12.2, 8.3 Hz, 4 H).

^{13}C NMR (DMSO-d_6, 100 MHz): δ = 34.4, 109.3, 117.6, 124.7, 129.0 (2C), 129.4, 130.8, 131.0 (2C), 133.1, 139.6, 162.5.

1-tert-butyl 2-methyl 5-(4-chlorophenyl)-3-methyl-1H-pyrrole-1,2-dicarboxylate (6)

In a Schlenk tube, $PdCl_2(PPh_3)_2$ (0.75 g, 0.8 mmol, 5 mol %) was added under an argon atmosphere to a solution of **5** (7.37 g, 21.6 mmol) in anhydrous DMF (80 mL) and the reaction was left stirring for about 5 min at rt. Then the p-Cl-phenyl acetylene (4.40 g, 32.2 mmol, 1.5 equiv), CuI (0.81 g, 4.3 mmol, 20 mol %) and Cs_2CO_3 (14.00 g, 43.0 mmol, 2.0 equiv) were successively added, and the solution was stirred at 50 °C for several hours. The reaction was monitored by TLC, following the disappearance of the dehydroamino acid. After cooling, the reaction mixture was diluted with ether and washed three times with water. Then the organic layer was collected, dried over $MgSO_4$, filtered and concentrated under reduced pressure. The resulting oil was purified by column chromatography (eluent hexanes/EtOAc, 10:1). M = 4.64 g. Yield = 61%.

^{1}H NMR ($CDCl_3$, 400 MHz): δ = 1.43 (s, 9 H), 2.32 (s, 3 H), 3.88 (s, 3 H), 7.37 (s, 4 H).

methyl 5-(4-chlorophenyl)-3-methyl-1H-pyrrole-2-carboxylate (7)

N-Boc pyrrole **6** (4.64 g, 13.3 mmol) was dissolved in MeOH (46 mL) and NaH (60% suspension in mineral oil, 0.64 g, 16 mmol, 1.2 equiv) was added in several portions under nitrogen atmosphere. The reaction mixture was stirred for 1 day and the precipitate was filtered. M = 2.07 g. Yield = 62%.

^{1}H NMR: (DMSO-d_6, 400 MHz) δ = 2.28 (s, 3 H), 3.79 (s, 3 H), 6.53 (s, 1 H), 7.42 (d, *J*=7.8 Hz, 2 H), 7.85 (d, *J*=8.0 Hz, 2 H), 11.75 (br. s., 1 H).

sodium 5-(4-chlorophenyl)-3-methyl-1H-pyrrole-2-carboxylate (8)

The ester **7** (2.07 g, 8.3 mmol) was suspended in ethanol (4.1 mL) - THF (4.1 mL) mixture and a solution of NaOH (332 mg, 8.3 mmol) in water (4.1 mL) was added. The resulting mixture was heated under reflux for a week, filtered and evaporated. When acidification was attempted, immediate decarboxylation was observed. M = 1.79 g. Yield = 84%.

^{1}H NMR: (DMSO-d_6, 400 MHz) δ = 2.28 (s, 3 H), 6.31 (s, 1 H), 7.27 (d, *J*=8.6 Hz, 2 H), 7.73 (d, *J*=8.6 Hz, 2 H), 10.72 (br. s, 1 H).

^{13}C NMR (DMSO-d_6, 100 MHz): δ = 12.8, 109.2, 121.3, 125.5 (2C), 127.9, 128.4 (2C), 129.5, 129.5, 131.8, 167.1.

ethyl 1-acetyl-5-(4-chlorophenyl)-4-methyl-1H-pyrrole-2-carboxylate (11)

A mixture of the enamide **9** (2.89 g, 18.4 mmol), the alkyne **10** (3.60 g, 23.9 mmol, 1.1 equiv.), $[RuCl_2(p\text{-cymene})]_2$ (563 mg, 0.92 mmol, 5.0 mol %), $Cu(OAc)_2 \cdot H_2O$ (8.14 g, 40.8 mmol, 2.2 equiv) and AgOTf (0.95 g, 3.7 mmol, 20 mol %) were successively dissolved in a mixture of DCE (92 mL) and MeOH (92 mL). The mixture was stirred at 110 °C in a pressure vessel for 12 h under Ar atmosphere (no reaction proceeded when heated under reflux). Afterwards, it was diluted with DCM and transferred to a round bottom flask. Silica was added to the flask and volatiles were evaporated under reduced pressure. The purification was performed by flash column chromatography on silica gel (eluent: hexane/EtOAc, 10:1). M = 4.32 g. Yield = 77%.

^{1}H NMR ($CDCl_3$, 400 MHz): δ = 1.37 (t, *J*=7.2 Hz, 3 H), 1.99 (s, 3 H), 2.34 (s, 3 H), 4.32 (q, *J*=7.1 Hz, 2 H), 6.88 (s, 1 H), 7.25 (d, *J*=8.6 Hz, 2 H), 7.41 (d, *J*=8.6 Hz, 2 H).

^{13}C NMR ($CDCl_3$, 100 MHz): δ = 11.1, 14.3, 28.7, 60.8, 120.0, 120.5, 123.3, 128.7 (2C), 129.5, 131.3 (2C), 134.4, 134.6, 160.7, 173.4.

5-(4-chlorophenyl)-4-methyl-1H-pyrrole-2-carboxylic acid (12)

N-Acetyl pyrrole **11** (4.32 g, 14.1 mmol) was suspended in ethanol (70 mL) and a solution of NaOH (2.85 g, 71.3 mmol, 4.0 equiv) in water (70 mL) was added. The resulting mixture was heated under reflux for 4 h, cooled to rt and acidified with conc. HCl (5.94 mL) and the acid was filtered off. M = 2.98 g. Yield = 90%.

^{1}H NMR: (DMSO-d_6, 400 MHz) δ = 2.16 (s, 3 H), 6.68 (s, 1 H), 7.46 (d, *J*=7.9 Hz, 2 H), 7.58 (d, *J*=7.9 Hz, 2 H), 11.72 (s, 1 H), 12.15 (br. s, 1 H).

^{13}C NMR (DMSO-d_6, 100 MHz): δ = 12.5, 117.5, 117.9, 122.5, 128.4 (2C), 129.1 (2C), 131.0, 131.4, 132.0, 161.8

methyl 4-(2-chloroacetyl)-5-(4-chlorophenyl)-1H-pyrrole-2-carboxylate (13)

Chloroacetyl chloride (7.06 mL, 88.6 mmol, 4.0 equiv) was added dropwise to an ice-cooled suspension of $AlCl_3$ (11.5 g, 86.3 mmol, 3.9 equiv) in anhydrous DCM (90 mL), Pyrrole **2** (5.21 g, 22.2 mmol) was added to the resulting mixture in several portions, and the mixture was stirred for 2 h at rt. The reaction was quenched by pouring the mixture into the brine. The aqueous layer was extracted with EtOAc, and the organic phase was washed with a saturated $NaHCO_3$ solution, brine and then dried over Na_2SO_4. The solvent was evaporated under reduced pressure to give the residue which was used without purification. M = 6.76 g. Yield = 98%.

^{1}H NMR ($CDCl_3$, 400 MHz): δ = 3.87 (s, 3 H), 4.47 (s, 2 H), 7.36 (d, *J*=2.6 Hz, 1 H), 7.44 (dt, *J* = 8.6, 2.2 Hz, 2 H), 7.59 (dt, *J* = 8.7, 2.2 Hz, 2 H), 9.74 (br. s, 1 H).

methyl 4-(2-chloroacetoxy)-5-(4-chlorophenyl)-1H-pyrrole-2-carboxylate (14)

Na_2HPO_4 (12.30 g, 86.6 mmol, 4 equiv) and *m*-chloroperbenzoic acid 70 % (10.7 g, 43.4 mmol, 2 equiv) were added to a suspension of pyrrole **13** (6.76 g, 21.7 mmol) in DCM (90 mL). During the addition of mCPBA a slightly exothermic reaction occurred accompanied by dissolution of the starting material. The mixture was stirred for 5 h at rt, washed with water and saturated $NaHCO_3$ solution, and then dried (Na_2SO_4). The solvent was evaporated under reduced pressure to give a crude material, which was purified by crystallization from MeOH. M = 5.19 g. Yield = 73%.

^{1}H NMR ($CDCl_3$, 400 MHz): δ = 3.87 (s, 3 H), 4.30 (s, 2 H), 7.01 (d, *J*=2.8 Hz, 1 H), 7.42 (d, *J*=8.7 Hz, 2 H), 7.57 (d, *J*=8.4 Hz, 2 H), 9.61 (br. s., 1 H).

methyl 5-(4-chlorophenyl)-4-hydroxy-1H-pyrrole-2-carboxylate (15)

A solution of K_2CO_3 (3.27 g, 23.7 mmol, 1.5 equiv) in water (32 mL) was added to a solution of pyrrole **14** (5.19 g, 15.8 mmol) in MeOH (142 mL), and the mixture was stirred at rt for 15 min. After evaporation of the solvent in vacuo, a crude material was obtained. After the addition of water, it was acidified (2 N HCl pH =5-6) and extracted with EtOAc (3x100 mL). The combined organic phases were washed with brine and dried (Na_2SO_4). The solvent was evaporated, and the residue purified by chromatography (eluent hexane\EtOAc, 3:1) and then triturated in the same system to give the pure compound. M = 1.167 g. Yield = 29%.

^{1}H NMR: (DMSO-d_6, 400 MHz) δ = 3.75 (s, 3 H), 6.36 (d, *J*=2.6 Hz, 1 H), 7.38 (d, *J*=8.8 Hz, 2 H), 7.98 (d, *J*=8.7 Hz, 2 H), 9.25 (s, 1 H), 11.50 (br. s., 1 H).

^{13}C NMR (DMSO-d_6, 100 MHz): δ = 51.1, 104.7, 118.4, 119.0, 126.4 (2C), 128.2 (2C), 129.8, 130.4, 143.1, 160.6.

methyl 5-(4-chlorophenyl)-4-methoxy-1H-pyrrole-2-carboxylate (16)

The ester **15** (712 mg, 2.84 mmol) was dissolved in DMF (7.1 mL) and under a nitrogen atmosphere at 0 °C NaH (60% suspension in mineral oil, 113 mg, 2.83 mmol) was added in several portions. After 5 min MeI (0.177 mL, 2.84 mmol) was added. The reaction mixture was stirred for 1 day at rt. The reaction mixture was evaporated. The residue was suspended in DCM and dry loaded on silica. Elution with hexane\EtOAc (10:1) gave the title compound as a yellow solid. M = 455 mg. Yield = 61%.

^{1}H NMR ($CDCl_3$, 400 MHz): δ = 3.87 (s, 3 H), 3.88 (s, 3 H), 6.66 (d, *J*=2.8 Hz, 1 H), 7.36 (d, *J*=8.8 Hz, 2 H), 7.67 (d, *J*=8.8 Hz, 2 H), 9.00 (br. s, 1 H).

^{13}C NMR ($CDCl_3$, 100 MHz): δ = 51.8, 58.4, 102.0, 118.8, 119.8, 126.1 (2C), 129.1 (2C), 129.2, 132.4, 146.8, 161.6.

A dimethylated (211 mg, 27%) product was also isolated:

methyl 5-(4-chlorophenyl)-4-methoxy-1-methyl-1H-pyrrole-2-carboxylate

^{1}H NMR ($CDCl_3$, 400 MHz): δ = 3.75 (s, 3 H), 3.82 (s, 3 H), 3.84 (s, 3 H), 6.70 (s, 1 H), 7.35 (dt, *J*=8.6, 2.2 Hz, 2 H), 7.40 - 7.44 (dt, *J*=8.7, 2.2 Hz, 2 H).

5-(4-chlorophenyl)-4-methoxy-1H-pyrrole-2-carboxylic acid (17)

The ester **16** (455 mg, 1.72 mmol) was suspended in ethanol (5 mL) and a solution of NaOH (206 mg, 5.15 mmol, 3.0 equiv) in water (5 mL) was added. The resulting mixture was heated under reflux for 1 day, cooled to rt and acidified with conc. HCl (0.43 mL). The precipitate was filtered and air dried. M = 405 mg. Yield = 94%.

^{1}H NMR: (DMSO-d_6, 400 MHz) δ = 3.78 (s, 3 H), 6.62 (s, 1 H), 7.36 (d, *J* = 8.0 Hz, 2H), 7.89 (d, *J* = 8.6 Hz, 2H), 11.71 (br. s, 1 H), 12.37 (br. s, 1 H).

^{13}C NMR (DMSO-d_6, 100 MHz): δ = 58.0, 101.6, 118.7, 119.9, 126.7 (2C), 128.3 (2C), 129.9, 130.1, 146.3, 161.6.

1-(4-chlorophenyl)-2,2-dihydroxyethanone (18)

To a stirred solution of the 1-(4-chlorophenyl)ethanone (26 mL, 200 mmol) in 340 mL of DMSO was added slowly 58 mL (600 mmol, 3 equiv) of 48% aqueous HBr (8.8 M). The solution was stirred in an open flask at 55 °C, and the reaction was monitored by TLC. When the starting material was consumed, the solution was poured onto ice. The crude product was extracted into EtOAc, and the solution was washed with brine, dried, and concentrated. M = 19.57 g. Yield = 52%.

^{1}H NMR ($CDCl_3$, 400 MHz): δ = 4.84 (br. s., 2 H), 6.29 (s, 1 H), 7.45 (d, *J*=8.6 Hz, 2 H), 8.07 (d, *J*=8.6 Hz, 2 H).

ethyl 5-(4-chlorophenyl)-1H-imidazole-2-carboxylate (19)

To a solution of ammonium acetate (24.3 g, 315 mmol, 3 equiv) in water (72 mL) and acetonitrile (144 mL) at 0 °C was added ethyl glyoxylate (50% soln. in toluene, 62 mL, 313 mmol, 3 equiv) followed by 1-(4-chlorophenyl)-2,2-dihydroxyethanone **18** (19.57 g, 104.9 mmol) in acetonitrile (144 mL) over a period of 20 min at 0 °C. The mixture was stirred at 0-5 °C for 30 min and at rt overnight. After removal of acetonitrile, the mixture was partitioned between ethyl acetate (~200 mL) and water (~100 mL). The organic layer was washed with brine and dried over Na_2SO_4, filtered and concentrated. The residue was triturated with hot hexane\EtOAc 1:1 mixture (100 mL) and filtered to provide 5.72 g (22%) of a pale yellow solid.

^{1}H NMR: (DMSO-d_6, 400 MHz) δ = 1.33 (t, *J*=7.1 Hz, 3 H), 4.35 (q, *J*=7.1 Hz, 2 H), 7.44 (d, *J*=8.3 Hz, 2 H), 7.88 (d, *J*=8.4 Hz, 2 H), 7.96 (br. s, 1 H), 13.51 (br. s, 1 H).

^{13}C NMR (DMSO-d_6, 100 MHz): δ = 14.2, 60.8, 117.9 (br.), 126.4 (2C), 128.6 (2C), 131.4, 132.6 (br.), 137.4, 141.3 (br.), 158.4.

5-(4-chlorophenyl)-1H-imidazole-2-carboxylic acid (20)

The ester **19** (4.72 g, 18.8 mmol) was suspended in ethanol (95 mL) and a solution of NaOH (3.80 g, 95.0 mmol, 5.0 equiv) in water (95 mL) was added. The resulting mixture was heated under reflux for 1 day, cooled to rt and acidified with conc. HCl (7.9 mL). The acid was filtered and dried on air. M = 4.31 g. Yield = 100%.

^{1}H NMR: (DMSO-d_6, 400 MHz) δ = 6.53 (br. s, 2 H), 7.43 (d, *J*=8.3 Hz, 2 H), 7.86 (d, *J*=8.0 Hz, 2 H), 7.87 (s, 1H).

^{13}C NMR (DMSO-d_6, 100 MHz): δ = 118.6, 126.5 (2C), 128.7 (2C), 131.5, 132.0, 138.9, 139.8, 159.5.

2-(4-chlorophenyl)-5-(trifluoromethyl)-1H-imidazole (21)

10.85 g (5.00 mL, 40.2 mmol) of 1,1-dibromo-3,3,3-trifluoro acetone was dissolved in 20 mL of water containing sodium acetate (6.60 g, 80.5 mmol, 2 equiv). It was stirred at 90° C. for 30 min, then cooled to ambient temperature, and 5.65 g (40.2 mmol) of *p*-Cl-benzaldehyde was added as a solution in the mixture of 70 ml methanol and 70 ml of aqueous ammonia. The reaction mixture was stirred overnight. Then the methanol was evaporated. The remaining aqueous phase was extracted with ethyl acetate and the organic phase was further washed with brine. The organic phase was dried over Na_2SO_4, filtered and evaporated. The residue was subjected to the

chromatographic purification. Eluent: hexane/EtOAc (10:1) first fraction is unreacted *p*-Cl-benzaldehyde than the title compound (2.85 g, 29%). After that eluent was changed to the hexane/EtOAc (3:1) a side product-nitrile was obtained (1.87 g, 23%).

^{1}H NMR: (DMSO-d_6, 400 MHz) δ = 7.56 (d, *J*=8.6 Hz, 2 H), 7.94 (s, 1 H), 7.99 (d, *J*=8.4 Hz, 2 H), 13.27 (br. s, 1 H).

^{13}C NMR (DMSO-d_6, 100 MHz): δ = 119.2 (q, *J* = 3.7 Hz), 122.2 (q, *J* = 266.4 Hz), 127.1 (2C), 128.3, 129.0 (2C), 130.8 (q, *J* = 38.1 Hz), 133.7, 146.3.

For **2-(4-chlorophenyl)-1H-imidazole-5-carbonitrile**:

^{1}H NMR: (DMSO-d_6, 400 MHz) δ = 7.58 (d, *J*=8.7 Hz, 2 H), 7.97 (d, *J*=8.7 Hz, 2 H), 8.28 (s, 1 H), 13.52 (br. s, 1 H).

2-(4-chlorophenyl)-1H-imidazole-5-carboxylic acid (22)

Imidazole **21** (2.85 g, 11.6 mmol) was suspended in the solution of NaOH (4.63 g, 116 mmol, 10 equiv) in water (46 mL) and heated under reflux for 1 day. The reaction mixture was cooled to rt and acidified with conc. HCl (9.65 mL). The precipitate was filtered. M =1.649 g. Yield = 64%. Nitrile did not react under the same conditions.

^{1}H NMR: (DMSO-d_6, 400 MHz) δ = 7.52 (d, 2 H), 7.75 (s, 1 H), 8.07 (d, *J*=8.3 Hz, 2 H). two exchangeable protons are missing.

^{13}C NMR (DMSO-d_6, 100 MHz): δ = 127.3 (2C), 128.8 (2C), 128.9, 133.3, 146.1, 163.4. two signals are missing, probably due to broadening.

General procedure for amide coupling

DIPEA (10 mmol) was added to an appropriate acid (10 mmol) followed by DMF (10 mL per 1 g of acid) and then HBTU (10 mmol). The resulting solution was stirred for 10 min and added to a solution of appropriate amine (10 mmol) in DMF (10 mL per 1 g of amine) in several portions. The reaction mixture was stirred overnight; DMF was evaporated, and the residue was dissolved in DCM (50 mL) and successively washed with 5% aqueous NaOH and 10% tartaric acid solutions (50 mL). The organic layer was dried over Na_2SO_4, filtered, evaporated and dry loaded on silica. Eluting with hexanes/EtOAc (1:1, then pure EtOAc) gave the target compounds.

The products were used in the next step without analysis.

General procedure for deprotection

To a solution containing protected compound (5 mmol) and N,N'–diethyl barbituric acid (NDMBA, 15 mmol, 3 equiv) in MeOH (50 mL), PPh_3 (10 mol. %) was added under a nitrogen atmosphere followed by $Pd(dba)_2$ (5 mol. %). The mixture was stirred for 1 day under reflux. After cooling, 50 ml DCM was added, and the organic phase was shaken with 10% aqueous K_2CO_3 (50 mL) to remove the unreacted NDMBA. The organic layer was separated, and the aqueous layer was extracted with DCM/EtOH (~4:1, 2-4 x 50 mL). The combined organic layers were dried over Na_2SO_4, filtered and concentrated. Purification by flash chromatography (eluent: DCM/MeOH (saturated with NH_3~ 7M), 10:1) afforded amine as a slightly brown or yellowish solid.

HCl salt of the amine: pure amine was dissolved in a minimal amount of 1M MeOH-HCl, and evaporated. The added mass exactly corresponds to two molecules of HCl per one molecule of amine.

N-(2-amino-1-(5-(hydroxymethyl)-4-methylthiazol-2-yl)ethyl)-5-(3,4-difluorophenyl)-1H-pyrrole-2-carboxamide (25)

Compound **25** was obtained following the general procedure for amide coupling and then the general procedure for deprotection from amine **24** and acid **23**.

*f*S-**25A**: m = 255 mg. Yield = 38% (over two steps).

^{t}R = 1.159 min. Purity = 100%. LC–MS: m/z $[M+H]^+$ = 393 Da.

*f*R-**25B**: m = 204 mg. Yield = 30% (over two steps).

^{t}R = 1.156 min. Purity = 100%. LC–MS: m/z $[M+H]^+$ = 393 Da.

mp = 105-110 °C.

^{1}H NMR: (DMSO-d_6, 400 MHz) δ = 1.74 (br. s, 2 H), 2.25 (s, 3 H), 2.96 (dd, *J*=13.1, 7.8 Hz, 1 H), 3.09 (dd, *J*=13.2, 5.3 Hz, 1 H), 4.52 (s, 2 H), 5.13 (dd, *J*=13.4, 7.9 Hz, 1 H), 5.36 (br. s., 1 H), 6.66 (d, *J*=3.8 Hz, 1 H), 6.99 (d, *J*=3.9 Hz, 1 H), 7.42 (dd, *J*=19.3, 8.7 Hz, 1 H), 7.61 - 7.68 (m, 1 H), 7.94 (ddd, *J*=12.6, 7.8, 2.0 Hz, 1 H), 8.51 (d, *J*=7.7 Hz, 1 H), 11.85 (br. s, 1 H).

^{13}C NMR (DMSO-d_6, 100 MHz): δ = 14.8, 45.6, 54.3, 55.0, 107.9, 112.7, 113.5 (d, *J* = 19.0 Hz), 117.7 (d, *J* = 17.6 Hz), 121.4 (dd, *J* = 5.9, 2.9 Hz), 127.7, 129.6 (dd, *J* = 7.3, 3.7 Hz), 132.5, 132.8, 146.8, 148.1 (dd, *J* = 245.9, 13.2 Hz), 149.6 (dd, *J* = 244.4, 12.4 Hz), 160.4, 169.3.

HRMS (ESI): m/z calcd for $C_{18}H_{19}F_2N_4O_2S$ $[M+H]^+$ 393.1191, found 393.1186.

N-(2-amino-1-(5-(hydroxymethyl)-4-methylthiazol-2-yl)ethyl)-5-(4-chlorophenyl)-1-methyl-1H-pyrrole-2-carboxamide (26)

Compound **26** was obtained following the general procedure for amide coupling and then the general procedure for deprotection from amine **24** and acid **4**.

*f*S-**26A**: M = 373 mg. Yield = 29% (over two steps).

^{t}R = 1.282 min. Purity = 96%. LC–MS: m/z $[M+H]^+$ = 405 Da.

*f*R-**26B**: M = 290 mg. Yield = 37% (over two steps).

^{t}R = 1.315 min. Purity = 95%. LC–MS: m/z $[M+H]^+$ = 405 Da.

mp = 85-90°C.

^{1}H NMR: (DMSO-d_6, 400 MHz) δ = 2.26 (s, 3 H), 2.98 (dd, *J* = 13.2, 8.1 Hz, 1 H), 3.10 (dd, *J* = 13.2, 5.1 Hz, 1 H), 3.33 (br. s., 2 H), 3.79 (s, 3 H), 4.54 (s, 2 H), 5.10 (td, *J*=7.7, 5.3 Hz, 1 H), 5.37 (br. s., 1 H), 6.26 (d, *J*=3.9 Hz, 1 H), 7.05 (d, *J*=4.0 Hz, 1 H), 7.47 - 7.55 (m, 4 H), 8.51 (d, *J*=7.9 Hz, 1 H).

^{13}C NMR (DMSO-d_6, 100 MHz): δ = 14.8, 34.1, 45.6, 54.5, 55.0, 108.4, 113.1, 127.1, 128.6 (2C), 130.6 (2C), 130.8, 132.3, 132.5, 137.8, 146.9, 161.5, 169.7

HRMS (ESI): m/z calcd for $C_{19}H_{22}ClN_4O_2S$ $[M+H]^+$ 405.1147, found 405.1146.

N-(2-amino-1-(5-(hydroxymethyl)-4-methylthiazol-2-yl)ethyl)-5-(4-chlorophenyl)-3-methyl-1H-pyrrole-2-carboxamide (27)

Compound **27** was obtained following the general procedure for amide coupling (sodium salt was used, no DIPEA was added) and then the general procedure for deprotection from amine **24** and acid **8**.

*f*S-**27A**: M = 99.3 mg. Yield = 22% (over two steps).

^{t}R = 1.443 min. Purity = 89%. LC–MS: m/z $[M+H]^+$ = 405 Da.

*f*R-**27B**: M = 97.4 mg. Yield = 18% (over two steps).

^{t}R = 1.356 min. Purity = 100%. LC–MS: m/z $[M+H]^+$ = 405 Da.

mp = 140-160 °C (decomp).

^{1}H NMR ($CDCl_3$, 400 MHz): δ = 2.28 (s, 3 H), 2.34 (s, 3 H), 3.13 (dd, *J* = 13.2, 5.0 Hz, 1 H), 3.22 (dd, *J* = 13.2, 5.8 Hz, 1 H), 3.74 (br. s., 5 H), 4.60 (s, 2 H), 5.34 (t, *J*=5.4 Hz, 1 H), 6.29 (s, 1 H), 7.26 (d, *J*=8.6 Hz, 2 H), 7.47 (d, *J*=8.6 Hz, 2 H).

^{1}H NMR: (DMSO-d_6, 400 MHz) δ = 2.26 (s, 3 H), 2.30 (s, 3 H), 3.06 (dd, *J* = 13.2, 7.7 Hz, 1 H), 3.12 -3.19 (m, 2 H), 3.38 (br. s, 1H), 4.53 (s, 2 H), 5.21 (q, *J*=6.6 Hz, 1 H), 5.37 (br. s., 1 H), 6.49 (s, 1 H), 7.44 (d, *J*=8.2 Hz, 2 H), 7.77 (d, *J*=8.2 Hz, 2 H), 8.42 (d, *J*=7.9 Hz, 1 H), 11.46 (br. s., 1 H).

^{13}C NMR (DMSO-d_6, 100 MHz): δ = 12.9, 14.8, 45.0, 53.0, 55.0, 110.1, 122.8, 126.1, 126.3 (2C), 128.7 (2C), 130.6, 131.1, 131.6, 132.7, 146.9, 160.8, 168.7.

HRMS (ESI): m/z calcd for $C_{19}H_{22}ClN_4O_2S$ $[M+H]^+$ 405.1147, found 405.1141.

N-(2-amino-1-(5-(hydroxymethyl)-4-methylthiazol-2-yl)ethyl)-5-(4-chlorophenyl)-4-methyl-1H-pyrrole-2-carboxamide (28)

Compound **28** was obtained following the general procedure for amide coupling and then the general procedure for deprotection from amine **24** and acid **12**.

*f*S-**28A**: M = 141.1 mg. Yield = 12% (over two steps).

^{t}R = 1.386 min. Purity = 100%. LC–MS: m/z $[M+H]^+$ = 405 Da.

*f*R-**28B**: M = 635 mg. Yield = 33% (over two steps).

^{t}R = 1.507 min. Purity = 100%. LC–MS: m/z $[M+H]^+$ = 405 Da.

mp = 120-125°C.

^{1}H NMR ($CDCl_3$, 400 MHz): δ = 2.12 (s, 3 H), 2.19 (s, 3 H), 2.50 - 3.60 (br. s, 3H), 2.99 (d, *J*=8.9 Hz, 1 H), 3.15 (d, *J*=8.4 Hz, 1 H), 4.58 (s, 2 H), 5.21 (br. s., 1 H), 6.68 (s, 1 H), 7.21 (d, *J*=8.3 Hz, 2 H), 7.31 (d, *J*=8.1 Hz, 2 H), 7.81 (d, *J*=6.1 Hz, 1 H), 10.73 (br. s., 1 H).

^{13}C NMR ($CDCl_3$, 100 MHz): δ = 12.6, 14.8, 45.3, 52.7, 55.9, 114.7, 118.1, 124.3, 128.3 (2C), 128.7 (2C), 131.0, 132.1, 132.3, 132.6, 148.7, 161.4, 168.2.

HRMS (ESI): m/z calcd for $C_{19}H_{22}ClN_4O_2S$ $[M+H]^+$ 405.1147, found 405.1155.

N-(2-amino-1-(5-(hydroxymethyl)-4-methylthiazol-2-yl)ethyl)-5-(4-chlorophenyl)-4-methoxy-1H-pyrrole-2-carboxamide (29)

Compound **29** was obtained following the general procedure for amide coupling and then the general procedure for deprotection from amine **24** and acid **17**.

*f*S-**29A**: M = 149.7 mg. Yield = 59% (over two steps).

^{t}R = 1.293 min. Purity = 100%. LC–MS: m/z $[M+H]^+$ = 421 Da.

*f*R-**29B**: M = 188.7 mg. Yield = 45% (over two steps).

^{t}R = 1.295 min. Purity = 98%. LC–MS: m/z $[M+H]^+$ = 421 Da.

mp = 115-120°C.

^{1}H NMR: (DMSO-d_6, 400 MHz) δ = 1.51 - 1.94 (br. s, 2 H), 2.25 (s, 3 H), 2.96 (dd, *J*=13.1, 7.9 Hz, 1 H), 3.09 (dd, *J*=13.1, 5.4 Hz, 1 H), 3.81 (s, 3 H), 4.52 (s, 2 H), 5.12 (dd, *J*=13.0, 7.7 Hz, 1 H), 5.35 (br. s., 1 H), 6.86 (s, 1 H), 7.39 (d, *J*=8.7 Hz, 2 H), 7.87 (d, *J*=8.6 Hz, 2 H), 8.47 (d, *J*=7.7 Hz, 1 H), 11.39 (br. s, 1 H).

^{13}C NMR (DMSO-d_6, 100 MHz): δ = 14.8, 45.7, 54.3, 55.0, 57.9, 98.9, 116.9, 122.9, 126.2 (2C), 128.3 (2C), 129.7, 130.2, 132.4, 146.1, 146.8, 160.1, 169.1.

HRMS (ESI): m/z calcd for $C_{19}H_{22}ClN_4O_3S$ $[M+H]^+$ 421.1096, found 421.1093.

N-(2-amino-1-(5-(hydroxymethyl)-4-methylthiazol-2-yl)ethyl)-5-(4-chlorophenyl)-1H-imidazole-2-carboxamide (30)

Compound **30** was obtained following the general procedure for amide coupling and then the general procedure for deprotection from amine **24** and acid **20**.

*f*S-**30A**: M = 225 mg. Yield = 11% (over two steps).

^{t}R = 1.253 min. Purity = 100%. LC–MS: m/z $[M+H]^+$ = 392 Da.

*f*R-**30B**: M = 167 mg. Yield = 14% (over two steps).

^{t}R = 1.287 min. Purity = 95%. LC–MS: m/z $[M+H]^+$ = 392 Da.

mp = 120-125°C.

^{1}H NMR: (DMSO-d_6, 400 MHz) δ = 2.27 (s, 3 H), 3.08 (dd, *J* = 13.0, 5.3 Hz, 1 H), 3.15 (dd, *J* = 13.1, 6.6 Hz, 1 H), 3.20 - 3.56 (br. s, 2 H), 4.54 (s, 2 H), 5.15 (q, *J*=5.8 Hz, 1 H), 5.46 (br. s., 2 H), 7.45 (d, *J*=8.6 Hz, 2 H), 7.85 (br. s., 1 H), 7.91 (d, *J*=8.6 Hz, 2 H), 8.84 (d, *J*=7.6 Hz, 1 H).

^{13}C NMR (DMSO-d_6, 100 MHz): δ = 14.8, 45.0, 53.4, 55.0, 117.2 (br.), 126.4, 128.5, 131.2, 132.7, 140.9, 146.9, 158.2, 168.2. several signals are missing due to broadening.

HRMS (ESI): m/z calcd for $C_{17}H_{19}ClN_5O_2S$ $[M+H]^+$ 392.0942, found 392.0943.

N-(2-amino-1-(5-(hydroxymethyl)-4-methylthiazol-2-yl)ethyl)-2-(4-chlorophenyl)-1H-imidazole-5-carboxamide(31)

Compound **31** was obtained following the general procedure for amide coupling and then the general procedure for deprotection from amine **24** and acid **22**.

*f*S-**31A**: M = 200 mg. Yield = 24% (over two steps).

^{t}R = 0.913 min. Purity = 100%. LC–MS: m/z $[M+H]^+$ = 392 Da.

*f*R-**31B**: M = 229 mg. Yield = 32% (over two steps).

^{t}R = 0.980 min. Purity = 100%. LC–MS: m/z $[M+H]^+$ = 392 Da.

mp = 125-130°C.

^{1}H NMR: (DMSO-d_6, 400 MHz) δ = 2.27 (s, 3 H), 3.06 (dd, *J* = 13.0, 5.2 Hz, 1 H), 3.13 (dd, *J* = 12.9, 6.3 Hz, 1 H), 3.33 (br. s, 3 H), 4.53 (s, 2 H), 5.15 (dd, *J* = 13.5, 5.8 Hz, 1 H), 5.38 (br. s, 1 H), 7.56 (d, *J*=8.6 Hz, 2 H), 7.85 (s, 1 H), 8.04 (d, *J*=8.6 Hz, 2 H), 8.46 (d, *J*=6.6 Hz, 1 H).

^{13}C NMR (DMSO-d_6, 100 MHz): δ = 14.9, 45.2, 53.0, 55.0, 122.0 (br.), 127.1 (2C), 128.7, 128.9 (2C), 132.6, 133.3, 144.9 (br.), 146.9, 161.6 (br.), 168.9.

HRMS (ESI): m/z calcd for $C_{17}H_{19}ClN_5O_2S$ $[M+H]^+$ 392.0942, found 392.0944.

allyl (2,2-dimethoxyethyl)(methyl)carbamate (33)

Allyl 2,2-dimethoxyethylcarbamate **32**[14] (91.59 g, 484 mmol) was dissolved in DMF (500 mL) and NaH (60% dispersion in mineral oil, 23.2 g, 580 mmol, 1.20 equiv) was added in several portions. When hydrogen evolution stopped MeI (39 mL, 626 mmol, 1.30 equiv) was added dropwise with external water bath cooling. After 10 min the TLC shows the disappearance of the starting material. The reaction mixture was diluted with water (1000 mL) and extracted with EtOAc (3x200 mL). The combined organic layers were washed with brine (200 mL), dried over Na_2SO_4, filtered and evaporated. M = 91.92 g. Yield = 93%.

^{1}H NMR ($CDCl_3$, 400 MHz): δ = (3.35, 3.35) (s, 3H), (3.39, 3.41) (bs., 6H), 3.94 - 4.02 (m, 1H), 4.43 - 4.55 (m, 1H), 4.59 - 4.66 (m, 1H), 5.08 - 5.25 (m, 2H), 5.31 (d, *J* = 17.0 Hz, 1H), 5.71 - 5.85 (m, 1H), 5.86 - 6.01 (m, 1H).

allyl methyl(2-oxoethyl)carbamate (34)

33 (91.92 g, 452 mmol) was dissolved in formic acid (500 mL) and water (50 mL) was added to the solution. After 30 min TLC shows disappearance of the starting material. After 1 day HCOOH and water was evaporated to provide a residue which is pure enough (~95% yield). To obtain very

pure compound it was distilled under reduced pressure. bp = 90 - 110 °C (2-3 torr). The product was obtained as slightly yellow oil. M = 55.73 g. Yield = 78%.

^{1}H NMR ($CDCl_3$, 400 MHz): δ = 2.97 (s, 3H), 4.04 (d, *J* = 16.4 Hz, 2H), 4.55 (dd, *J* = 16.3, 5.3 Hz, 2H), 5.11 - 5.33 (m, 2H), 5.77 - 5.97 (m, 1H), 9.58 (s, 1H).

^{13}C NMR ($CDCl_3$, 100 MHz): δ = (35.5, 36.2), (58.8, 59.1), (66.4, 66.5), (117.5, 117.7), (132.6, 132.7), (197.8, 197.9).

(*E*)-allyl (2-((tert-butyl sulfinyl)imino)ethyl)(methyl)carbamate (35)

To a solution of aldehyde **34** (7.80 g, 49.6 mmol) in DCM (22 mL) was added commercially available (*S*)-*N*-*tert*-butyl sulfinyl amide (6.62 g, 54.6 mmol, 1.10 equiv), PPTS (0.62 g, 0.050 equiv) and $MgSO_4$ (29.77 g, 248.1 mmol, 5.000 equiv). The mixture was stirred at rt for 30 h; the inorganic material was filtered and washed several times with DCM. The filtrate was concentrated in vacuo to yield pure enough title compound (S)-35. Chromatographic purification: Hexanes/EtOAc 3:1. The product always contains an inseparable mixture of aldehyde. M = 13.32 g. Yield > 100 %.

(*R*)-**35** was prepared using the same procedure from aldehyde **34** (7.90 g). M = 14.68 g. Yield > 100 %.

Alternatively **35** was prepared using the following method (faster reaction times, lower yields):

To a solution of aldehyde **34** (5.00 g, 31.8 mmol) in Et_2O (32 mL) was added commercially available (*S*)-*N*-*tert*-butylsulfinylamide (4.25 g, 35.1 mmol, 1.10 equiv) followed by $Ti(O\textit{i}Pr)_4$ (10.4 mL, 35.1 mmol, 1.1 equiv). The mixture was stirred at rt for 8 h, diluted with Et_2O (100 mL) silica gel (~50 mL) was added and water (2.53 mL, 140.4 mmol, 4.4 equiv) was added under vigorous stirring. After 10 min the mixture was evaporated. Chromatographic purification gave

imine (eluent: EtOAc). The product always contains inseparable mixture of aldehyde. M = 6.20 g. Yield = 75%.

(*R*)-**35** was prepared using the same alternate procedure from aldehyde **34** (5.00 g). M = 6.27 g. Yield = 75%.

^{1}H NMR ($CDCl_3$, 400 MHz): δ = 1.19 (s, 9H), 3.00 (d, *J* = 1.8 Hz, 3H), 4.21 - 4.40 (m, 2H), 4.50 - 4.66 (m, 2H), 5.17 - 5.35 (m, 2H), 5.83 – 6.00 (m, 1H), 7.98 (t, *J* = 2.8 Hz, 1H).

^{13}C NMR ($CDCl_3$, 100 MHz): δ = 14.2, (22.2, 22.4) (3C), 24.8, 28.2, 29.8, (35.2, 35.9), (53.3, 53.6), 57.2, (66.4, 66.5), (117.5, 117.9), (132.7, 132.9), (155.9, 156.4), (164.6, 164.8).

General procedure for 1,2-addition

Appropriate thiazole (130 mmol, 1.3 equiv) was dissolved in THF (130 mL) and cooled to -78 °C. At this temperature *n*-BuLi (2.5 M, 140 mmol, 1.4 equiv) was added dropwise under a nitrogen atmosphere. The reaction mixture was stirred for 20 min at -78 °C, and appropriate imine (100 mmol) was added dropwise as a solution in THF (100 mL). The reaction mixture was slowly (~1 h) warmed to 0 °C, and poured into water (0.5 L). The biphasic mixture was extracted with DCM (3x100 mL). The combined organic phases were dried over Na_2SO_4, filtered and evaporated to give a brown oil which was purified by column chromatography. Eluent: hexanes/EtOAc (10:1, 5:1, 1:1, 0:1).

allyl (2-(5-(((tert-butyldimethylsilyl)oxy)methyl)-4-methylthiazol-2-yl)-2-(1,1-dimethylethylsulfinamido)ethyl)(methyl)carbamate (37)

Compound **37** was obtained following the general procedure for 1,2-addition from imine **35** and thiazole **36**. Rf = 0.5 (EtOAc)

*f*S-**37**: M = 16.50 g. Yield = 65%.

*f*R-**37**: M = 11.07 g. Yield = 44%.

^{1}H NMR ($CDCl_3$, 400 MHz): δ = 0.08 (s, 6H), 0.89 (s, 9H), 1.26 (s, 9H), 2.31 (s, 3H), 2.98 (s, 3H), 3.48 (dd, *J* = 14.5, 2.9 Hz, 1H), 4.01 (dd, *J* = 14.5, 10.0 Hz, 1H), 4.53 - 4.67 (m, 2H), 4.75 (s, 2H), 4.84 - 4.91 (m, 1H), 5.19 (d, *J* = 10.5 Hz, 1H), 5.30 (dd, *J* = 17.2, 1.6 Hz, 1H), 5.37 (d, *J* = 3.1 Hz, 1H), 5.93 (ddt, *J* = 16.8, 11.0, 5.4, 5.4 Hz, 1H).

^{13}C NMR ($CDCl_3$, 100 MHz): δ = -5.2 (2C), 15.3, 18.3, 22.9, 25.8 (3C), 35.1, 54.4, 56.2, 57.3, 58.0, 66.7, 117.5, 132.9, 133.1, 147.9, 158.7, 170.5.

General procedure for amine deprotection:

1M HCl-MeOH solution was prepared by dropwise addition of AcCl to a MeOH (100 mmol). The resulting solution was cooled to an ambient temperature and added to a flask containing appropriately protected compound (10 mmol). After dissolution the reaction mixture was stirred for 1 h, evaporated, dissolved in DCM and washed with 10 % aqueous K_2CO_3. The organic layer was dried over Na_2SO_4, filtered and evaporated and loaded on silica. Eluting with DCM/MeOH (50:1) provided pure amine as a yellow oil.

allyl (2-amino-2-(5-(hydroxymethyl)-4-methylthiazol-2-yl)ethyl)(methyl)carbamate (38)

Compound **38** was obtained following the general procedure for amine deprotection from **37**.

*f*S-**38**: M = 5.99 g. Yield = 65%.

*f*R-**38** M = 5.39 g. Yield = 86%.

^{1}H NMR ($CDCl_3$, 400 MHz): δ = 2.25 (s, 3H), 2.84 (s + br. s, 3+2H), 3.37 - 3.67 (m, 2H), 4.30 (dd, *J* = 7.8, 5.6 Hz, 1H), 4.49 (br. s., 2H), 4.64 (s, 2H), 5.14 (d, *J* = 10.3 Hz, 1H), 5.23 (d, *J* = 17.2 Hz, 1H), 5.76 - 5.92 (m, 1H).

^{13}C NMR ($CDCl_3$, 100 MHz): δ = 14.9, 35.1, 35.6, 52.7, (55.6, 56.0), 56.1, 66.2, (117.3, 117.7), 131.8, 132.8, 148.5, (156.3, 157.0), (171.6, 172.2).

5-(4-chlorophenyl)-N-(1-(5-(hydroxymethyl)-4-methylthiazol-2-yl)-2-(methylamino)ethyl)-1H-pyrrole-2-carboxamide (41)

Compound **41** was obtained following the general procedure for amide coupling and then the general procedure for deprotection from amine **38** and acid **1**.

*f*S-**41A**: M = 1.393 g. Yield = 44% (over two steps).

^{t}R = 1.409 min. Purity = 100%. LC–MS: m/z $[M+H]^+$ = 405 Da.

*f*R-**41B**: M = 1.146 g. Yield = 49% (over two steps).

^{t}R = 1.230 min. Purity = 100%. LC–MS: m/z $[M+H]^+$ = 405 Da.

mp = 120-125 °C.

^{1}H NMR ($CDCl_3$, 400 MHz): δ = 2.25 (s, 3H), 2.45 (s, 3H), 2.99 - 3.09 (m, 1H), 3.30 (m, *J* = 11.6, 5.9 Hz, 1H), 3.35 - 3.95 (br. s, 2H), 4.64 (s, 2H), 5.44 - 5.55 (m, 1H), 6.43 (d, *J* = 3.7 Hz, 1H), 6.86 (d, *J* = 3.7 Hz, 1H), 7.24 (d, *J* = 8.2 Hz, 2H), 7.50 (d, *J* = 8.4 Hz, 2H), 7.92 (br. s, 1H), 10.64 (br. s, 1H)

^{13}C NMR ($CDCl_3$, 100 MHz): δ = 15.0, 35.9, 50.2, 54.2, 56.2, 107.9, 113.5, 126.1 (2C), 127.6, 129.0 (2C), 130.2, 132.4, 133.0, 135.5, 148.9, 161.4, 168.3.

HRMS (ESI): m/z calcd for $C_{19}H_{22}ClN_4O_2S$ $[M+H]^+$ 405.1147, found 405.1144.

5-(4-chloro-3-fluorophenyl)-N-(1-(5-(hydroxymethyl)-4-methylthiazol-2-yl)-2-(methylamino)ethyl)-1H-pyrrole-2-carboxamide (42)

Compound **42** was obtained following the general procedure for amide coupling and then the general procedure for deprotection from amine **38** and acid **39**.

*f*S-**42A**: M = 1.17 g. Yield = 37% (over two steps).

^{t}R = 1.425 min. Purity = 92%. LC–MS: m/z $[M+H]^+$ = 423 Da.

*f*R-**42B**: M = 1.55 g. Yield = 60% (over two steps).

^{t}R = 1.297 min. Purity = 94%. LC–MS: m/z $[M+H]^+$ = 423 Da.

mp = 120-125 °C.

^{1}H NMR ($CDCl_3$, 400 MHz): δ = 2.22 (s, 3H), 2.40 (s, 3H), 2.97 (dd, *J* = 12.2, 4.4 Hz, 1H), 3.29 (dd, *J* = 12.2, 5.1 Hz, 1H), 3.20 - 3.90 (br. s, 2H), 4.63 (s, 2H), 5.37 - 5.50 (m, 1H), 6.43 (d, J = 3.9 Hz, 1H), 6.83 (d, *J* = 3.9 Hz, 1H), 7.20 - 7.31 (m, 2H), 7.36 (d, *J* = 10.9 Hz, 1H), 7.89 (d, *J* = 7.3 Hz, 1H), 10.97 (br. s, 1H).

^{13}C NMR ($CDCl_3$, 100 MHz): δ = 15.0, 36.1, 50.4, 54.4, 56.2, 108.4, 112.9 (d, *J* = 22.7 Hz), 113.2, 119.4 (d, *J* = 17.6 Hz), 121.1, 126.8, 131.0, 132.2, 132.4 (d, *J* = 7.3 Hz), 134.3, 149.0, 158.4 (d, *J* = 248.1 Hz), 161.3, 168.4.

HRMS (ESI): m/z calcd for $C_{19}H_{21}ClFN_4O_2S$ $[M+H]^+$ 423.1052, found 423.1049.

5-(3-fluoro-4-methylphenyl)-N-(1-(5-(hydroxymethyl)-4-methylthiazol-2-yl)-2-(methylamino)ethyl)-1H-pyrrole-2-carboxamide (43)

Compound **43** was obtained following the general procedure for amide coupling and then the general procedure for deprotection from amine **38** and acid **40**.

*f*S-**43A**: M = 796 mg. Yield = 28% (over two steps).

^{t}R = 1.409 min. Purity = 98%. LC–MS: m/z $[M+H]^+$ = 403 Da.

*f*R-**43B**: M = 1.447 g. Yield = 57% (over two steps).

^{t}R = 1.244 min. Purity = 98%. LC–MS: m/z $[M+H]^+$ = 403 Da.

mp = 115-120 °C.

^{1}H NMR ($CDCl_3$, 400 MHz): δ = 2.23 (s, 3H), 2.24 (s, 3H), 2.43 (s, 3H), 3.03 (dd, *J* = 12.1, 4.4 Hz, 1H), 3.31 (dd, *J* = 12.2, 5.8 Hz, 1H), 3.84 (br. s, 2H), 4.63 (s, 2H), 5.46 - 5.55 (m, 1H), 6.41 (d, *J* = 3.8 Hz, 1H), 6.86 (d, *J* = 3.8 Hz, 1H), 7.10 (t, *J* = 7.9 Hz, 1H), 7.19 - 7.28 (m, 2H), 7.96 (d, *J* = 6.0 Hz, 1H), 10.63 (br. s, 1H).

^{13}C NMR ($CDCl_3$, 100 MHz): δ = 14.4 (d, *J* = 2.9 Hz), 14.9, 35.9, 50.3, 54.4, 56.1, 107.6, 111.4 (d, *J* = 24.2 Hz), 113.3, 120.2 (d, *J* = 2.9 Hz), 123.8 (d, *J* = 16.8 Hz), 126.1, 131.3 (d, *J* = 8.8 Hz), 131.9 (d, *J* = 5.1 Hz), 132.2, 135.5, 148.9, 161.33, 161.6 (d, *J* = 244.4 Hz), 168.5.

HRMS (ESI): m/z calcd for $C_{20}H_{24}FN_4O_2S$ $[M+H]^+$ 403.1599, found 403.1593.

General procedure for reductive amination:

Amine was dissolved in MeOH (0.1 M), formic acid (10 equiv) was added followed by formaldehyde solution (37 wt. % in H_2O, contains 10-15% methanol, 10 equiv) and $NaBH_3CN$ (4 equiv, *gas evolution!*). The reaction mixture was stirred for a day, quenched with a saturated aqueous K_2CO_3 solution (volume is equal to the volume of methanol) and dry loaded on silica. Chromatography using $CHCl_3$/MeOH 10:1 mixture gave the title compounds as white or slightly brown solids.

5-(4-chlorophenyl)-N-(2-(dimethylamino)-1-(5-(hydroxymethyl)-4-methylthiazol-2-yl)ethyl)-1H-pyrrole-2-carboxamide (44)

Compound **44** was obtained following the general procedure for reductive amination from **41**.

*f*S-**44A**: M = 183 mg. Yield = 35%.

^{t}R = 1.446 min. Purity = 100%. LC–MS: m/z $[M+H]^+$ = 419 Da.

*f*R-**44B**: M = 212 mg. Yield = 39%.

^{t}R = 1.419 min. Purity = 97%. LC–MS: m/z $[M+H]^+$ = 419 Da.

mp = 110-115 °C.

^{1}H NMR: ($CDCl_3$, 400 MHz) δ = 2.27 (s, 6H), 2.30 (s, 3H), 2.76 (dd, *J* = 11.6, 4.5 Hz, 1H), 2.93 (t, *J* = 10.3 Hz, 1H), 3.34 - 4.03 (br. s, 1H), 4.70 (s., 2H), 5.27 - 5.37 (m, 1H), 6.44 - 6.50 (m, 1H), 6.79 - 6.84 (m, 1H), 7.24 - 7.30 (m, 2H), 7.49 (dd, *J* = 8.6, 3.7 Hz, 2H), 7.55 (br. s, 1H), 10.48 (br. s, 1H).

^{13}C NMR ($CDCl_3$, 100 MHz): δ = 15.0, 45.3, 49.7, 56.6, 62.1, 76.8, 77.2, 77.5, 107.9, 113.0, 126.1, 126.4, 129.1, 130.3, 131.7, 133.1, 135.3, 149.0, 161.5, 169.4.

HRMS (ESI): m/z calcd for $C_{20}H_{24}ClN_4O_2S$ $[M+H]^+$ 419.1303, found 419.1298.

5-(4-chloro-3-fluorophenyl)-N-(2-(dimethylamino)-1-(5-(hydroxymethyl)-4-methylthiazol-2-yl)ethyl)-1H-pyrrole-2-carboxamide (45)

Compound **45** was obtained following the general procedure for reductive amination from **42**.

*f*S-**45A**: M = 454 mg. Yield = 48%.

^{t}R = 1.478 min. Purity = 91%. LC–MS: m/z $[M+H]^+$ = 437 Da.

*f*R-**45B**: M = 580 mg. Yield = 55%.

^{t}R = 1.369 min. Purity = 94%. LC–MS: m/z $[M+H]^+$ = 437 Da.

mp = 115-120 °C.

^{1}H NMR: ($CDCl_3$, 400 MHz) δ = 2.28 (s., 6H), 2.29 (s., 3H), 2.76 (dd, *J* = 12.7, 5.7 Hz, 1H), 2.94 (dd, *J* = 12.1, 9.0 Hz, 1H), 3.49 (br. s, 1H), 4.70 (s, 2H), 5.33 (q, *J* = 6.4 Hz, 1H), 6.46 - 6.50 (m, 1H), 6.79 - 6.83 (m, 1H), 7.29 - 7.40 (m, 3H), 7.53 - 7.61 (m, 1H), 10.62 (br. s, 1H).

^{13}C NMR ($CDCl_3$, 100 MHz): δ = 15.0, 45.4, 49.8, 56.5, 62.2, 108.5, 112.8, 113.0 (d, *J* = 3.7 Hz), 119.5 (d, *J* = 18.3 Hz), 121.1 (d, *J* = 2.9 Hz), 126.9, 131.1, 131.7, 132.4 (d, *J* = 7.3 Hz), 134.2, 149.0, 158.4 (d, *J* = 248.1 Hz), 161.5, 169.3.

HRMS (ESI): m/z calcd for $C_{20}H_{23}ClFN_4O_2S$ $[M+H]^+$ 437.1209, found 437.1204.

N-(2-(dimethylamino)-1-(5-(hydroxymethyl)-4-methylthiazol-2-yl)ethyl)-5-(3-fluoro-4-methylphenyl)-1H-pyrrole-2-carboxamide (46)

Compound **46** was obtained following the general procedure for reductive amination from **43**.

*f*S-**46A**: M = 191 mg. Yield = 39%.

^{t}R = 1.425 min. Purity = 96%. LC–MS: m/z $[M+H]^+$ = 417 Da.

*f*R-**46B**: M = 450 mg. Yield = 57%.

^{t}R = 1.449 min. Purity = 97%. LC–MS: m/z $[M+H]^+$ = 417 Da.

mp = 140-150 °C (decomp.; dihydrochloride).

^{1}H NMR: ($CDCl_3$, 400 MHz) δ = 2.27 (s, 9H), 2.30 (s, 3H), 2.75 (dd, *J* = 12.4, 5.8 Hz, 1H), 2.90 (dd, *J* = 12.0, 9.4 Hz, 1H), 3.60 (br. s, 1H), 4.70 (s, 2H), 5.33 (dt, *J* = 8.5, 6.1 Hz, 1H), 6.46 (dd, *J* = 3.6, 2.7 Hz, 1H), 6.78 - 6.83 (m, 1H), 7.10 - 7.17 (m, 1H), 7.18 - 7.25 (m, 2H), 7.52 (d, *J* = 5.7 Hz, 1H), 10.28 (br. s., 1H).

^{13}C NMR ($CDCl_3$, 100 MHz): δ = 14.4 (d, *J* = 3.2 Hz), 15.1, 45.3 (2C), 49.8, 56.7, 62.2, 107.7, 111.4 (d, *J* = 24.1 Hz), 112.8, 120.1, 124.0 (d, *J* = 17.7 Hz), 126.1, 131.3 (d, *J* = 8.0 Hz), 131.5, 132.1 (d, *J* = 4.8 Hz), 135.2, 149.1, 161.4, 161.7 (d, *J* = 244.1 Hz), 169.4.

HRMS (ESI): m/z calcd for $C_{21}H_{26}FN_4O_2S$ $[M+H]^+$ 417.1755, found 417.1754.

allyl (3-((*tert*-butyldimethylsilyl)oxy)propyl)carbamate (48)

52 (36.7 g, 0.231 mol) was dissolved in DCM (230 mL), imidazole (18.8 g, 0.276 mol, 1.2 equiv) was added in one portion followed by portion wise addition of TBSCl (38.3 g, 0.254 mol, 1.1 equiv) with cooling on a water bath. The reaction mixture was stirred overnight and diluted with water (0.5 L). The organic layer was separated, and the aqueous layer was extracted with DCM (100 mL). The combined organic phases were dried over Na_2SO_4 and evaporated to give a clear oil, which was pure enough for all purposes. The title compound can be purified by flash chromatography on silica using hexanes/EtOAc 10:1 mixture as an eluent.

M = 65.4 g, Yield >100%.

^{1}H NMR ($CDCl_3$, 400 MHz): δ = 0.07 (s, 6H), 0.91 (s, 9H), 1.73 (quin, *J* = 6.0 Hz, 1H), 3.32 (q, *J* = 5.7 Hz, 1H), 3.72 (t, *J* = 5.6 Hz, 1H), 4.56 (d, *J* = 4.9 Hz, 1H), 5.20 (d, *J* = 10.4 Hz, 1H), 5.25 - 5.34 (m, 2H), 5.92 (ddt, *J* = 16.7, 10.9, 5.3 Hz, 1H).

^{13}C NMR ($CDCl_3$, 100 MHz): δ = -5.4 (2C), 18.1, 26.0 (3C), 32.1, 39.6, 62.0, 65.4, 117.3, 133.2, 156.4.

allyl allyl(3-((*tert*-butyldimethylsilyl)oxy)propyl)carbamate (49)

48 (65.4 g, 239 mmol) was dissolved in THF (360 mL) and NaH (60% dispersion in mineral oil, 12.5 g, 313 mmol, 1.30 equiv) was added in several portions. When hydrogen evolution stops allyl bromide (31 mL, 0.36 mol, 1.5 equiv) was added dropwise. The reaction mixture was heated under reflux. After 1 h TLC shows the disappearance of the starting material. The excess of NaH was

quenched by careful dropwise addition of ethanol (~100 mL). The reaction mixture was poured into water (500 mL) and extracted with DCM (3x100 mL). Combined organic layers were dried over Na_2SO_4 and evaporated to yield a clear oil.

In the case of an incomplete reaction, the title compound was separated by flash chromatography on silica using hexanes/EtOAc 20:1 mixture as an eluent.

M = 70.7 g. Yield = 94%.

^{1}H NMR ($CDCl_3$, 400 MHz): δ = 0.06 (s, 6H), 0.91 (s, 9H), 1.77 (quin, *J* = 6.5 Hz, 2H), 3.34 (t, *J* = 7.0 Hz, 2H), 3.65 (t, *J* = 5.7 Hz, 2H), 3.87 - 3.94 (m, 2H), 4.61 (d, *J* = 5.5 Hz, 2H), 5.11 - 5.23 (m, 3H), 5.31 (d, *J* = 16.8 Hz, 1H), 5.81 (ddt, *J* = 16.7, 10.8, 5.6 Hz, 1H), 5.95 (ddt, *J* = 11.2, 11.2, 5.5 Hz, 1H).

Allyl 3-(tert-butyldimethylsilyloxy)propyl(methyl)carbamate (50)

48 (50.17 g, 183.5 mmol) was dissolved in THF (190 mL) and NaH (60% dispersion in mineral oil, 14.7 g, 368 mmol, 2.00 equiv) was added in several portions. When hydrogen evolution stops MeI (34 mL, 0.546 mol, 3.0 equiv) was added dropwise. The reaction mixture was heated under reflux. After 1 h TLC shows the disappearance of the starting material. The excess of NaH was quenched by careful dropwise addition of ethanol (~100 mL). The reaction mixture was poured into water (500 mL) and extracted with DCM (3x100 mL). Combined organic layers were dried over Na_2SO_4, filtered and evaporated. The residue was used without purification. M = 41.78 g. Yield = 79%.

^{1}H NMR ($CDCl_3$, 400 MHz): δ = 0.06 (s, 6 H), 0.91 (s, 9 H), 1.72 - 1.81 (m, 2 H), 2.94 (s, 3 H), 3.36 (t, *J*=7.2 Hz, 2 H), 3.65 (t, *J*=5.6 Hz, 2 H), 4.59 (d, *J*=5.5 Hz, 2 H), 5.20 (d, *J*=10.4 Hz, 1 H), 5.31 (dd, *J*=17.2, 1.5 Hz, 1 H), 5.88 - 6.01 (m, 1 H).

allyl allyl(3-hydroxypropyl)carbamate (51)

To a solution of **49** (70.7 g, 226 mmol) in MeOH (230 mL) was added KF*2H_2O (63.7 g, 0.677 mol, 3 equiv) and the resulting solution was heated under reflux for 24 h. When TLC showed the disappearance of the starting material, the reaction mixture was cooled to rt, diluted with water (0.5 L) and extracted with DCM (3x100 mL). Combined organic layers were dried over Na_2SO_4, filtered and evaporated. The residue contains the title compound along with a large amount of unknown TBS-containing admixture, but it was used in the next step without purification.

M = 37.75 g. Yield = 84%.

^{1}H NMR ($CDCl_3$, 400 MHz): δ = 1.66 - 1.74 (m, 1H), 3.43 (t, *J* = 5.1 Hz, 1H), 3.58 (t, *J* = 4.9 Hz, 1H), 3.85 (d, *J* = 4.1 Hz, 1H), 4.61 (d, *J* = 5.5 Hz, 1H), 5.16 (d, *J* = 11.3 Hz, 1H), 5.22 (d, *J* = 10.6 Hz, 1H), 5.30 (d, *J* = 17.2 Hz, 1H), 5.79 (ddt, *J* = 15.7, 10.8, 5.7 Hz, 1H), 5.93 (ddt, *J* = 15.4, 9.8, 4.7 Hz, 1H).

allyl (3-hydroxypropyl)(methyl)carbamate (52)

To a solution of **50** (41.78 g, 145.3 mmol) in MeOH (150 mL) was added KF*2H_2O (41.0 g, 0.436 mol, 3 equiv) and the resulting solution was heated under reflux for 24 h. When TLC showed the disappearance of the starting material, the reaction mixture was cooled to rt, diluted with water (0.5 L) and extracted with DCM (3x100 mL). The combined organic layers were dried over Na_2SO_4 and evaporated. The resulting product was subjected to a gradient chromatography purification (Hexanes/EtOAc 3:1, 1:1, pure EtOAc), leading to the title compound along with an admixture of unknown TBS-based compounds. This admixture was used in the next step without purification.

M = 17.1 g. Yield = 68%.

^{1}H NMR ($CDCl_3$, 400 MHz): δ = 1.65 - 1.80 (m, 2 H), 2.90 (s, 3 H), 3.08 (br. s, 1 H), 3.36 - 3.45 (m, 2 H), 3.51 - 3.66 (m, 2 H), 4.58 (d, *J*=5.5 Hz, 2 H), 5.21 (d, *J*=1.2 Hz, 1 H), 5.29 (dq, *J*=17.2, 1.5 Hz, 1 H), 5.84 - 5.99 (m, 1 H).

^{13}C NMR ($CDCl_3$, 100 MHz): δ = 29.8, 34.0, 45.2, 58.3, 66.3, 117.4, 133.0, 157.4.

allyl allyl(3-oxopropyl)carbamate (53)

A solution of oxalyl chloride (18 mL, 212 mmol, 1.5 equiv) in DCM (150 mL) was added dropwise at –70 to –80 °C, to 25 mL of DMSO. The reaction mixture was stirred for 10 min and a solution of **51** (28.5 g, 143 mmol) in DCM (150 mL), was added dropwise at the same temperature. After 15 min, Et_3N (99 mL, 0.71 mol, 5.0 equiv) was added, and after 5 min the reaction mixture was allowed to warm to ambient temperature (~1-2 h). The reaction mixture was quenched with water (500 mL), and the layers were separated. The organic layer was dried over Na_2SO_4, filtered, and evaporated to give pure enough compound as yellow oil (Mixture of rotamers). If necessary, the substance can be purified using chromatography (hexanes/EtOAc 10:1, 3:1).

M = 28.05 g. Yield = 99%.

^{1}H NMR ($CDCl_3$, 400 MHz): δ = 2.72 (t, *J* = 5.8 Hz, 2H), 3.55 (t, *J* = 6.7 Hz, 2H), 3.89 (d, *J* = 4.9 Hz, 2H), 4.57 (d, *J* = 4.3 Hz, 2H), 5.08 - 5.22 (m, 3H), 5.27 (d, *J* = 17.2 Hz, 1H), 5.70 - 5.82 (m, 1H), 5.90 (m, *J* = 10.9, 5.2, 5.2 Hz, 1H), 9.77 (s, 1H).

^{13}C NMR ($CDCl_3$, 100 MHz): δ = (40.2, 41.2), (43.1, 43.5), 50.3, 66.1, (116.9, 117.8), 117.4, 132.9, 133.6, 155.8, (200.5, 200.9).

allyl methyl(3-oxopropyl)carbamate (54)

A solution of oxalyl chloride (13 mL, 154 mmol, 1.5 equiv) in DCM (108 mL) was added dropwise at –70 to –80 °C to 18 mL of DMSO. The reaction mixture was stirred for 10 min and a solution of **52** (17.1 g, 98.8 mmol) in DCM (108 mL), was added dropwise at the same temperature. After 15 min, Et_3N (69 mL, 0.495 mol, 5.0 equiv) was added, and after 5 min the reaction mixture was allowed to warm to ambient temperature (~1-2 h). The reaction mixture was quenched with water (500 mL), and the layers were separated. The organic layer was dried over Na_2SO_4, filtered and evaporated to give pure enough compound as yellow oil (Mixture of rotamers). M = 15.35 g. Yield = 91%.

^{1}H NMR ($CDCl_3$, 400 MHz): δ = 2.69 (t, *J*=6.5 Hz, 2 H), 2.91 (s, 3 H), 3.57 (t, *J*=6.6 Hz, 2 H), 4.54 (d, *J*=3.9 Hz, 2 H), 5.17 (d, *J*=10.4 Hz, 1 H), 5.26 (dd, *J*=17.2, 1.5 Hz, 1 H), 5.83 - 5.95 (m, 1 H), 9.78 (s, 1 H).

^{13}C NMR ($CDCl_3$, 100 MHz): δ = 42.5, (42.8, 43.2), 45.8, 66.1, (117.3, 117.6), 132.9, 156.5, (200.5, 200.9).

(*E*)-allyl allyl(3-((*tert*-butyl sulfinyl)imino)propyl)carbamate (55)

To a solution of aldehyde **53** (7.30 g, 37.0 mmol) in DCM (37 mL) was added (*S*)-*N*-*tert*-butyl sulfinyl amide (4.71 g, 38.9 mmol, 1.05 equiv), PPTS (0.46 g, 0.050 equiv) and $MgSO_4$ (22.2 g, 185 mmol, 5.00 equiv). To control the progress of the reaction, 0.5 mL of the DCM solution from the reaction mixture was evaporated and analyzed by NMR (once a day).The mixture was stirred at rt for 3-7 days; the inorganic material was filtered and washed several times with DCM. The

filtrate was concentrated in vacuo to give pure enough title compound as a clear oil. M = 10.98 g. Yield = 99% (not purified).

The reaction with (*R*)-*N*-*tert*-butyl sulfinyl amide was conducted in the same manner, but the product was purified by flash chromatography on silica using hexanes/EtOAc 1:1, 0:1 mixture as an eluent.

M = 12.30 g. Yield = 81%.

^{1}H NMR ($CDCl_3$, 400 MHz): δ = 1.19 (s, 9H), 2.73 - 2.85 (m, 2H), 3.58 (d, *J* = 12.7 Hz, 1H), 3.87 - 3.95 (m, 2H), 4.60 (d, *J* = 4.7 Hz, 2H), 5.12 - 5.23 (m, 3H), 5.29 (d, *J* = 17.2 Hz, 1H), 5.73 - 5.85 (m, 1H), 5.85 - 6.00 (m, 1H), 8.08 (t, *J* = 4.2 Hz, 1H).

^{13}C NMR ($CDCl_3$, 100 MHz): δ = 22.4 (3C), 24.8, 25.8, 28.2, (35.0, 35.5), (42.8, 43.6), 50.2, 56.7, 66.2, 117.0, (117.4, 117.6), 132.9, 133.6, 155.8, 167.0.

(*E*)-allyl (3-((tert-butyl sulfinyl)imino)propyl)(methyl)carbamate (56)

To a solution of aldehyde **54** (7.60 g, 44.4 mmol) in DCM (44 mL) was added commercially available (*S*)-*N*-*tert*-butyl sulfinyl amide (5.65 g, 46.6 mmol, 1.05 equiv), PPTS (0.56 g, 0.05 equiv) and $MgSO_4$ (26.6 g, 222 mmol, 5.00 equiv). To control the progress of the reaction, 0.5 mL of the DCM solution from the reaction mixture was evaporated and analyzed by NMR (once a day).The mixture was stirred at rt for 3-7 days; the inorganic material was filtered and washed several times with DCM. The filtrate was concentrated in vacuo to give pure enough title compound as a clear oil. M = 12.26 g. Yield = 100% (not purified).

The reaction with (*R*)-*N*-*tert*-butyl sulfinyl amide was conducted in the same manner.

M = 12.18 g. Yield = 100%.

^{1}H NMR ($CDCl_3$, 400 MHz): δ = 1.16 (s, 9 H), 2.71 - 2.81 (m, 2 H), 2.92 (s, 3 H), 3.58 (t, *J*=7.2 Hz, 2 H), 4.55 (d, *J*=5.1 Hz, 2 H), 5.17 (dd, *J*=10.5, 1.2 Hz, 1 H), 5.26 (dd, *J*=17.2, 1.4 Hz, 1 H), 5.85 - 5.96 (m, 1 H), 8.06 (t, *J*=4.2 Hz, 1 H).

^{13}C NMR ($CDCl_3$, 100 MHz): δ = 22.3 (3C), 24.7, 25.9, 28.2, (34.4, 34.9), (45.1, 45.6), 56.7, (66.1, 66.2), (117.3, 117.5), 133.0, 155.9 (br.), (166.8, 167.0).

allyl allyl(3-(5-(((*tert*-butyldimethylsilyl)oxy)methyl)-4-methylthiazol-2-yl)-3-(1,1-dimethylethylsulfinamido)propyl)carbamate (57)

Compound **57** was obtained following the general procedure for 1,2-addition from imine **55** and thiazole **36**.

*f*S-**57**: M = 9.90 g. Yield = 50%.

fR-**57**: M = 9.80 g. Yield = 44%.

^{1}H NMR ($CDCl_3$, 400 MHz): δ = 0.08 (s, 3H), 0.09 (s, 3H), 0.90 (s, 9H), 1.26 (br. s., 3H), 1.30 (d, *J* = 5.7 Hz, 6H), 2.09 - 2.58 (m, 6H), 3.11 - 3.37 (m, 1H), 3.55 - 3.97 (m, 3H), 4.36 - 4.70 (m, 3H), 4.74 (d, *J* = 6.7 Hz, 2H), 5.05 - 5.43 (m, 4H), 5.63 - 5.98 (m, 2H).

^{13}C NMR ($CDCl_3$, 100 MHz): δ = -5.2, 15.3, 18.4, 22.9, 25.9, 33.9, 42.4, 49.3, 56.6, 56.9, 57.9, 66.2, 117.0, 117.1, 133.0, 133.4, 147.3, 156.0. (Few signals are missing due to broadening).

allyl (3-(5-(((tert-butyldimethylsilyl)oxy)methyl)-4-methylthiazol-2-yl)-3-(1,1-dimethylethylsulfinamido)propyl)(methyl)carbamate (58)

Compound **58** was obtained following the general procedure for 1,2-addition from imine **56** and thiazole **36**.

*f*S-**58**: M = 10.09 g. Yield = 44%.

fR-**58**: M = 7.12 g. Yield = 31%.

^{1}H NMR ($CDCl_3$, 400 MHz): δ = 0.09 (s, 6 H), 0.91 (s, 9 H), 1.32 (s, 9 H), 2.30 (m, 3H), 2.18 - 2.38 (m, 1 H), 2.56 - 2.98 (m, 4 H), 3.06 - 3.93 (m, 3 H), 4.34 - 4.64 (m, 2 H), 4.64 - 4.81 (m, 2 H), 5.11 - 5.35 (m, 2 H), 5.45 (br. s, 1 H), 5.78 - 6.00 (m, 1H).

allyl allyl(3-amino-3-(5-(hydroxymethyl)-4-methylthiazol-2-yl)propyl)carbamate (59)

Compound **59** was obtained following the general procedure for amine deprotection from **57**.

*f*S-**59**: M = 5.20 g. Yield = 88%.

fR-**59**: M = 6.46 g. Yield = 100%.

^{1}H NMR ($CDCl_3$, 400 MHz): δ = 1.78 - 1.95 (m, 1H), 2.09 - 2.23 (m, 1H), 2.33 (s, 3H), 2.69 (br. s., 3H), 3.23 - 3.47 (m, 1H), 3.50 - 3.66 (m, 1H), 3.71 - 3.99 (m, 2H), 4.13 (dd, *J* = 8.0, 4.9 Hz, 1H), 4.57 (d, *J* = 4.5 Hz, 2H), 4.72 (s, 2H), 5.15 (s, 3H), 5.28 (d, *J* = 17.0 Hz, 1H), 5.76 (ddt, *J* = 16.0, 11.2, 5.7, Hz, 1H), 5.90 (ddt, *J* = 15.6, 10.1, 5.1, 5.1 Hz, 1H).

^{13}C NMR ($CDCl_3$, 100 MHz): δ = 15.0, 21.6, (36.5, 37.0), (43.2, 43.4), (49.3, 49.8), (51.8, 52.0), 56.5, 66.2, 117.4, (117.0, 117.7), 131.1, 132.9, 133.5, 148.7, (155.9, 156.4), 174.3.

allyl (3-amino-3-(5-(hydroxymethyl)-4-methylthiazol-2-yl)propyl)(methyl)carbamate (60)

Compound **60** was obtained following the general procedure for amine deprotection from **58**.

*f*S-**60**: M = 2.00 g. Yield = 34%.

fR-**60**: M = 1.95 g. Yield = 47%.

^{1}H NMR ($CDCl_3$, 400 MHz): δ = 1.74 - 1.93 (m, 1 H), 2.08 - 2.23 (m, 1 H), 2.31 (s, 3 H), 2.57 - 2.76 (m, 2 H), 2.88 (s, 3 H), 3.19 - 3.29 (m, 1 H), 3.30 - 3.50 (m, 1 H), 3.63 (dt, *J*=14.1, 7.2 Hz, 1

H), 4.10 (dd, *J*=8.7, 4.6 Hz, 1 H), 4.54 (d, *J*=5.3 Hz, 2 H), 4.69 (s, 2 H), 5.18 (dd, *J*=10.4, 1.3 Hz, 1 H), 5.27 (dd, *J*=17.2, 1.5 Hz, 1 H), 5.84 - 5.96 (ddt, *J*=17.1, 10.6, 5.4 Hz, 1 H).

^{13}C NMR ($CDCl_3$, 100 MHz): δ = 15.0, (34.0, 34.7), (36.0, 36.5), 45.7, (51.6, 51.9), 56.4, 66.2, (117.3, 117.7), 131.2, 133.0, 148.6, (156.1, 156.6), (174.2, 174.4).

_N_-(3-amino-1-(5-(hydroxymethyl)-4-methylthiazol-2-yl)propyl)-5-(4-chlorophenyl)-1H-pyrrole-2-carboxamide (61)

Compound **61** was obtained following the general procedure for amide coupling and then the general procedure for deprotection from amine **59** and acid **1**.

*f*S-**61A**: M = 580 mg. Yield = 44% (over two steps).

^{t}R = 1.249 min. Purity = 100%. LC–MS: m/z $[M+H]^+$ =405 Da.

*f*R-**61B**: M = 845 mg. Yield = 46% (over two steps).

^{t}R = 1.329 min. Purity = 100%. LC–MS: m/z $[M+H]^+$ =405 Da.

mp = 230-240 °C (decomp.; dihydrochloride).

^{1}H NMR (CD_3OD, 400 MHz): δ = 2.08 (s, 1H), 2.18 - 2.30 (m, 1H), 2.35 (s, 3H), 2.75 - 2.82 (m, 2H), 4.67 (s, 2H), 5.46 (dd, *J* = 9.6, 5.1 Hz, 1H), 6.57 (d, *J* = 3.9 Hz, 1H), 6.98 (d, *J* = 3.9 Hz, 1H), 7.37 (d, *J* = 8.4 Hz, 2H), 7.65 (d, *J* = 8.6 Hz, 2H). (Five exchangeable protons are missing)

^{13}C NMR (CD_3OD, 100 MHz): δ = 14.9, 39.0, 39.5, 50.8, 56.7, 108.9, 114.7, 127.4 (2C), 127.9, 130.1 (2C), 132.2, 133.4, 133.9, 136.6, 149.7, 163.3, 173.1.

HRMS (ESI): m/z calcd for $C_{19}H_{22}ClN_4O_2S$ $[M+H]^+$ 405.1147, found 405.1144.

_N_-(3-amino-1-(5-(hydroxymethyl)-4-methylthiazol-2-yl)propyl)-5-(4-chloro-3-fluorophenyl)-1H-pyrrole-2-carboxamide (62)

Compound **62** was obtained following the general procedure for amide coupling and then the general procedure for deprotection from amine **59** and acid **39**.

*f*S-**62A**: M = 820 mg. Yield = 61% (over two steps).

^{t}R= 1.325 min. Purity = 89%. LC–MS: m/z $[M+H]^+$ =423 Da.

*f*R-**62B**: M = 986 mg. Yield = 50% (over two steps).

^{t}R = 1.406 min. Purity = 100%. LC–MS: m/z $[M+H]^+$ =423 Da.

mp = 220-230 °C (decomp.; dihydrochloride).

^{1}H NMR (CD_3OD, 400 MHz): δ = 2.04 - 2.15 (m, 1H), 2.18 - 2.30 (m, 1H), 2.36 (s, 3H), 2.75 - 2.84 (m, 1H), 4.68 (s, 2H), 5.46 (dd, *J* = 9.8, 5.1 Hz, 1H), 6.63 (d, *J* = 3.9 Hz, 1H), 6.98 (d, *J* = 3.9 Hz, 1H), 7.43 - 7.51 (m, 1H), 7.59 (dd, *J* = 10.7, 1.9 Hz, 1H). (Five exchangeable protons are missing).

^{13}C NMR (CD_3OD, 100 MHz): δ = 14.9, 39.0, 39.5, 50.8, 56.7, 109.6, 113.8 (d, *J* = 22.7 Hz), 114.5, 120.0 (d, *J* = 18.3 Hz), 122.6 (d, *J* = 3.7 Hz), 128.4, 132.2, 133.4, 134.5 (d, *J* = 8.1 Hz), 135.4, 149.7, 159.8 (d, *J* = 246.6 Hz), 163.1, 173.1.

HRMS (ESI): m/z calcd for $C_{19}H_{21}ClFN_4O_2S$ $[M+H]^+$ 423.1052, found 423.1051.

_N_-(3-amino-1-(5-(hydroxymethyl)-4-methylthiazol-2-yl)propyl)-5-(3-fluoro-4-methylphenyl)-1H-pyrrole-2-carboxamide (63)

Compound **63** was obtained following the general procedure for amide coupling and then the general procedure for deprotection from amine **59** and acid **40**.

*f*S-**63A**: M = 880 mg. Yield = 69% (over two steps).

^{t}R = 1.279 min. Purity = 93%. LC–MS: m/z $[M+H]^+$ =403 Da.

*f*R-**63B**: M = 719 mg. Yield = 45% (over two steps).

^{t}R = 1.385 min. Purity = 100%. LC–MS: m/z $[M+H]^+$ =403 Da.

mp = 220-230 °C (decomp.; dihydrochloride).

^{1}H NMR (CD_3OD, 400 MHz): δ = 2.03 - 2.15 (m, 1H), 2.19 - 2.31 (m, 1H), 2.26 (s, 3H), 2.35 (s, 3H), 2.73 - 2.86 (m, 2H), 4.67 (s, 2H), 5.46 (dd, *J* = 9.8, 5.1 Hz, 1H), 6.55 (d, *J* = 3.9 Hz, 1H), 6.97 (d, *J* = 3.9 Hz, 1H), 7.23 (t, *J* = 8.1 Hz, 1H), 7.33 - 7.40 (m, 2H). (Five exchangeable protons are missing).

^{13}C NMR (CD_3OD, 100 MHz): δ = 14.4 (d, *J* = 3.7 Hz), 14.9, 38.9, 39.4, 50.8, 56.7, 108.7, 112.2 (d, *J* = 24.2 Hz), 114.7, 121.5 (d, *J* = 3.7 Hz), 124.7 (d, *J* = 17.6 Hz), 127.5, 133.1 (d, *J* = 5.1 Hz), 133.2 (d, *J* = 8.1 Hz), 133.5, 136.7, 149.7, 163.1 (d, *J* = 243.0 Hz), 163.3, 173.1.

HRMS (ESI): m/z calcd for $C_{20}H_{24}FN_4O_2S$ $[M+H]^+$ 403.1599, found 403.1597.

5-(4-chlorophenyl)-N-(1-(5-(hydroxymethyl)-4-methylthiazol-2-yl)-3-(methylamino)propyl)-1H-pyrrole-2-carboxamide (64)

Compound **64** was obtained following the general procedure for amide coupling and then the general procedure for deprotection from amine **60** and acid **1**.

*f*S-**64A**: M = 498 mg. Yield = 51% (over two steps).

^{t}R = 1.279 min. Purity = 100%. LC–MS: m/z $[M+H]^+$ =419 Da.

*f*R-**64B**: M = 644 mg. Yield = 65% (over two steps).

^{t}R = 1.407 min. Purity = 100%. LC–MS: m/z $[M+H]^+$ =419 Da.

mp = 215-220°C (decomp.; dihydrochloride).

^{1}H NMR ($CDCl_3$, 400 MHz): δ = 2.07 - 2.22 (m, 3 H), 2.27 (s, 3 H), 2.43 (s, 3 H), 2.70 - 2.82 (m, 2 H), 3.83 (br. s, 1 H), 4.66 (s, 2 H), 5.40 (t, *J*=5.0 Hz, 1 H), 6.45 (d, *J*=3.8 Hz, 1 H), 6.76 (d, *J*=3.8 Hz, 1 H), 7.23 (d, *J*=8.6 Hz, 2 H), 7.51 (d, *J*=8.6 Hz, 2 H), 9.26 (br. s., 1 H), 10.61 (br. s., 1 H).

^{13}C NMR ($CDCl_3$, 100 MHz): δ = 15.0, 32.9, 35.8, 48.1, 51.4, 56.3, 107.8, 112.6, 126.1 (2C), 126.8, 129.0 (2C), 130.4, 131.7, `132.9, 135.2, 149.1, 161.3, 171.0.

HRMS (ESI): m/z calcd for $C_{20}H_{24}ClN_4O_2S$ $[M+H]^+$ 419.1303, found 419.1299.

5-(4-chloro-3-fluorophenyl)-N-(1-(5-(hydroxymethyl)-4-methylthiazol-2-yl)-3-(methylamino)propyl)-1H-pyrrole-2-carboxamide (65)

Compound **65** was obtained following the general procedure for amide coupling and then the general procedure for deprotection from amine **60** and acid **39**.

*f*S-**65A**: M = 508 mg. Yield = 51% (over two steps).

^{t}R = 1.293 min. Purity = 92%. LC–MS: m/z $[M+H]^+$ =437 Da.

*f*R-**65B**: M = 596 mg. Yield = 59% (over two steps).

^{t}R = 1.462 min. Purity = 94%. LC–MS: m/z $[M+H]^+$ =437 Da.

mp = 215-220°C (decomp.; dihydrochloride).

^{1}H NMR ($CDCl_3$, 400 MHz): δ = 2.08 - 2.21 (m, 2 H), 2.25 (s, 3 H), 2.46 (s, 3 H), 2.72 - 2.84 (m, 2 H), 3.76 (br. s., 2 H), 4.66 (s, 2 H), 5.38 (t, *J*=5.3 Hz, 1 H), 6.47 (d, *J*=3.9 Hz, 1 H), 6.75 (d, *J*=3.9 Hz, 1 H), 7.24 - 7.29 (m, 1 H), 7.30 - 7.34 (m, 1 H), 7.40 (dd, *J*=10.3, 1.8 Hz, 1 H), 9.36 (br. s., 1 H), 10.79 (br. s., 1 H).

^{13}C NMR ($CDCl_3$, 100 MHz): δ = 15.0, 32.6, 35.6, 48.0, 51.5, 56.3, 108.5, 112.7, 112.9 (d, *J* = 17.6 Hz), 119.3 (d, *J* = 19.0 Hz), 121.2 (d, *J* = 2.9 Hz), 127.2, 131.0, 131.6, 132.4 (d, *J* = 7.3 Hz), 134.1, 149.1, 158.4 (d, *J* = 247.4 Hz), 161.3, 170.8.

HRMS (ESI): m/z calcd for $C_{20}H_{23}ClFN_4O_2S$ $[M+H]^+$ 437.1209, found 437.1205.

5-(3-fluoro-4-methylphenyl)-N-(1-(5-(hydroxymethyl)-4-methylthiazol-2-yl)-3-(methylamino)propyl)-1H-pyrrole-2-carboxamide (66)

Compound **66** was obtained following the general procedure for amide coupling and then the general procedure for deprotection from amine **60** and acid **40**.

*f*S-**66A**: M = 424 mg. Yield = 47% (over two steps).

^{t}R = 1.265 min. Purity = 97%. LC–MS: m/z $[M+H]^+$ =417 Da.

*f*R-**66B**: M = 528 mg. Yield = 54% (over two steps).

^{t}R = 1.383 min. Purity = 98%. LC–MS: m/z $[M+H]^+$ =417 Da.

mp = 210-220°C (decomp.; dihydrochloride).

^{1}H NMR ($CDCl_3$, 400 MHz): δ = 2.04 - 2.19 (m, 2 H), 2.25 (s, 6 H), 2.42 (s, 3 H), 2.73 (t, *J*=5.5 Hz, 2 H), 3.68 (br. s., 2 H), 4.65 (s, 2 H), 5.34 - 5.43 (m, 1 H), 6.44 (d, *J*=3.8 Hz, 1 H), 6.75 (d, *J*=3.7 Hz, 1 H), 7.11 (t, *J*=7.9 Hz, 1 H), 7.20 - 7.27 (m, 2 H), 9.25 (br. s., 1 H), 10.55 (br. s., 1 H).

^{13}C NMR ($CDCl_3$, 100 MHz): δ = 14.5 (d, *J* = 2.9 Hz), 15.0, 32.7, 35.4, 48.0, 51.3, 56.4, 107.7, 111.4 (d, *J* = 23.4 Hz), 112.9, 120.2 (d, *J* = 2.9 Hz), 123.9 (d, *J* = 17.6 Hz), 126.4, 131.3 (d, *J* = 7.3 Hz), 131.7, 132.0 (d, *J* = 5.9 Hz), 135.2, 149.1. 161.3, 161.7 (d, *J* = 244.4 Hz), 170.8.

HRMS (ESI): m/z calcd for $C_{21}H_{26}FN_4O_2S$ $[M+H]^+$ 417.1755, found 417.1749.

5-(4-chlorophenyl)-N-(3-(dimethylamino)-1-(5-(hydroxymethyl)-4-methylthiazol-2-yl)propyl)-1H-pyrrole-2-carboxamide (67)

Compound **67** was obtained following the general procedure for reductive amination from **61**.

*f*S-**67A**: M = 236 mg. Yield = 90%.

^{t}R = 1.313 min. Purity = 100%. LC–MS: m/z $[M+H]^+$ =433 Da.

*f*R-**67B**: M = 338 mg. Yield = 84%.

^{t}R = 1.313 min. Purity = 97%. LC–MS: m/z $[M+H]^+$ =433 Da.

^{1}H NMR ($CDCl_3$, 400 MHz): δ = 2.07 - 2.18 (m, 1H), 2.18 - 2.28 (m, 2H), 2.33 (s 6H), 2.34 (s, 3H), 2.29 - 2.43 (m, 1H), 2.55 - 2.64 (m, 1H), 3.68 (br. s, 1H), 4.71 (s, 2H), 5.43 (q, *J* = 5.2 Hz, 1H), 6.49 (d, *J* = 3.5 Hz, 1H), 6.66 (d, *J* = 3.5 Hz, 1H), 7.24 (d, *J* = 8.4 Hz, 1H), 7.52 (d, *J* = 8.4 Hz, 2H), 9.69 (d, *J* = 6.3 Hz, 1H), 10.59 (br. s, 1H).

For dihydrochloride:

mp = 150-155 °C.

^{1}H NMR: (DMSO-d_6, 400 MHz) δ = 2.27 (s, 3 H), 2.38 - 2.53 (m, 2 H), 2.75 (s, 3 H), 2.77 (s, 3 H), 3.16 - 3.32 (m, 2 H), 4.54 (s, 2 H), 5.28 - 5.36 (m, 1 H), 6.46 (br. s., 2 H), 6.64 (t, *J* = 2.7 Hz, 1 H), 6.96 (t, *J* = 2.6 Hz, 1 H), 7.40 (d, *J*=8.3 Hz, 1 H), 7.92 (d, *J*=8.3 Hz, 2 H), 9.36 (d, *J* = 8.0 Hz, 1 H), 10.68 (br. s., 1 H), 12.27 (s, 1 H).

^{13}C NMR (DMSO-d_6, 100 MHz): δ = 14.6, 28.2, 41.8, 42.5, 48.8, 54.1, 55.0, 107.5, 114.1, 126.4 (2C), 127.2, 128.6, 130.6, 131.1, 133.6, 133.9, 146.1, 160.0, 169.9.

HRMS (ESI): m/z calcd for $C_{21}H_{26}ClN_4O_2S$ $[M+H]^+$ 433.1460, found 433.1455.

5-(4-chloro-3-fluorophenyl)-N-(3-(dimethylamino)-1-(5-(hydroxymethyl)-4-methylthiazol-2-yl)propyl)-1H-pyrrole-2-carboxamide (68)

Compound **68** was obtained following the general procedure for reductive amination from **62**.

*f*S-**68A**: M = 190 mg. Yield = 59%.

^{t}R = 1.396 min. Purity = 96%. LC–MS: m/z $[M+H]^+$ =451 Da.

*f*R-**68B**: M = 418 mg. Yield = 82%.

^{t}R = 1.435 min. Purity = 96%. LC–MS: m/z $[M+H]^+$ =451 Da.

^{1}H NMR ($CDCl_3$, 400 MHz): δ = 2.12 - 2.23 (m, 1H), 2.31 (s, 3H), 2.24 - 2.36 (m, 1H), 2.40 (s, 6H), 2.46 - 2.57 (m, 1H), 2.62 - 2.73 (m, 1H), 3.68 (br. s, 1H), 4.70 (s, 2H), 5.41 (q, *J* = 4.9 Hz, 1H), 6.51 (d, *J* = 3.1 Hz, 1H), 6.69 (d, *J* = 2.9 Hz, 1H), 7.30 - 7.38 (m, 2H), 7.42 (d, *J* = 10.4 Hz, 1H), 9.66 - 9.79 (br. s, 1H), 10.63 - 10.82 (br. s, 1H).

For dihydrochloride:

mp = 160-165 °C.

^{1}H NMR: (DMSO-d_6, 400 MHz) δ = 2.27 (s, 3 H), 2.41 - 2.48 (m, 2 H), 2.76 (s, 3 H), 2.77 (s, 3 H), 3.16 - 3.32 (m, 2 H), 4.54 (s, 2 H), 5.27 -5.37 (m, 1 H), 6.39 (br. s, 2 H), 6.74 (s, 1 H), 6.97 (s, 1 H), 7.54 (t, *J*=8.2 Hz, 1 H), 7.76 (d, *J*=8.4 Hz, 1 H), 8.04 (d, *J*=11.4 Hz, 1 H), 9.41 (d, *J*=7.9 Hz, 1 H), 10.69 (br. s, 1 H), 12.40 (s, 1 H).

^{13}C NMR (DMSO-d_6, 100 MHz): δ = 14.5, 28.2, 41.8, 42.5, 48.8, 54.0, 55.0, 108.5, 112.7 (d, *J* = 22.7 Hz), 114.1, 117.1 (d, *J* = 17.6 Hz), 121.8 (d, *J* = 3.7 Hz), 127.7, 130.8, 132.85, 132.93, 133.6, 146.0, 157.5 (d, *J* = 244.4 Hz), 159.9, 169.9.

HRMS (ESI): m/z calcd for $C_{21}H_{25}ClFN_4O_2S$ $[M+H]^+$ 451.1365, found 451.1363.

N-(3-(dimethylamino)-1-(5-(hydroxymethyl)-4-methylthiazol-2-yl)propyl)-5-(3-fluoro-4-methylphenyl)-1H-pyrrole-2-carboxamide (69)

Compound **69** was obtained following the general procedure for reductive amination from **63**.

*f*S-**69A**: M = 203 mg. Yield = 66%.

^{t}R = 1.332 min. Purity = 94%. LC–MS: m/z $[M+H]^+$ =431 Da.

*f*R-**69B**: M = 201 mg. Yield = 89%.

^{t}R = 1.417 min. Purity = 95%. LC–MS: m/z $[M+H]^+$ =431 Da.

^{1}H NMR ($CDCl_3$, 400 MHz): δ = 2.07 - 2.19 (m, 1H), 2.28 (s, 3H), 2.20 -2.30 (m, 1H), 2.32 (s, 3H), 2.34 (s, 6H), 2.30 - 2.42 (m, 1H), 2.54 - 2.66 (m, 1H), 3.10 - 3.52 (m, 1H), 4.71 (s, 2H), 5.44 (q, *J* = 5.1 Hz, 1H), 6.48 (t, *J* = 2.5 Hz, 1H), 6.61 - 6.65 (m, 1H), 7.15 (t, *J* = 7.9 Hz, 1H), 7.24 (s, 2H), 9.65 -9.75 (br. s., 1H), 10.08 - 10.32 (br. s, 1H).

For dihydrochloride:

mp = 165-170 °C.

^{1}H NMR: (DMSO-d_6, 400 MHz) δ = 2.21 (s, 3 H), 2.28 (s, 3 H), 2.42 - 2.51 (m, 2 H), 2.76 (s, 3 H), 2.77 (s, 3 H), 3.17 - 3.34 (m, 2 H), 4.54 (s, 2 H), 5.29 - 5.37 (m, 1 H), 6.55 - 6.62 (m, 2 H), 6.63 (s, 1 H), 6.94 (s, 1 H), 7.24 (t, *J*=8.2 Hz, 1 H), 7.62 (d, *J*=7.9 Hz, 1 H), 7.74 (d, *J*=11.6 Hz, 1 H), 9.39 (d, *J*=7.8 Hz, 1 H), 10.71 (br. s, 1 H), 12.24 (s, 1 H).

^{13}C NMR (DMSO-d_6, 100 MHz): δ = 13.9 (d, *J* = 2.9 Hz), 14.4, 28.2, 41.8, 42.5, 48.8, 54.0, 55.0, 107.4, 111.0 (d, *J* = 23.4 Hz), 114.1, 120.5, 122.4 (d, *J* = 16.8 Hz), 126.9, 131.6 (d, *J* = 8.8 Hz), 131.8 (d, *J* = 5.1 Hz), 133.8, 134.1 (d, *J* = 2.2 Hz), 145.8, 160.0, 161.0 (d, *J* = 242.2 Hz), 170.2.

HRMS (ESI): m/z calcd for $C_{22}H_{28}FN_4O_2S$ $[M+H]^+$ 431.1912, found 431.1910.

ethyl 2-chloro-3-oxopropanoate (70)

NaO*t*Bu (106 g, 1.1 mol, 1.1 eqiuv) was dissolved in THF (2L) and the solution was cooled to 0 °C. At this temperature with a vigorous mechanical stirring, a mixture of ethyl chloroacetate (108 mL, 1.0 mol) and ethyl formate (104 mL, 1.3 moles, 1.3 equiv) was added dropwise. The mixture was left overnight, and aqueous HCl (100 mL +400 mL H_2O) was added. The resulting solution was extracted with DCM (3x200 mL). The combined organic layers were dried over Na_2SO_4, filtered and evaporated. The residue was distilled at reduced pressure (bp = 60 - 90 °C, 30 torr) to give a viscous oil which crystallizes upon standing. M = 71.28 g, yield = 47%.

^{1}H NMR: (DMSO-d_6, 400 MHz) δ = 1.20 (td, *J*=7.1, 0.6 Hz, 3 H), 4.13 (q, *J*=7.1 Hz, 2 H), 7.93 (s, 1 H), 11.75 (br. s., 1 H).

^{13}C NMR ($CDCl_3$, 100 MHz): δ = 14.2, 60.7, 100.4, 154.1, 163.5.

ethyl thiazole-5-carboxylate (71)

To a solution of formamide (19.2 mL, 0.483 mol, 1.5 equiv) in 1,4-dioxane (130 mL), P_2S_5 (21.50 g, 96.7 mmol, 0.3 equiv) was added in small portions in the course of 0.5 h under vigorous stirring. The reaction mixture was stirred for 0.5 h, and melted **70** (48.6 g, 0.323 mol) was added in several portions. The reaction mixture was heated at ~60 °C for 8 h, poured into water (300 mL), and extracted with DCM (3x100 mL). The combined organic phases were washed with 5% K_2CO_3, dried over anhydrous Na_2SO_4, filtered, evaporated and purified using column chromatography (eluent hexane/EtOAc, 20:1, 10:1). M = 45.01 g (total mass from two identical batches). Yield = 44%. The reaction can be scaled up to 30 ml of formamide. When larger quantities were used, the reaction mixture could not be stirred even on a mechanical stirrer.

^{1}H NMR ($CDCl_3$, 400 MHz): δ = 1.38 (t, *J*=7.2 Hz, 3 H), 4.38 (q, *J*=7.1 Hz, 2 H), 8.49 (s, 1 H), 8.93 (s, 1 H).

^{13}C NMR ($CDCl_3$, 100 MHz): δ = 14.3, 61.8, 103.1, 148.7, 158.0, 161.2.

thiazol-5-ylmethanol (72)

A solution of **71** (45.01 g, 0.287 mol) in THF (280 mL) was added dropwise to a suspension of $LiAlH_4$ (10.90 g, 0.287 mmol) in THF (280 mL) at 0 °C. The reaction mixture was stirred for 30 min at 0 °C (at this point TLC indicated consumption of the SM). It was then quenched by successive addition of EtOAc (50 mL), water (11 mL), 10% NaOH (11 mL) solution, and water

(33 mL) (the temperature should not exceed 0 °C). The precipitate was filtered and washed several times with THF. The filtrate was evaporated to give **72** which was used without purification. M = 29.67 g. Yield = 90%.

^{1}H NMR ($CDCl_3$, 400 MHz): δ = 3.51 (br. s, 1 H), 4.88 (s, 2 H), 7.71 (s, 1 H), 8.73 (s, 1 H).

^{13}C NMR ($CDCl_3$, 100 MHz): δ = 57.0, 139.4, 140.6, 153.6.

5-(((tert-butyldimethylsilyl)oxy)methyl)thiazole (73)

Alcohol **72** (29.67 g, 0.258 mol) was dissolved in DMF (250 mL), and imidazole (26.3 g, 0.387 mol, 1.5 equiv) was added in one portion, followed by portion wise addition of TBSCl (58.4 g, 0.388 mol, 1.5 equiv). The reaction mixture was stirred overnight at 50–60 °C, cooled to rt, diluted with water (0.5 L), and extracted with hexane (3x100 mL). The combined organic phases were dried over anhydrous Na_2SO_4, filtered and evaporated to give an oil, which was purified by distillation at reduced pressure (bp = 80 -120 °C, 2 torr). M = 45.14 g, yield = 76%.

^{1}H NMR ($CDCl_3$, 400 MHz): δ = 0.12 (s, 6 H), 0.93 (s, 9 H), 4.94 (d, *J*=0.7 Hz, 2 H), 7.74 (s, 1 H), 8.78 (s, 1 H).

^{13}C NMR ($CDCl_3$, 100 MHz): δ = -5.2 (2C), 18.4, 25.9 (3C), 58.3, 139.5, 140.0, 153.0.

allyl allyl(2-(5-(((tert-butyldimethylsilyl)oxy)methyl)thiazol-2-yl)-2-(1,1-dimethylethylsulfinamido)ethyl)carbamate (75)

Compound **75** was obtained following the general procedure for 1,2-addition from imine **74**[14] and thiazole **73**.

*f*S-**75**: M = 6.10 g. Yield = 66%.

*f*R-**75**: M = 9.54 g. Yield = 79%.

^{1}H NMR ($CDCl_3$, 400 MHz): δ = 0.05 - 0.16 (m, 6 H), 0.86 - 0.95 (m, 9 H), 1.29 (s, 9 H), 3.59 (dd, *J*=14.7, 2.5 Hz, 1 H), 3.85 (dd, *J*=15.8, 5.6 Hz, 1 H), 3.93 - 4.06 (m, 2 H), 4.57 - 4.70 (m, 2 H), 4.86 (s, 2 H), 4.93 - 4.99 (m, 1 H), 5.12 - 5.26 (m, 3 H), 5.32 (d, *J*=17.2 Hz, 1 H), 5.61 (d, *J*=2.7 Hz, 1 H), 5.83 (dddd, *J*=16.6, 10.9, 5.6, 5.4 Hz, 1 H), 5.87 - 6.00 (m, 1 H), 7.55 (s, 1 H).

allyl (2-(5-(((tert-butyldimethylsilyl)oxy)methyl)thiazol-2-yl)-2-(1,1-dimethylethylsulfinamido)ethyl)(methyl)carbamate (76)

Compound **76** was obtained following the general procedure for 1,2-addition from imine **35** and thiazole **73**.

*f*S-**76**: M = 6.88 g. Yield = 58%.

*f*R-**76**: M = 6.14 g. Yield = 53%.

^{1}H NMR ($CDCl_3$, 400 MHz): δ = 0.09 (s, 6 H), 0.90 (s, 9 H), 1.27 (s, 9 H), 2.97 (s, 3 H), 4.03 (dd, *J*=14.5, 9.8 Hz, 1 H), 4.53 - 4.67 (m, 2 H), 4.84 (s, 2 H), 4.89 - 4.97 (m, 1 H), 5.20 (d, *J*=10.4 Hz, 1 H), 5.31 (dd, *J*=17.2, 1.5 Hz, 1 H), 5.41 (d, *J*=2.8 Hz, 1 H), 5.86 - 6.00 (m, 1 H), 7.54 (s, 1 H). (NH proton is missed)

allyl allyl(2-amino-2-(5-(hydroxymethyl)thiazol-2-yl)ethyl)carbamate (77)

Compound **77** was obtained following the general procedure for amine deprotection from **75**.

*f*S-**77**: M = 2.44 g. Yield = 69%.

*f*R-**77**: M = 4.04 g. Yield = 73%.

^{1}H NMR ($CDCl_3$, 400 MHz): δ = 2.86 (br. s, 3 H), 3.50 - 3.72 (m, 2 H), 3.75 - 3.83 (m, 1 H), 3.84 - 3.97 (m, 1 H), 4.44 (t, *J*=6.6 Hz, 1 H), 4.58 (d, *J*=5.3 Hz, 2 H), 4.78 (s, 2 H), 5.07 - 5.18 (m, 2 H),

5.20 (dq, *J*=10.5, 1.3 Hz, 1 H), 5.29 (dq, *J*=17.2, 1.5 Hz, 1 H), 5.68 - 5.82 (ddt, *J*=16.4, 10.7, 5.3, 5.3 Hz, 1 H), 5.84 - 5.97 (ddt, *J*=17.2, 10.7, 5.4, 5.4 Hz, 1 H), 7.51 (s, 1 H).

^{13}C NMR ($CDCl_3$, 100 MHz): δ = (50.6, 50.7), 53.3, 54.0, 57.0, 66.5, (117.1, 118.0), 117.5, 132.7, 133.1, 139.4, 139.9, (156.1, 156.9), (174.4, 174.9).

allyl (2-amino-2-(5-(hydroxymethyl)thiazol-2-yl)ethyl)(methyl)carbamate (78)

Compound **78** was obtained following the general procedure for amine deprotection from **76**.

*f*S-**78**: M = 2.21 g. Yield = 58%.

*f*R-**78**: M = 2.69 g. Yield = 79%.

^{1}H NMR ($CDCl_3$, 400 MHz): δ = 2.20 - 3.18 (br. s, 3H), 2.85 (s, 3 H), 3.43 - 3.70 (m, 2 H), 4.34 - 4.42 (m, 1 H), 4.52 (s, 2 H), 4.74 (s, 2 H), 5.17 (d, *J*=10.4 Hz, 1 H), 5.25 (d, *J*=17.0 Hz, 1 H), 5.79 - 5.95 (m, 1 H), 7.46 (s, 1 H).

^{13}C NMR ($CDCl_3$, 100 MHz): δ = (35.3, 35.8), 52.9, (55.7, 56.1), 57.1, 66.3, (117.5, 117.9), 132.8, 139.4, 140.0, (156.3, 157.1), (174.6, 175.2).

N-(2-amino-1-(5-(hydroxymethyl)thiazol-2-yl)ethyl)-5-(4-chlorophenyl)-1H-pyrrole-2-carboxamide (81)

Compound **81** was obtained following the general procedure for amide coupling and then the general procedure for deprotection from amine **77** and acid **1**.

*f*S-**81A**: M = 252 mg. Yield = 40% (over two steps).

^{t}R = 1.234 min. Purity = 97%. LC–MS: m/z $[M+H]^+$ =377 Da.

*f*R-**81B**: M = 364 mg. Yield = 43% (over two steps).

^{t}R = 1.184 min. Purity = 97%. LC–MS: m/z $[M+H]^+$ =377 Da.

mp = 200-205 °C.

^{1}H NMR: (DMSO-d_6, 400 MHz) δ = 1.71 (br. s, 2 H), 3.01 (dd, *J*=13.2, 7.8 Hz, 1 H), 3.14 (dd, *J*=13.2, 5.2 Hz, 1 H), 4.61 (s, 2 H), 5.20 (dd, *J*=13.0, 7.6 Hz,1 H), 5.48 (br. s., 1 H), 6.65 (d, *J*=3.8 Hz, 1 H), 7.01 (d, *J*=3.8 Hz, 1 H), 7.43 (d, *J*=8.6 Hz, 2 H), 7.55 (s, 1 H), 7.84 (d, *J*=8.6 Hz, 2 H), 8.55 (d, *J*=7.9 Hz, 1 H), 11.74 (br. s, 1 H).

^{13}C NMR (DMSO-d_6, 100 MHz): δ = 45.6, 54.4, 55.8, 107.6, 113.0, 126.4 (2), 127.5, 128.6 (2C), 130.7, 131.1, 133.7, 139.0, 140.0, 160.4, 172.0.

HRMS (ESI): m/z calcd for $C_{17}H_{18}ClN_4O_2S$ $[M+H]^+$ 377.0834, found 377.0827.

N-(2-amino-1-(5-(hydroxymethyl)thiazol-2-yl)ethyl)-5-(4-chloro-3-fluorophenyl)-1H-pyrrole-2-carboxamide (82)

Compound **82** was obtained following the general procedure for amide coupling and then the general procedure for deprotection from amine **77** and acid **39**.

*f*S-**82A**: M = 474 mg. Yield = 51% (over two steps).

^{t}R = 1.229 min. Purity = 96%. LC–MS: m/z $[M+H]^+$ =395 Da.

*f*R-**82B**: M = 396 mg. Yield = 33% (over two steps).

^{t}R = 1.199 min. Purity = 97%. LC–MS: m/z $[M+H]^+$ =395 Da.

mp = 145-150 °C.

^{1}H NMR: (DMSO-d_6, 400 MHz) δ = 1.81 (br. s., 2 H), 3.01 (dd, *J*=13.1, 7.9 Hz, 1 H), 3.14 (dd, *J*=13.1, 5.3 Hz, 1 H), 4.61 (s, 2 H), 5.20 (dd, *J*= 13.1, 7.3 Hz, 1 H), 5.47 (br. s., 1 H), 6.75 (d, *J*=3.9 Hz, 1 H), 7.02 (d, *J*=3.8 Hz, 1 H), 7.52 - 7.61 (m, 2 H), 7.69 (dd, *J*=8.4, 1.7 Hz, 1 H), 7.94 (dd, *J*=11.4, 1.8 Hz, 1 H), 8.58 (d, *J*=7.7 Hz, 1 H), 11.87 (br. s., 1 H).

^{13}C NMR (DMSO-d_6, 100 MHz): δ = 45.6, 54.4, 55.7, 108.6, 112.6 (d, *J*= 22.7 Hz), 112.8, 117.0 (d, *J*= 17.6 Hz), 121.8 (d, *J*= 2.9 Hz), 128.0, 130.8, 132.6 (d, *J*= 2.2 Hz), 132.9 (d, *J*= 8.1 Hz), 139.0, 140.0, 157.5 (d, *J*= 244.4 Hz), 160.4, 171.9.

HRMS (ESI): m/z calcd for $C_{17}H_{17}ClFN_4O_2S$ $[M+H]^+$ 395.0739, found 395.0737.

N-(2-amino-1-(5-(hydroxymethyl)thiazol-2-yl)ethyl)-5-(3-fluoro-4-methylphenyl)-1H-pyrrole-2-carboxamide (83)

Compound **83** was obtained following the general procedure for amide coupling and then the general procedure for deprotection from amine **77** and acid **40**.

*f*S-**83A**: M = 383 mg. Yield = 50% (over two steps).

^{t}R = 1.201 min. Purity = 97%. LC–MS: m/z $[M+H]^+$ =375 Da.

*f*R-**83B**: M = 304 mg. Yield = 40% (over two steps).

^{t}R = 1.224 min. Purity = 100%. LC–MS: m/z $[M+H]^+$ =375 Da.

mp = 160-170 °C.

^{1}H NMR: (DMSO-d_6, 400 MHz) δ = 1.77 (br. s., 2 H), 2.23 (s, 3 H), 3.01 (dd, *J*=13.0, 8.0 Hz, 1 H), 3.14 (dd, *J*=13.4, 5.1 Hz, 1 H), 4.61 (s, 2 H), 5.20 (dd, *J*=13.0, 7.6 Hz, 1 H), 5.48 (br. s., 1 H), 6.65 (d, *J*=3.8 Hz, 1 H), 6.99 (d, *J*=3.8 Hz, 1 H), 7.27 (t, *J*=8.1 Hz, 1 H), 7.52 - 7.58 (m, 2 H), 7.66 (d, *J*=11.4 Hz, 1 H), 8.53 (d, *J*=7.9 Hz, 1 H), 11.75 (br. s., 1 H).

^{13}C NMR (DMSO-d_6, 100 MHz): δ = 13.9 (d, *J*= 2.9 Hz), 45.6, 54.4, 55.8, 107.4, 111.1 (d, *J*= 24.2 Hz), 112.9, 120.4 (d, *J*= 2.2 Hz), 122.3 (d, *J*= 17.6 Hz), 127.2, 131.6 (d, *J*= 8.1 Hz), 131.8 (d, *J*= 5.1 Hz), 133.9, 139.0, 140.0, 160.4, 161.0 (d, *J*= 241.5 Hz), 172.0.

HRMS (ESI): m/z calcd for $C_{18}H_{20}FN_4O_2S$ $[M+H]^+$ 375.1286, found 375.1285.

N-(2-amino-1-(5-(hydroxymethyl)thiazol-2-yl)ethyl)-5-(4-chloro-3,5-difluorophenyl)-1H-pyrrole-2-carboxamide (84)

Compound **84** was obtained following the general procedure for amide coupling and then the general procedure for deprotection from amine **77** and acid **79**.

*f*S-**84A**: M = 30 mg (after pHPLC). Yield = ~3% (over two steps).

^{t}R = 1.360 min. Purity = 90%. LC–MS: m/z $[M+H]^+$ =413 Da.

*f*R-**84B**: M = 724 mg. Yield = 28% (over two steps).

^{t}R = 1.355 min. Purity = 98%. LC–MS: m/z $[M+H]^+$ =413 Da.

mp = 165-170 °C.

^{1}H NMR: (DMSO-d_6, 400 MHz) δ = 1.76 (br. s., 2 H), 2.99 (dd, *J*=13.1, 7.8 Hz, 1 H), 3.13 (dd, *J*=13.3, 5.2 Hz, 1 H), 4.59 (s, 2 H), 5.18 (dd, *J*= 13.3, 7.2 Hz, 1 H), 5.46 (br. s., 1 H), 6.84 (d, *J*=3.8 Hz, 1 H), 7.02 (d, *J*=3.9 Hz, 1 H), 7.53 (s, 1 H), 7.85 (d, *J*=9.3 Hz, 2 H), 8.61 (d, *J*=7.7 Hz, 1 H), 12.04 (br. s., 1 H).

^{13}C NMR (DMSO-d_6, 100 MHz): δ = 45.5, 54.5, 55.7, 105.3, (t, *J* = 21.2 Hz), 108.3 (d, *J* = 25.6 Hz, 2C), 109.5, 112.7, 128.5, 131.8 (t, *J* = 2.6 Hz), 132.8 (t, *J* = 10.2 Hz), 139.0, 140.1, 158.3 (dd, *J* = 245.9, 4.4 Hz, 2C), 160.3. 171.8.

HRMS (ESI): m/z calcd for $C_{17}H_{16}ClF_2N_4O_2S$ $[M+H]^+$ 413.0645, found 413.0645.

N-(2-amino-1-(5-(hydroxymethyl)thiazol-2-yl)ethyl)-5-(3,4-dimethoxyphenyl)-1H-pyrrole-2-carboxamide (85)

Compound **85** was obtained following the general procedure for amide coupling and then the general procedure for deprotection from amine **77** and acid **80**.

*f*S-**85A**: M = 342 mg, yield = 36% (over two steps).

^{t}R = 1.081 min. Purity = 100%. LC–MS: m/z $[M+H]^+$ =403 Da.

*f*R-**85B**: M = 430 mg, yield = 42% (over two steps).

^{t}R = 1.085 min. Purity = 100%. LC–MS: m/z $[M+H]^+$ =403 Da.

mp = 100-105 °C.

^{1}H NMR: (DMSO-d_6, 400 MHz) δ = 1.75 (br. s, 2 H), 3.00 (dd, *J*=13.1, 7.9 Hz, 1 H), 3.13 (dd, *J*=13.1, 5.3 Hz, 1 H), 3.75 (s, 3 H), 3.82 (s, 3 H), 4.59 (s, 2 H), 5.18 (dd, *J*=13.2, 7.6 Hz, 1 H), 5.45 (br. s., 1 H), 6.51 (d, *J*=3.5 Hz, 1 H), 6.93 (d, *J*=8.6 Hz, 1 H), 6.98 (d, *J*=3.7 Hz, 1 H), 7.30 (dd, *J*=8.3, 1.6 Hz, 1 H), 7.47 (s, 1 H), 7.53 (s, 1 H), 8.45 (d, *J*=7.8 Hz, 1 H), 11.69 (br. s, 1 H).

^{13}C NMR (DMSO-d_6, 100 MHz): δ = 45.6, 54.4, 55.5, 55.6, 55.8, 106.1, 108.8, 112.0, 112.7, 117.2, 124.9, 126.3, 135.4, 139.0, 140.0, 147.8, 148.9, 160.7, 172.3.

HRMS (ESI): m/z calcd for $C_{19}H_{23}N_4O_4S$ $[M+H]^+$ 403.1435, found 403.1443.

5-(4-chloro-3-fluorophenyl)-N-(1-(5-(hydroxymethyl)thiazol-2-yl)-2-(methylamino)ethyl)-1H-pyrrole-2-carboxamide (86)

Compound **86** was obtained following the general procedure for amide coupling and then the general procedure for deprotection from amine **78** and acid **39**.

*f*S-**86A**: M = 473 mg. Yield = 58% (over two steps).

^{t}R = 1.328 min. Purity = 96%. LC–MS: m/z $[M+H]^+$ =409 Da.

*f*R-**86B**: M = 392 mg. Yield = 48% (over two steps).

^{t}R = 1.184 min. Purity = 97%. LC–MS: m/z $[M+H]^+$ =409 Da.

mp = 100-110 °C.

^{1}H NMR: (DMSO-d_6, 400 MHz) δ = 1.88 (br. s, 1 H), 2.32 (s, 3 H), 3.00 (dd, *J* = 12.4, 8.3 Hz, 1H), 3.07 (dd, *J* = 12.5, 5.6 Hz, 1H), 4.60 (d, *J*=2.6 Hz, 2 H), 5.40 (dd, *J* = 8.1, 5.6 Hz, 1H), 5.45

(br. s, 1H), 6.73 (d, *J*=3.8 Hz, 1 H), 6.99 (d, *J*=3.8 Hz, 1 H), 7.51 - 7.58 (m, 2 H), 7.67 (dd, *J*=8.5, 1.7 Hz, 1 H), 7.92 (dd, *J*=11.2, 1.8 Hz, 1 H), 8.58 (d, *J*=8.1 Hz, 1 H), 11.81 (br. s, 1 H).

^{13}C NMR (DMSO-d_6, 100 MHz): δ = 35.5, 50.4, 54.5, 55.7, 108.5, 112.6 (d, *J* = 23.4 Hz), 112.8, 117.0 (d, *J* = 17.6 Hz), 121.7 (d, *J* = 3.7 Hz), 128.0, 130.7, 132.6, 132.9 (d, *J* = 8.1 Hz), 138.9, 140.1, 157.5 (d, *J* = 245.2 Hz), 160.2, 171.9.

HRMS (ESI): m/z calcd for $C_{18}H_{19}ClFN_4O_2S$ $[M+H]^+$ 409.0896, found 409.0894.

5-(3-fluoro-4-methylphenyl)-N-(1-(5-(hydroxymethyl)thiazol-2-yl)-2-(methylamino)ethyl)-1H-pyrrole-2-carboxamide (87)

Compound **87** was obtained following the general procedure for amide coupling and then the general procedure for deprotection from amine **78** and acid **40**.

*f*S-**87A**: M = 414 mg. Yield = 51% (over two steps).

^{t}R = 1.298 min. Purity = 100%. LC–MS: m/z $[M+H]^+$ =389 Da.

*f*R-**87B**: M = 535 mg. Yield = 64% (over two steps).

^{t}R = 1.144 min. Purity = 100%. LC–MS: m/z $[M+H]^+$ =389 Da.

mp = 100-110 °C.

^{1}H NMR: (DMSO-d_6, 400 MHz) δ = 1.95 (br. s., 1 H), 2.21 (s, 3 H), 2.32 (s, 3 H), 3.00 (dd, *J* = 12.5, 8.6 Hz, 1H), 3.05 (dd, *J* = 12.2, 5.4 Hz, 1H), 4.60 (d, *J*=2.6 Hz, 2 H), 5.40 (dd, *J* = 13.7, 7.9 Hz, 1 H), 5.46 (br. s., 1 H), 6.63 (d, *J*=3.5 Hz, 1 H), 6.96 (d, *J*=3.5 Hz, 1 H), 7.25 (t, *J*=8.1 Hz, 1 H), 7.53 (d, *J*=3.9 Hz, 2 H), 7.64 (dd, *J*=11.7, 0.9 Hz, 1 H), 8.53 (d, *J*=8.1 Hz, 1 H), 11.77 (s, 1 H).

^{13}C NMR (DMSO-d_6, 100 MHz): δ = 13.9 (d, *J* = 2.9 Hz), 35.5, 50.4, 54.5, 55.7, 107.4, 110.9 (d, *J* = 24.2 Hz), 112.9, 120.4 (d, *J* = 2.9 Hz), 122.3 (d, *J* = 17.6 Hz), 127.2, 131.6 (d, *J* = 8.8 Hz), 131.8 (d, *J* = 5.9 Hz), 133.8 (d, *J* = 2.2 Hz), 138.9, 140.1, 160.2, 161.0 (d, *J* = 241.5 Hz), 172.0.

HRMS (ESI): m/z calcd for $C_{19}H_{22}FN_4O_2S$ $[M+H]^+$ 389.1442, found 389.1441.

5-(4-chloro-3,5-difluorophenyl)-N-(1-(5-(hydroxymethyl)thiazol-2-yl)-2-(methylamino)ethyl)-1H-pyrrole-2-carboxamide (88)

Compound **88** was obtained following the general procedure for amide coupling and then the general procedure for deprotection from amine **78** and acid **79**.

*f*S-**88A**: M = 500 mg. Yield = 29% (over two steps).

^{t}R = 1.362 min. Purity = 96%. LC–MS: m/z $[M+H]^+$ =427 Da.

*f*R-**88B**: M = 980 mg. Yield = 39% (over two steps).

^{t}R = 1.352 min. Purity = 92%. LC–MS: m/z $[M+H]^+$ =427 Da.

mp = 105-110 °C.

^{1}H NMR: (DMSO-d_6, 400 MHz) δ = 1.90 (br. s., 1 H), 2.32 (s, 3 H), 3.00 (dd, *J*=12.5, 8.4 Hz, 1 H), 3.07 (dd, *J*=12.5, 5.6 Hz, 1 H), 4.60 (s, 2 H), 5.40 (dd, *J*=13.7, 8.1 Hz, 1 H), 5.46 (br. s., 1 H), 6.84 (d, *J*=3.9 Hz, 1 H), 7.01 (d, *J*=3.9 Hz, 1 H), 7.53 (s, 1 H), 7.85 (d, *J*=9.0 Hz, 2 H), 8.62 (d, *J*=8.2 Hz, 1 H), 12.01 (br. s., 1 H)

^{13}C NMR (DMSO-d_6, 100 MHz): δ = 35.5, 50.5, 54.4, 55.7, 105.3, (t, *J* = 21.7 Hz), 108.3 (d, *J* = 24.1 Hz, 2C), 109.5, 112.7, 128.5, 131.8, 132.8 (t, *J* = 9.6 Hz), 138.9, 140.2, 158.3 (dd, *J* = 245.8, 4.0 Hz, 2C), 160.1. 171.8.

HRMS (ESI): m/z calcd for $C_{18}H_{18}ClF_2N_4O_2S$ $[M+H]^+$ 427.0802, found 427.0800.

ASSOCIATED CONTENT

Supporting Information

Table S1. Crystallographic data collection and refinement statistics

Figure S1. Comparison of Surface/Shape Complementarity of 90 in the absence (a and c) and presence (b and d) of fluorine.

Molecular formula strings are also available.

Accession Codes

X-ray crystallographic structure of 90 with HIV-1 Clade A/E gp120 $core_e$ H375S (PDB ID: 5U6E) has been deposited at RCSB PDB (http://www.pdb.org).

AUTHOR INFORMATION

Corresponding Author

***(A.K.D.),** Laboratory of Molecular Modeling and Drug Design, Lindsey F. Kimball Research Institute, New York Blood Center, New York, NY 10065, USA. Tel. 001-212-570-3373; E-mail: adebnath@nybc.org

ABBREVIATIONS USED

HIV-1, Human Immunodeficiency Virus Type 1; Env, Envelope; AIDS, acquire immunodeficiency syndrome; VSV-G, Vesicular stomatitis virus-G; ADMET, absorption, distribution, metabolism and excretion; mCPBA, meta-Chloroperoxybenzoic acid; DCM, dichloromethane; DIPEA, N,N-Diisopropylethylamine; HBTU, N,N,N′,N′-Tetramethyl-O-(1H-benzotriazol-1-yl)uronium hexafluorophosphate; TBSCl, tert-Butyldimethylsilyl chloride; DIPEA, N,N-Diisopropylethylamine**;** Alloc, allyloxycarbonyl

ACKNOWLEDGEMENTS

This study was supported by funds from NIH Grant RO1 AI104416 (AKD) and the New York Blood Center (AKD). We would like to thank Andy Clarkson of Cyprotex Discovery Ltd, UK for

help in interpreting the ADMET data. We thank J. Stuckey for assistance with figures, and members of the structural biology section for comments on the manuscript. This work was supported by the Intramural AIDS Targeted Antiviral Program (IATAP) and the Intramural Research Program of the Vaccine Research Center, National Institute of Allergy and Infectious Diseases, National Institutes of Health. X-ray data were collected at the SER-CAT 22-ID and 22-BM beamlines at the Advanced Photon Source (APS), Argonne National Laboratory. Use of APS was supported by the US Department of Energy, Basic Energy Sciences, Office of Science under contract no. W-31-109-Eng-38.

REFERENCES

1. Caffrey, M. Hiv Envelope: Challenges and Opportunities for Development of Entry Inhibitors. *Trends Microbiol.* **2011,** *19*, 191-197.

2. Didigu, C. A.; Doms, R. W. Novel Approaches to Inhibit Hiv Entry. *Viruses* **2012,** *4*, 309-324.

3. Yu, F.; Lu, L.; Du, L.; Zhu, X.; Debnath, A. K.; Jiang, S. Approaches for Identification of Hiv-1 Entry Inhibitors Targeting Gp41 Pocket. *Viruses* **2013,** *5*, 127-149.

4. Lu, L.; Yu, F.; Cai, L.; Debnath, A. K.; Jiang, S. Development of Small-Molecule Hiv Entry Inhibitors Specifically Targeting Gp120 or Gp41. *Curr. Top. Med. Chem.* **2016,** *16*, 1074-1090.

5. Duffalo, M. L.; James, C. W. Enfuvirtide: A Novel Agent for the Treatment of Hiv-1 Infection. *Ann. Pharmacother.* **2003,** *37*, 1448-1456.

6. Hardy, H.; Skolnik, P. R. Enfuvirtide, a New Fusion Inhibitor for Therapy of Human Immunodeficiency Virus Infection. *Pharmacotherapy* **2004,** *24*, 198-211.

7. Dorr, P.; Westby, M.; Dobbs, S.; Griffin, P.; Irvine, B.; Macartney, M.; Mori, J.; Rickett, G.; Smith-Burchnell, C.; Napier, C.; Webster, R.; Armour, D.; Price, D.; Stammen, B.; Wood, A.; Perros, M. Maraviroc (Uk-427,857), a Potent, Orally Bioavailable, and Selective Small-Molecule Inhibitor of Chemokine Receptor Ccr5 with Broad-Spectrum Anti-Human Immunodeficiency Virus Type 1 Activity. *Antimicrob. Agents Chemother.* **2005,** *49*, 4721-4732.

8. Hunt, J. S.; Romanelli, F. Maraviroc, a Ccr5 Coreceptor Antagonist That Blocks Entry of Human Immunodeficiency Virus Type 1. *Pharmacotherapy* **2009,** *29*, 295-304.

9. Meanwell, N. A.; Kadow, J. F. Maraviroc, a Chemokine Ccr5 Receptor Antagonist for the Treatment of Hiv Infection and Aids. *Curr. Opin. Investig. Drugs* **2007,** *8*, 669-681.

10. Nowicka-Sans, B.; Gong, Y. F.; McAuliffe, B.; Dicker, I.; Ho, H. T.; Zhou, N.; Eggers, B.; Lin, P. F.; Ray, N.; Wind-Rotolo, M.; Zhu, L.; Majumdar, A.; Stock, D.; Lataillade, M.; Hanna, G. J.; Matiskella, J. D.; Ueda, Y.; Wang, T.; Kadow, J. F.; Meanwell, N. A.; Krystal, M. In Vitro Antiviral Characteristics of Hiv-1 Attachment Inhibitor Bms-626529, the Active Component of the Prodrug Bms-663068. *Antimicrobial Agents and Chemotherapy* **2012,** *56*, 3498-3507.

11. Lalezari, J. P.; Latiff, G. H.; Brinson, C.; Echevarr+¡a, J.; Trevi+¦o-P+¬rez, S.; Bogner, J. R.; Thompson, M.; Fourie, J.; Sussmann Pena, O. A.; Mendo Urbina, F. C.; Martins, M.; Diaconescu, I. G.; Stock, D. A.; Joshi, S. R.; Hanna, G. J.; Lataillade, M. Safety and Efficacy of the Hiv-1 Attachment Inhibitor Prodrug Bms-663068 in Treatment-Experienced Individuals: 24 Week Results of Ai438011, a Phase 2b, Randomised Controlled Trial. *The Lancet HIV 2*, e427-e437.

12. Zhao, Q.; Ma, L.; Jiang, S.; Lu, H.; Liu, S.; He, Y.; Strick, N.; Neamati, N.; Debnath, A. K. Identification of N-Phenyl-N'-(2,2,6,6-Tetramethyl-Piperidin-4-Yl)-Oxalamides as a New Class of Hiv-1 Entry Inhibitors That Prevent Gp120 Binding to Cd4. *Virology* **2005,** *339*, 213-225.

13. Si, Z.; Madani, N.; Cox, J. M.; Chruma, J. J.; Klein, J. C.; Schon, A.; Phan, N.; Wang, L.; Biorn, A. C.; Cocklin, S.; Chaiken, I.; Freire, E.; Smith, A. B., III; Sodroski, J. G. Small-Molecule Inhibitors of Hiv-1 Entry Block Receptor-Induced Conformational Changes in the Viral Envelope Glycoproteins. *Proc. Natl. Acad. Sci. U S A* **2004,** *101*, 5036-5041.

14. Curreli, F.; Kwon, Y. D.; Zhang, H.; Scacalossi, D.; Belov, D. S.; Tikhonov, A. A.; Andreev, I. A.; Altieri, A.; Kurkin, A. V.; Kwong, P. D.; Debnath, A. K. Structure-Based Design

of a Small Molecule Cd4-Antagonist with Broad Spectrum Anti-Hiv-1 Activity. *J. Med. Chem.* **2015,** *58*, 6909-6927.

15. Curreli, F.; Kwon, Y. D.; Zhang, H.; Yang, Y.; Scacalossi, D.; Kwong, P. D.; Debnath, A. K. Binding Mode Characterization of Nbd Series Cd4-Mimetic Hiv-1 Entry Inhibitors by X-Ray Structure and Resistance Study. *Antimicrob. Agents Chemother.* **2014,** *58*, 5478-5491.

16. Curreli, F.; Choudhury, S.; Pyatkin, I.; Zagorodnikov, V. P.; Bulay, A. K.; Altieri, A.; Kwon, Y. D.; Kwong, P. D.; Debnath, A. K. Design, Synthesis and Antiviral Activity of Entry Inhibitors That Target the Cd4-Binding Site of Hiv-1. *J. Med. Chem.* **2012,** *55*, 4764-4775.

17. Curreli, F.; Belov, D. S.; Ramesh, R. R.; Patel, N.; Altieri, A.; Kurkin, A. V.; Debnath, A. K. Design, Synthesis and Evaluation of Small Molecule Cd4-Mimics as Entry Inhibitors Possessing Broad Spectrum Anti-Hiv-1 Activity. *Bioorg. Med. Chem.* **2016,** *24*, 5988-6003.

18. Courter, J. R.; Madani, N.; Sodroski, J.; Schon, A.; Freire, E.; Kwong, P. D.; Hendrickson, W. A.; Chaiken, I. M.; Lalonde, J. M.; Smith, A. B., III. Structure-Based Design, Synthesis and Validation of Cd4-Mimetic Small Molecule Inhibitors of Hiv-1 Entry: Conversion of a Viral Entry Agonist to an Antagonist. *Acc. Chem. Res.* **2014,** *47*, 1228-1237.

19. Lalonde, J. M.; Elban, M. A.; Courter, J. R.; Sugawara, A.; Soeta, T.; Madani, N.; Princiotto, A. M.; Kwon, Y. D.; Kwong, P. D.; Schon, A.; Freire, E.; Sodroski, J.; Smith, A. B., III. Design, Synthesis and Biological Evaluation of Small Molecule Inhibitors of Cd4-Gp120 Binding Based on Virtual Screening. *Bioorg. Med. Chem.* **2011,** *19*, 91-101.

20. Lalonde, J. M.; Le-Khac, M.; Jones, D. M.; Courter, J. R.; Park, J.; Schon, A.; Princiotto, A. M.; Wu, X.; Mascola, J. R.; Freire, E.; Sodroski, J.; Madani, N.; Hendrickson, W. A.; Smith, A. B., III. Structure-Based Design and Synthesis of an Hiv-1 Entry Inhibitor Exploiting X-Ray and Thermodynamic Characterization. *ACS Med. Chem. Lett.* **2013,** *4*, 338-343.

21. Melillo, B.; Liang, S.; Park, J.; Schon, A.; Courter, J. R.; Lalonde, J. M.; Wendler, D. J.; Princiotto, A. M.; Seaman, M. S.; Freire, E.; Sodroski, J.; Madani, N.; Hendrickson, W. A.; Smith, A. B., III. Small-Molecule Cd4-Mimics: Structure-Based Optimization of Hiv-1 Entry Inhibition. *ACS Med. Chem. Lett.* **2016,** *7*, 330-334.

22. Hashimoto, C.; Narumi, T.; Otsuki, H.; Hirota, Y.; Arai, H.; Yoshimura, K.; Harada, S.; Ohashi, N.; Nomura, W.; Miura, T.; Igarashi, T.; Matsushita, S.; Tamamura, H. A Cd4 Mimic as an Hiv Entry Inhibitor: Pharmacokinetics. *Bioorg. Med. Chem.* **2013,** *21*, 7884-7889.

23. Narumi, T.; Arai, H.; Yoshimura, K.; Harada, S.; Hirota, Y.; Ohashi, N.; Hashimoto, C.; Nomura, W.; Matsushita, S.; Tamamura, H. Cd4 Mimics as Hiv Entry Inhibitors: Lead Optimization Studies of the Aromatic Substituents. *Bioorg. Med. Chem.* **2013,** *21*, 2518-2526.

24. Narumi, T.; Arai, H.; Yoshimura, K.; Harada, S.; Nomura, W.; Matsushita, S.; Tamamura, H. Small Molecular Cd4 Mimics as Hiv Entry Inhibitors. *Bioorg. Med. Chem.* **2011,** *19*, 6735-6742.

25. van de Waterbeemd, H.; Gifford, E. Admet in Silico Modelling: Towards Prediction Paradise? *Nat. Rev. Drug Discov.* **2003,** *2*, 192-204.

26. Waring, M. J.; Arrowsmith, J.; Leach, A. R.; Leeson, P. D.; Mandrell, S.; Owen, R. M.; Pairaudeau, G.; Pennie, W. D.; Pickett, S. D.; Wang, J.; Wallace, O.; Weir, A. An Analysis of the Attrition of Drug Candidates from Four Major Pharmaceutical Companies. *Nat. Rev. Drug Discov.* **2015,** *14*, 475-486.

27. Queiroz, M. J. ú.; Begouin, A.; Pereira, G.; Ferreira, P. M. T. New Synthesis of Methyl 5-Aryl or Heteroaryl Pyrrole-2-Carboxylates by a Tandem Sonogashira Coupling/5-Endo-Dig-Cyclization from +¦-Iododehydroamino Acid Methyl Esters and Terminal Alkynes. *Tetrahedron* **2008,** *64*, 10714-10720.

28. Li, B.; Wang, N.; Liang, Y.; Xu, S.; Wang, B. Ruthenium-Catalyzed Pyrrole Synthesis Via Oxidative Annulation of Enamides and Alkynes. *Org. Lett.* **2013,** *15*, 136-139.

29. Balsamini, C.; Bedini, A.; Diamantini, G.; Spadoni, G.; Tontini, A.; Tarzia, G.; Di, F. R.; Feriani, A.; Reggiani, A.; Tedesco, G.; Valigi, R. (E)-3-(2-(N-Phenylcarbamoyl)Vinyl)Pyrrole-2-Carboxylic Acid Derivatives. A Novel Class of Glycine Site Antagonists. *J. Med. Chem.* **1998,** *41*, 808-820.

30. Ferreira, P. M. T.; Monteiro, L. s. S.; Pereira, G. Synthesis of Substituted Oxazoles from N-Acyl-+¦-Hydroxyamino Acid Derivatives. *Eur. J. Org. Chem.* **2008,** *2008*, 4676-4683.

31. Weiss, H. M.; Touchette, K. M.; Angell, S.; Khan, J. The Concerted Addition of Hbr to Aryl Alkynes; Orthogonal Pi Bond Selectivity. *Org. Biomol. Chem.* **2003,** *1*, 2152-2156.

32. Devasthale, P.; Washburn, W. N.; Renduchintala, K. V.; R., S. Azolotriazinone Melanin Concentrating Hormone Receptor-1 Antagonists. WO2010/042682 A1, 2010.

33. Dhainaut, A.; Tizot, A.; Raimbaud, E.; Lockhart, B.; Lestage, P.; Goldstein, S. Synthesis, Structure, and Neuroprotective Properties of Novel Imidazolyl Nitrones. *J. Med. Chem.* **2000,** *43*, 2165-2175.

34. Kwon, Y. D.; Lalonde, J. M.; Yang, Y.; Elban, M. A.; Sugawara, A.; Courter, J. R.; Jones, D. M.; Smith, A. B., III; Debnath, A. K.; Kwong, P. D. Crystal Structures of Hiv-1 Gp120 Envelope Glycoprotein in Complex with Nbd Analogues That Target the Cd4-Binding Site. *PLoS. One* **2014,** *9*, e85940.

35. Lalonde, J. M.; Kwon, Y. D.; Jones, D. M.; Sun, A. W.; Courter, J. R.; Soeta, T.; Kobayashi, T.; Princiotto, A. M.; Wu, X.; Schon, A.; Freire, E.; Kwong, P. D.; Mascola, J. R.; Sodroski, J.; Madani, N.; Smith, A. B., III. Structure-Based Design, Synthesis, and

Characterization of Dual Hotspot Small-Molecule Hiv-1 Entry Inhibitors. *J. Med. Chem.* **2012,** *55*, 4382-4396.

36. Acharya, P.; Lusvarghi, S.; Bewley, C. A.; Kwong, P. D. Hiv-1 Gp120 as a Therapeutic Target: Navigating a Moving Labyrinth. *Expert Opin. Ther. Targets* **2015,** *19*, 765-783.

37. Haim, H.; Si, Z.; Madani, N.; Wang, L.; Courter, J. R.; Princiotto, A.; Kassa, A.; DeGrace, M.; Gee-Estrada, K.; Mefford, M.; Gabuzda, D.; Smith, A. B., III; Sodroski, J. Soluble Cd4 and Cd4-Mimetic Compounds Inhibit Hiv-1 Infection by Induction of a Short-Lived Activated State. *PLoS Pathog.* **2009,** *5*, e1000360.

38. Madani, N.; Schon, A.; Princiotto, A. M.; Lalonde, J. M.; Courter, J. R.; Soeta, T.; Ng, D.; Wang, L.; Brower, E. T.; Xiang, S. H.; Kwon, Y. D.; Huang, C. C.; Wyatt, R.; Kwong, P. D.; Freire, E.; Smith, A. B., III; Sodroski, J. Small-Molecule Cd4 Mimics Interact with a Highly Conserved Pocket on Hiv-1 Gp120. *Structure* **2008,** *16*, 1689-1701.

39. Narumi, T.; Ochiai, C.; Yoshimura, K.; Harada, S.; Tanaka, T.; Nomura, W.; Arai, H.; Ozaki, T.; Ohashi, N.; Matsushita, S.; Tamamura, H. Cd4 Mimics Targeting the Hiv Entry Mechanism and Their Hybrid Molecules with a Cxcr4 Antagonist. *Bioorg. Med. Chem. Lett.* **2010,** *20*, 5853-5858.

40. Yamada, Y.; Ochiai, C.; Yoshimura, K.; Tanaka, T.; Ohashi, N.; Narumi, T.; Nomura, W.; Harada, S.; Matsushita, S.; Tamamura, H. Cd4 Mimics Targeting the Mechanism of Hiv Entry. *Bioorg. Med. Chem. Lett.* **2010,** *20*, 354-358.

41. Lin, P. F.; Blair, W.; Wang, T.; Spicer, T.; Guo, Q.; Zhou, N.; Gong, Y. F.; Wang, H. G.; Rose, R.; Yamanaka, G.; Robinson, B.; Li, C. B.; Fridell, R.; Deminie, C.; Demers, G.; Yang, Z.; Zadjura, L.; Meanwell, N.; Colonno, R. A Small Molecule Hiv-1 Inhibitor That Targets the Hiv-1

Envelope and Inhibits Cd4 Receptor Binding. *Proc. Natl. Acad. Sci. U. S. A.* **2003,** *100*, 11013-11018.

42. Gillis, E. P.; Eastman, K. J.; Hill, M. D.; Donnelly, D. J.; Meanwell, N. A. Applications of Fluorine in Medicinal Chemistry. *J. Med. Chem.* **2015,** *58*, 8315-8359.

43. Hagmann, W. K. The Many Roles for Fluorine in Medicinal Chemistry. *J. Med. Chem.* **2008,** *51*, 4359-4369.

44. Park, B. K.; Kitteringham, N. R.; O'Neill, P. M. Metabolism of Fluorine-Containing Drugs. *Annu. Rev. Pharmacol. Toxicol.* **2001,** *41*, 443-470.

45. Thomas, V. H.; Bhattachar, S.; Hitchingham, L.; Zocharski, P.; Naath, M.; Surendran, N.; Stoner, C. L.; El-Kattan, A. The Road Map to Oral Bioavailability: An Industrial Perspective. *Expert. Opin. Drug Metab. Toxicol.* **2006,** *2*, 591-608.

46. International Transporter, C.; Giacomini, K. M.; Huang, S. M.; Tweedie, D. J.; Benet, L. Z.; Brouwer, K. L.; Chu, X.; Dahlin, A.; Evers, R.; Fischer, V.; Hillgren, K. M.; Hoffmaster, K. A.; Ishikawa, T.; Keppler, D.; Kim, R. B.; Lee, C. A.; Niemi, M.; Polli, J. W.; Sugiyama, Y.; Swaan, P. W.; Ware, J. A.; Wright, S. H.; Yee, S. W.; Zamek-Gliszczynski, M. J.; Zhang, L. Membrane Transporters in Drug Development. *Nat. Rev. Drug Discov.* **2010,** *9*, 215-236.

47. Smith, D. A.; Di, L.; Kerns, E. H. The Effect of Plasma Protein Binding on in Vivo Efficacy: Misconceptions in Drug Discovery. *Nat. Rev. Drug Discov.* **2010,** *9*, 929-939.

48. Zanger, U. M.; Schwab, M. Cytochrome P450 Enzymes in Drug Metabolism: Regulation of Gene Expression, Enzyme Activities, and Impact of Genetic Variation. *Pharmacol. Ther.* **2013,** *138*, 103-141.

49. Tang, C.; Lin, J. H.; Lu, A. Y. Metabolism-Based Drug-Drug Interactions: What Determines Individual Variability in Cytochrome P450 Induction? *Drug. Metab. Dispos.* **2005,** *33*, 603-613.

50. Priest, B. T.; Bell, I. M.; Garcia, M. L. Role of Herg Potassium Channel Assays in Drug Development. *Channels (Austin)* **2008,** *2*, 87-93.

51. Haertle, T.; Carrera, C. J.; Wasson, D. B.; Sowers, L. C.; Richman, D. D.; Carson, D. A. Metabolism and Anti-Human Immunodeficiency Virus-1 Activity of 2-Halo-2',3'-Dideoxyadenosine Derivatives. *J. Biol. Chem.* **1988,** *263*, 5870-5875.

52. Wei, X.; Decker, J. M.; Liu, H.; Zhang, Z.; Arani, R. B.; Kilby, J. M.; Saag, M. S.; Wu, X.; Shaw, G. M.; Kappes, J. C. Emergence of Resistant Human Immunodeficiency Virus Type 1 in Patients Receiving Fusion Inhibitor (T-20) Monotherapy. *Antimicrob. Agents Chemother.* **2002,** *46*, 1896-1905.

53. Chackerian, B.; Long, E. M.; Luciw, P. A.; Overbaugh, J. Human Immunodeficiency Virus Type 1 Coreceptors Participate in Postentry Stages in the Virus Replication Cycle and Function in Simian Immunodeficiency Virus Infection. *J. Virol.* **1997,** *71*, 3932-3939.

54. Bjorndal, A.; Deng, H.; Jansson, M.; Fiore, J. R.; Colognesi, C.; Karlsson, A.; Albert, J.; Scarlatti, G.; Littman, D. R.; Fenyo, E. M. Coreceptor Usage of Primary Human Immunodeficiency Virus Type 1 Isolates Varies According to Biological Phenotype. *J. Virol.* **1997,** *71*, 7478-7487.

55. Ciminale, V.; Felber, B. K.; Campbell, M.; Pavlakis, G. N. A Bioassay for Hiv-1 Based on Env-Cd4 Interaction. *AIDS Res. Hum. Retrov.* **1990,** *6*, 1281-1287.

56. Kolchinsky, P.; Mirzabekov, T.; Farzan, M.; Kiprilov, E.; Cayabyab, M.; Mooney, L. J.; Choe, H.; Sodroski, J. Adaptation of a Ccr5-Using, Primary Human Immunodeficiency Virus Type 1 Isolate for Cd4-Independent Replication. *J. Virol.* **1999,** *73*, 8120-8126.

57. Page, K. A.; Landau, N. R.; Littman, D. R. Construction and Use of a Human Immunodeficiency Virus Vector for Analysis of Virus Infectivity. *J. Virol.* **1990**, 5270-5276.

58. Blish, C. A.; Jalalian-Lechak, Z.; Rainwater, S.; Nguyen, M. A.; Dogan, O. C.; Overbaugh, J. Cross-Subtype Neutralization Sensitivity Despite Monoclonal Antibody Resistance among Early Subtype a, C, and D Envelope Variants of Human Immunodeficiency Virus Type 1. *J. Virol.* **2009,** *83*, 7783-7788.

59. Long, E. M.; Rainwater, S. M.; Lavreys, L.; Mandaliya, K.; Overbaugh, J. Hiv Type 1 Variants Transmitted to Women in Kenya Require the Ccr5 Coreceptor for Entry, Regardless of the Genetic Complexity of the Infecting Virus. *AIDS Res. Hum. Retrov.* **2002,** *18*, 567-576.

60. Kulkarni, S. S.; Lapedes, A.; Tang, H.; Gnanakaran, S.; Daniels, M. G.; Zhang, M.; Bhattacharya, T.; Li, M.; Polonis, V. R.; McCutchan, F. E.; Morris, L.; Ellenberger, D.; Butera, S. T.; Bollinger, R. C.; Korber, B. T.; Paranjape, R. S.; Montefiori, D. C. Highly Complex Neutralization Determinants on a Monophyletic Lineage of Newly Transmitted Subtype C Hiv-1 Env Clones from India. *Virology* **2009,** *385*, 505-520.

61. Li, M.; Gao, F.; Mascola, J. R.; Stamatatos, L.; Polonis, V. R.; Koutsoukos, M.; Voss, G.; Goepfert, P.; Gilbert, P.; Greene, K. M.; Bilska, M.; Kothe, D. L.; Salazar-Gonzalez, J. F.; Wei, X.; Decker, J. M.; Hahn, B. H.; Montefiori, D. C. Human Immunodeficiency Virus Type 1 Env Clones from Acute and Early Subtype B Infections for Standardized Assessments of Vaccine-Elicited Neutralizing Antibodies. *J. Virol.* **2005,** *79*, 10108-10125.

62. Wei, X.; Decker, J. M.; Wang, S.; Hui, H.; Kappes, J. C.; Wu, X.; Salazar-Gonzalez, J. F.; Salazar, M. G.; Kilby, J. M.; Saag, M. S.; Komarova, N. L.; Nowak, M. A.; Hahn, B. H.; Kwong, P. D.; Shaw, G. M. Antibody Neutralization and Escape by Hiv-1. *Nature* **2003,** *422*, 307-312.

63. Keele, B. F.; Giorgi, E. E.; Salazar-Gonzalez, J. F.; Decker, J. M.; Pham, K. T.; Salazar, M. G.; Sun, C.; Grayson, T.; Wang, S.; Li, H.; Wei, X.; Jiang, C.; Kirchherr, J. L.; Gao, F.; Anderson, J. A.; Ping, L. H.; Swanstrom, R.; Tomaras, G. D.; Blattner, W. A.; Goepfert, P. A.; Kilby, J. M.; Saag, M. S.; Delwart, E. L.; Busch, M. P.; Cohen, M. S.; Montefiori, D. C.; Haynes, B. F.; Gaschen, B.; Athreya, G. S.; Lee, H. Y.; Wood, N.; Seoighe, C.; Perelson, A. S.; Bhattacharya, T.; Korber, B. T.; Hahn, B. H.; Shaw, G. M. Identification and Characterization of Transmitted and Early Founder Virus Envelopes in Primary Hiv-1 Infection. *Proc. Natl. Acad. Sci. U. S. A.* **2008,** *105*, 7552-7557.

64. Derdeyn, C. A.; Decker, J. M.; Bibollet-Ruche, F.; Mokili, J. L.; Muldoon, M.; Denham, S. A.; Heil, M. L.; Kasolo, F.; Musonda, R.; Hahn, B. H.; Shaw, G. M.; Korber, B. T.; Allen, S.; Hunter, E. Envelope-Constrained Neutralization-Sensitive Hiv-1 after Heterosexual Transmission. *Science* **2004,** *303*, 2019-2022.

65. Li, M.; Salazar-Gonzalez, J. F.; Derdeyn, C. A.; Morris, L.; Williamson, C.; Robinson, J. E.; Decker, J. M.; Li, Y.; Salazar, M. G.; Polonis, V. R.; Mlisana, K.; Karim, S. A.; Hong, K.; Greene, K. M.; Bilska, M.; Zhou, J.; Allen, S.; Chomba, E.; Mulenga, J.; Vwalika, C.; Gao, F.; Zhang, M.; Korber, B. T.; Hunter, E.; Hahn, B. H.; Montefiori, D. C. Genetic and Neutralization Properties of Subtype C Human Immunodeficiency Virus Type 1 Molecular Env Clones from Acute and Early Heterosexually Acquired Infections in Southern Africa. *J. Virol.* **2006,** *80*, 11776-11790.

66. Williamson, C.; Morris, L.; Maughan, M. F.; Ping, L. H.; Dryga, S. A.; Thomas, R.; Reap, E. A.; Cilliers, T.; van, H. J.; Pascual, A.; Ramjee, G.; Gray, G.; Johnston, R.; Karim, S. A.; Swanstrom, R. Characterization and Selection of Hiv-1 Subtype C Isolates for Use in Vaccine Development. *AIDS Res. Hum. Retrov.* **2003,** *19*, 133-144.

67. Wu, X.; Parast, A. B.; Richardson, B. A.; Nduati, R.; John-Stewart, G.; Mbori-Ngacha, D.; Rainwater, S. M.; Overbaugh, J. Neutralization Escape Variants of Human Immunodeficiency Virus Type 1 Are Transmitted from Mother to Infant. *J. Virol.* **2006,** *80*, 835-844.

68. Zhang, H.; Zhao, Q.; Bhattacharya, S.; Waheed, A. A.; Tong, X.; Hong, A.; Heck, S.; Curreli, F.; Goger, M.; Cowburn, D.; Freed, E. O.; Debnath, A. K. A Cell-Penetrating Helical Peptide as a Potential Hiv-1 Inhibitor. *J. Mol. Biol.* **2008,** *378*, 565-580.

69. Lackman-Smith, C.; Osterling, C.; Luckenbaugh, K.; Mankowski, M.; Snyder, B.; Lewis, G.; Paull, J.; Profy, A.; Ptak, R. G.; Buckheit, R. W., Jr.; Watson, K. M.; Cummins, J. E., Jr.; Sanders-Beer, B. E. Development of a Comprehensive Human Immunodeficiency Virus Type 1 Screening Algorithm for Discovery and Preclinical Testing of Topical Microbicides. *Antimicrob. Agents Chemother.* **2008,** *52*, 1768-1781.

70. McMahon, J. B.; Currens, M. J.; Gulakowski, R. J.; Buckheit, R. W., Jr.; Lackman-Smith, C.; Hallock, Y. F.; Boyd, M. R. Michellamine B, a Novel Plant Alkaloid, Inhibits Human Immunodeficiency Virus-Induced Cell Killing by at Least Two Distinct Mechanisms. *Antimicrob. Agents Chemother.* **1995,** *39*, 484-488.

71. Kwon, Y. D.; Finzi, A.; Wu, X.; Dogo-Isonagie, C.; Lee, L. K.; Moore, L. R.; Schmidt, S. D.; Stuckey, J.; Yang, Y.; Zhou, T.; Zhu, J.; Vicic, D. A.; Debnath, A. K.; Shapiro, L.; Bewley, C. A.; Mascola, J. R.; Sodroski, J. G.; Kwong, P. D. Unliganded Hiv-1 Gp120 Core Structures

Assume the Cd4-Bound Conformation with Regulation by Quaternary Interactions and Variable Loops. *Proc. Natl. Acad. Sci. U. S. A.* **2012,** *109*, 5663-5668.

72. Otwinowski, Z.; Minor, W. Macromolecular Crystallography, Part A. In *Methods Enzymol.*, Otwinowski, Z.; Minor, W., Eds. Elsevier: Netherland, 1997; pp 307-326.

73. Adams, P. D.; Afonine, P. V.; Bunkoczi, G.; Chen, V. B.; Davis, I. W.; Echols, N.; Headd, J. J.; Hung, L. W.; Kapral, G. J.; Grosse-Kunstleve, R. W.; McCoy, A. J.; Moriarty, N. W.; Oeffner, R.; Read, R. J.; Richardson, D. C.; Richardson, J. S.; Terwilliger, T. C.; Zwart, P. H. Phenix: A Comprehensive Python-Based System for Macromolecular Structure Solution. *Acta Crystallogr. Sect. D* **2010,** *66*, 213-221.

74. Emsley, P.; Cowtan, K. Coot: Model-Building Tools for Molecular Graphics. *Acta Crystallogr. Sect. D* **2004,** *60*, 2126-2132.

FIGURE LEGENDS

Figure 1. Crystal structures of 90 in complex with HIV-1 gp120. (a) **90** inserting into the Phe43 cavity of gp120 shown in stick representation with *2fo-fc* electron density map (blue mesh) contoured at 1σ. (b) Superimposition of **89** (magenta) and **90** (orange). (c, d) Ordered water molecules (red spheres) hydrogen bonding with **90** and gp120. The nitrogen atom in the amine group of **90** makes a direct hydrogen bond with Asp368. Dotted lines represent hydrogen bonds.

Figure 2. **A. HIV-1 mediated cell-to-cell fusion inhibition assay.** Indicator cells MAGI-CCR5 were cocultured with Env- and Tat-expressing HL2/3 cells in the presence of escalating concentrations of NBD compounds**.** Two independent experiments were performed in triplicate, and the graph is representative of one experiment; the values represent the mean ± standard deviation.

B. Infectivity of Cf2Th−CCR5 cells by CD4-dependent HIV-1_{ADA}. Cf2Th−CCR5 cells were infected with CD4-dependent HIV-1_{ADA} in the presence of NBD compounds. The Relative virus infectivity indicates the amount of infection detected in the presence of the compounds divided by the amount of infection detected in the absence of the compounds. Three independent experiments were performed in triplicate, and the graph is representative of one experiment; the values represent the mean ± standard deviation.

Figure 3. Time-of-Addition of NBD compounds and reference compounds. TZMb-l cells were infected with HIV-1_{HXB2} and compounds were added to the culture at the time of infection (Time "0") and at 30 min, 1, 2, 4, 6 and 8 h postinfection (p.i.). Two independent experiments were performed in triplicate, and the graph is representative of one experiment; the values represent the mean ± standard deviation.

Table 1. Anti-HIV-1 activity (IC_{50}) and cytotoxicity (CC_{50}) of NBD compounds in single-cycle (TZM-bl cells) and multi-cycle (MT-2 cells) assays.

A.

Compd.No.	Structure	TZM-bl Cells (Mean ± SD)		MT-2 Cells (Mean ± SD)	
		IC_{50} (μM)	CC_{50} (μM)	IC_{50} (μM)	CC_{50} (μM)
89[a]	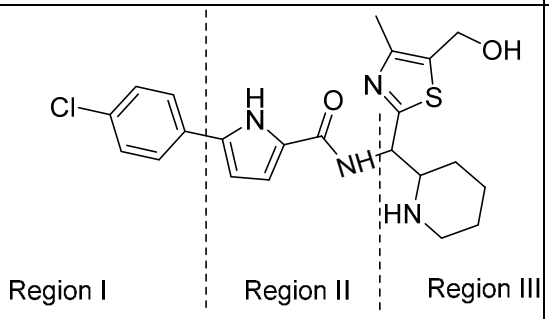	2.2 ± 0.2	23.6±1.1	0.85 ± 0.06	24.8±2.3

B.

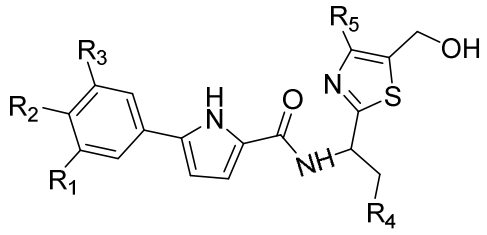

Compound No.	R_1	R_2	R_3	R_4	R_5	TZM-bl Cells (Mean ± SD)		MT-2 Cells (Mean ± SD)	
						IC_{50} (μM)	CC_{50} (μM)	IC_{50} (μM)	CC_{50} (μM)

25A	F	F	H	NH_2	CH_3	3.4±0.7	57.3±0.4	6±0.9	61.2±2.6
25B	F	F	H	NH_2	CH_3	3.3±0.3	58.6±0.2	4.8±0.8	64.6±2.9
41A	H	Cl	H	$NHCH_3$	CH_3	3.4±0.6	28.4±1.2	5.5±0.4	27.2±1.3
41B	H	Cl	H	$NHCH_3$	CH_3	3.3±0.5	31.7±0.7	3.1±0.6	26.4±1.4
42A	F	Cl	H	$NHCH_3$	CH_3	1.6±0.1	20.6±0.7	2.4±0.5	21.7±0.7
42B	F	Cl	H	$NHCH_3$	CH_3	1.6±0.6	21.3±0.3	2±0.8	18.1±0.7
43A	F	CH_3	H	$NHCH_3$	CH_3	2.1±0.9	33.5±0.3	1.1±0.3	34.4±0.8
43B	F	CH_3	H	$NHCH_3$	CH_3	1.6±0.6	34.2±0.7	0.95±0.2	30.6±1.4
44A	H	Cl	H	$NH(CH_3)_2$	CH_3	>40	>40	>40	>40
44B	H	Cl	H	$NH(CH_3)_2$	CH_3	>40	>40	>40	>40
45A	F	Cl	H	$NH(CH_3)_2$	CH_3	16.7±1	>40	>20	>40
45B	F	Cl	H	$NH(CH_3)_2$	CH_3	19±1	>40	19.2±0.7	>40
46A	F	CH_3	H	$NH(CH_3)_2$	CH_3	>40	>40	>20	>40
46B	F	CH_3	H	$NH(CH_3)_2$	CH_3	>40	>40	>20	>40

61A	H	Cl	H	CH_2NH_2	CH_3	5.1±0.1	40.3±0.5	4.6±0.1	31.1±1.2
61B	H	Cl	H	CH_2NH_2	CH_3	5.2±0.1	39.2±0.6	5.1±1.3	33.8±0.6
62A	F	Cl	H	CH_2NH_2	CH_3	6.6±2	25.5±0.6	7.8±1.5	25.1±1
62B	F	Cl	H	CH_2NH_2	CH_3	8±0.1	24.5±0.6	9.3±0.2	24.9±1.2
63A	F	CH_3	H	CH_2NH_2	CH_3	5.7±0.5	33±2.4	1.8±0.2	35.8±1.1
63B	F	CH_3	H	CH_2NH_2	CH_3	7.8±1.7	38.2±1.6	3±1.1	34.7±2.8
64A	H	Cl	H	CH_2NHCH_3	CH_3	6.3±1.1	23±0.6	7.8±2.4	25.1±0.6
64B	H	Cl	H	CH_2NHCH_3	CH_3	9.2±0.1	23±1.2	10.4±0.5	24.9±0.5
65A	F	Cl	H	CH_2NHCH_3	CH_3	1.5±0.4	22±0.6	3.9±0.1	22.6±0.1
65B	F	Cl	H	CH_2NHCH_3	CH_3	4.6±0.1	22.3±0.6	5.7±0.3	24.2±1.2
66A	F	CH_3	H	CH_2NHCH_3	CH_3	4.1±0.2	38.9±2.1	4.1±0.2	25.9±1.2
66B	F	CH_3	H	CH_2NHCH_3	CH_3	4.9±0.3	36.4±2.6	5±0.1	25.3±1.5
67A	H	Cl	H	$CH_2N(CH_3)_2$	CH_3	10.4±2	29.36±0.1	13.8±0.2	26±0.6
67B	H	Cl	H	$CH_2N(CH_3)_2$	CH_3	14.2±0.7	28.9±0.6	12.8±1	24.4±0.6

68A	F	Cl	H	$CH_2N(CH_3)_2$	CH_3	1.5±0.3	21.3±0.6	3.7±0.1	19.1±1.9
68B	F	Cl	H	$CH_2N(CH_3)_2$	CH_3	1.8±0.1	22±1	4.4±0.2	22±1.6
69A	F	CH_3	H	$CH_2N(CH_3)_2$	CH_3	1.9±0.1	23.7±0.8	2.1±0.3	25.1±2
69B	F	CH_3	H	$CH_2N(CH_3)_2$	CH_3	4.8±0.2	23.5±1.5	2.9±1	23.5±0.6
81A	H	Cl	H	NH_2	H	1.3±0.1	38±1.5	1.4±0.2	35.6±1
81B	H	Cl	H	NH_2	H	0.75±0.2	37.1±0.3	1.8±0.3	34.5±0.5
82A	F	Cl	H	NH_2	H	1.1±0.8	37.4±0.3	0.94±0.1	32±1
82B	F	Cl	H	NH_2	H	0.57±0.01	33±0.2	1.2±0.4	36±0.5
83A	F	CH_3	H	NH_2	H	0.85±0.06	39.2±0.8	1.6±0.08	35.2±0.8
83B	F	CH_3	H	NH_2	H	0.45±0.05	38.8±0.8	0.76±0.3	38±1
84A	F	Cl	F	NH_2	H	0.64±0.06	39.5±2.3	0.96±0.1	37±1.5
84B	F	Cl	F	NH_2	H	0.48±0.1	20.6±0.2	0.97±0.2	17.4±0.4
85A	OCH_3	OCH_3	H	NH_2	H	>50	>50	>50	>50
85B	OCH_3	OCH_3	H	NH_2	H	>50	>50	>50	>50

86A	F	Cl	H	$NHCH_3$	H	1.4±0.05	17.4±0.4	3.9±0.6	18.4±0.8
86B	F	Cl	H	$NHCH_3$	H	0.95±0.03	17.3±0.5	4±0.3	18.3±1
87A	F	CH_3	H	$NHCH_3$	H	2±0.3	22.3±0.8	4.4±0.2	26.6±1.5
87B	F	CH_3	H	$NHCH_3$	H	1±0.2	27.4±0.8	0.99±0.01	28.3±2.6
88A	F	Cl	F	$NHCH_3$	H	0.36±0.04	10.4±0.8	0.36±0.06	14±0.2
88B	F	Cl	F	$NHCH_3$	H	0.42±0.2	13.9±0.7	0.36±0.05	11.9±0.3

C.

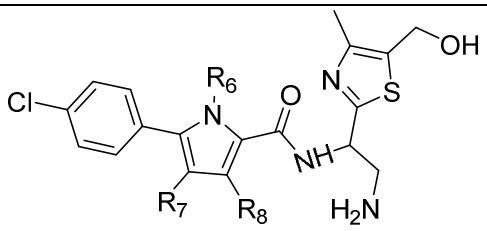

Compd. No.	R_6	R_7	R_8	TZM-bl Cells (Mean ± SD)		MT-2 Cells (Mean ± SD)	
				IC_{50} (μM)	CC_{50} (μM)	IC_{50} (μM)	CC_{50} (μM)
26A	CH_3	H	H	25.8±1.1	36.7±0.4	>25	26.6±0.3
26B	CH_3	H	H	26±1.4	35.8±0.3	>25	32.1±0.4

27A	H	CH_3	H	1.1±0.3	26.4±0.7	3.9±0.6	20.2±3.1
27B	H	CH_3	H	2.2±0.8	27.2±0.8	4.1±0.3	24.9±2.2
28A	H	H	CH_3	3.6±0.4	22.2±0.3	5.3±0.8	18±0.4
28B	H	H	CH_3	2.6±0.1	5.2±0.3	6.1±0.3	4.1±0.7
29A	H	H	OCH_3	22.2±0.7	25.4±2.7	>24	25±0.9
29B	H	H	OCH_3	16.9±0.3	16.4±1	>24	15.7±0.3

D.

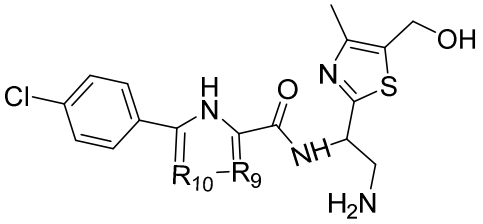

Compd. No.	R_9	R_{10}	TZM-bl Cells (Mean ± SD)		MT-2 Cells (Mean ± SD)	
			IC_{50} (μM)	CC_{50} (μM)	IC_{50} (μM)	CC_{50} (μM)
30A	N	CH	~51	>51	>26	>51
30B	N	CH	35±3	>51	>26	>51
31A	CH	N	>51	>51	>26	>51

31B	CH	N	>51	>51	>26	>51

a, Data from ref [14]

The reported IC_{50} values represent the means± standard deviations (SD), n=3.

Table 2. Antiviral activity of NBD compounds against HIV-1 Reverse Transcriptase

Inhibitors	IC_{50} (μM)
89	47
83B	7.2
84A	8.4
NBD-556 (control)	>300
Nevirapine (control)	0.2

Table 3. Neutralization activity of NBD compounds against a panel of HIV-1 Env Pseudoviruses

			IC_{50} (μM)[a]		
Subtype	**NIH #**	**ENVs**	**89**	**83B**	**84A**
A	11887	Q259env.w6	1.6±0.1[c]	0.5±0.08	0.36±0.04
	11888	QB726.70M.ENV.C4	1.3±0.3[c]	0.51±0.02	0.51±0.03
	11890	QF495.23M.ENV.A1	1.3±0.4[c]	0.33±0.03	0.46±0.09
	11891	QF495.23M.ENV.A3	0.88±0.4[c]	0.6±0.01	0.44±0.07
	11892	QF495.23M.ENV.B2	0.6±0.4[c]	0.27±0.03	0.68±0.06
		BG505-T332N	1±0.1[c]	0.39±0.03	0.41±0.02
		KNH1144	2.1±0.4[c]	0.4±0.03	0.53±0.09
A/D	11901	QA790.204I.ENV.A4	1.4±0.05[c]	0.57±0.08	0.4±0.03
	11903	QA790.204I.ENV.C8	1.5±0.02[c]	0.54±0.17	0.4±0.01
	11904	QA790.204I.ENV.E2	0.71±0.09[c]	0.33±0.04	0.61±0.03
A2/D	11906	QG393.60M.ENV.B7	0.8±0.3[c]	0.37±0.03	0.43±0.02
	11907	QG393.60M.ENV.B8	0.48±0.2[c]	0.38±0.02	0.27±0.01
A/E	11603	CRF01_AE clone 269	1.5±0.3[c]	0.3±0.02	0.62±0.05
		AA058	4.4±0.1[c]	0.32±0.03	0.39±0.1
A/G	11601	CRF02_AG clone 263	1.4±0.3[c]	0.5±0.02	0.6±0.09

	11602	CRF02_AG clone 266	1±0.2[c]	0.48±0.03	0.48±0.07
	11605	CRF02_AG clone 278	1.3±0.5[c]	0.64±0.1	0.5±0.03
B		B41	0.68±0.1[c]	0.51±0.03	0.36±0.04
	11563	p1058_11.B11.1550[b]	1.1±0.8[c]	0.28±0.01	0.34±0.01
	11578	pWEAUd15.410.5017[b]	3±0.1[c]	0.43±0.1	0.5±0.04
	11018	QH0692, clone 42	0.52±0.1[c]	0.39±0.07	0.35±0.06
	11022	PVO, clone 4	1.9±0.1[c]	0.72±0.03	0.5±0.05
	11023	TRO, clone 11	1.2±0.05[c]	0.65±0.1	0.83±0.2
	11024	AC10.0, clone 29	0.32±0.01[c]	0.4±0.08	0.5±0.02
	11035	pREJO4541 clone 67	1.6±0.3[c]	0.57±0.06	0.74±0.1
	11036	pRHPA4259 clone 7	1.4±0.2[c]	0.43±0.1	0.57±0.08
	11037	pTHRO4156 clone 18	1±0.2[c]	0.75±0.07	0.54±0.05
	11038	pCAAN5342 clone A2	0.6±0.07[c]	0.51±0.1	0.6±0.03
	11058	SC422661.8	0.33±0.01[c]	0.38±0.07	0.53±0.05
	11561	p1054.TC4.1499	2.5±0.3	0.4±0.08	0.65±0.03
	11571	p9014_01.TB1.4769	1.2±0.3	0.31±0.04	0.38±0.02
	11572	p9021_14.B2.4571	2.1±0.3	0.22±0.02	0.31±0.03
C	11306	Du156, clone 12	2.2±0.5[c]	0.32±0.03	0.62±0.2
	11307	Du172, clone 17	1.9±0.5[c]	0.62±0.08	0.61±0.05
	11308	Du422, clone 1	3.3±0.4[c]	0.36±0.01	0.32±0.02

	11309	ZM197M.PB7	2±0.2[c]	0.23±0.02	0.36±0.04
	11312	ZM249M.PL1	3.1±0.5[c]	0.41±0.03	0.71±0.07
	11313	ZM53M.PB12	1.5±0.2[c]	0.43±0.06	0.64±0.01
	11314	ZM109F.PB4	3.2±0.5[c]	0.2±0.01	0.66±0.08
	11315	ZM135M.PL10a	2.7±1.2[c]	0.25±0.03	0.53±0.1
	11316	CAP45.2.00.G3	1.5±0.1[c]	0.27±0.06	0.44±0.04
	11317	CAP210.2.00.E8	2.8±0.7[c]	0.49±0.04	0.61±0.03
	11502	HIV-16055-2, clone 3	2.3±0.1[c]	0.22±0.04	0.35±0.01
	11504	HIV-16936-2, clone 21	0.99±0.1	0.32±0.01	0.31±0.03
	11506	HIV-25711-2, clone 4	2±0.1	0.3±0.08	0.52±0.06
	11507	HIV-225925-2, clone 22	1.1±0.1	0.34±0.02	0.33±0.04
	11508	HIV-26191-2, clone 48	2.3±0.1	0.44±0.01	0.46±0.03
	11908	QB099.391M.ENV.B1	1.7±0.4[c]	0.35±0.02	0.51±0.03
D	11911	QA013.70I.ENV.H1	2.6±0.2[c]	0.43±0.03	0.46±0.02
	11912	QA013.70I.ENV.M12	0.79±0.08	0.24±0.05	0.5±0.02
	11916	QD435.100M.ENV.B5	1.4±0.06	0.41±0.1	0.41±0.04
	11917	QD435.100M.ENV.A4	1.2±0.1	0.25±0.08	0.32±0.04
	11918	QD435.100M.ENV.E1	2.3±0.1	0.47±0.06	0.5±0.05

D/A	11526 (Mother clone)	MF535.W0M.ENV.C1	1.8±0.5[c]	0.36±0.01	0.36±0.03
	11517 (Infant clone)	BF535.W6M.ENV.A1	2.8±0.6[c]	0.55±0.08	0.94±0.03
Control		VSV-G	7.1±0.7[c]	42.9±0.6	26±0.6
IC_{50} (µM) Color code			<0.5	>0.5 ≤1.0	>1.0
Mean ± SEM (µM)			**1.64±0.12**	**0.41±0.02**	**0.49±0.02**

[a] The reported IC_{50} values represent the means ± standard deviations (n = 3).

[b] R5X4-tropic viruses; all the rest were CCR5-tropic viruses.

[c] Data previously published[14, 17]

Table 4. *In vitro* ADMET profile of NBD compounds

In vitro ADMET		Compounds			
		83B	**84A**	**89**	**91**
*Solubility (μM)		>100	65	65	>100
Caco-2 permeability [Mean P_{app} (10^{-6} cms^{-1})	A2B (pH 7.4/7.4)	2.56	1.17	2.31	7.62
	B2A (pH 7.4/7.4)	19.5	17.2	31.3	37.4
	Efflux Ratio (Mean Papp B2A/ Mean P_{app} A2B	7.61	14.7	13.5	4.91
Metabolic stability (human microsomes)	$^{\Delta}$Compounds remaining at 45 min (% of 0 min)	101	97.4	84.0	87.0
	CL_{int} (μL/min/mg protein)	<10	<10	<10	<10
Protein binding (human plasma) (Mean fu)		0.0400	0.100	0.114	0.185
Cytochrome P450 inhibition, IC_{50} (μM)	CYP2C19 (Substrate=mephenytoin)	>25	>25	>25	>25
	CYP3A4 (Substrate=midazolam)	>25	>25	>25	>25
	CYP2D6 (Substrate=dextromethorphan)	>25	>25	>25	>25
	CYP2C9 (Substrate=tolbutamide)	>25	>25	>25	>25
	CYP1A (Substrate=ethoxyresorufin)	8.01	>25	>25	>25
hERG Channel inhibition (μM)		9.98	14.1	3.80	17.4

*Solubility based upon calculated mid-range from Turbidimetric Aqueous Solubility Assay

$^{\Delta}$, 45 minute was the limit of the assay

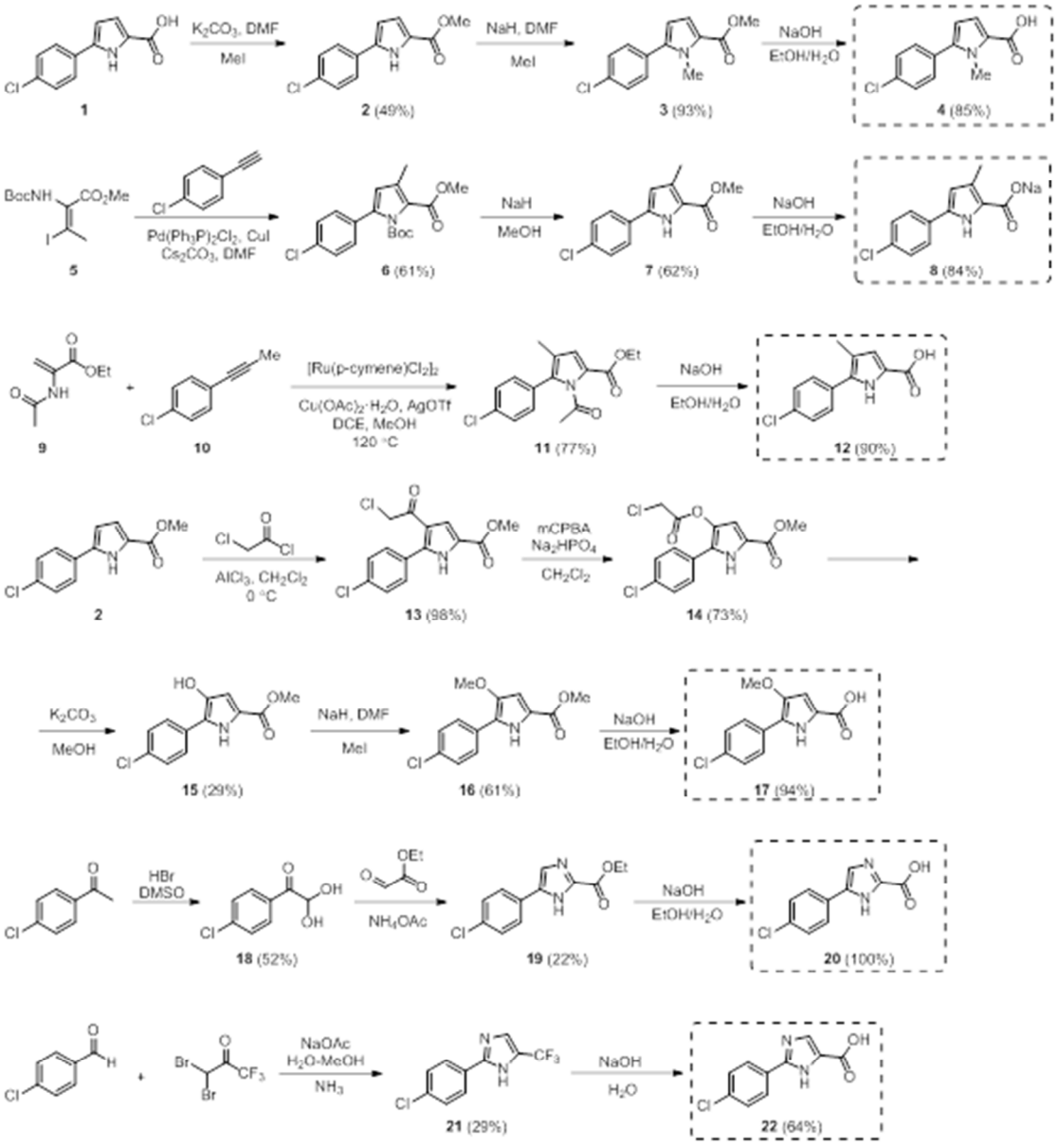

Scheme-1: Outline of synthesis to acid key intermediates **4**, **8**, **12**, **17**, **20** and **22**.

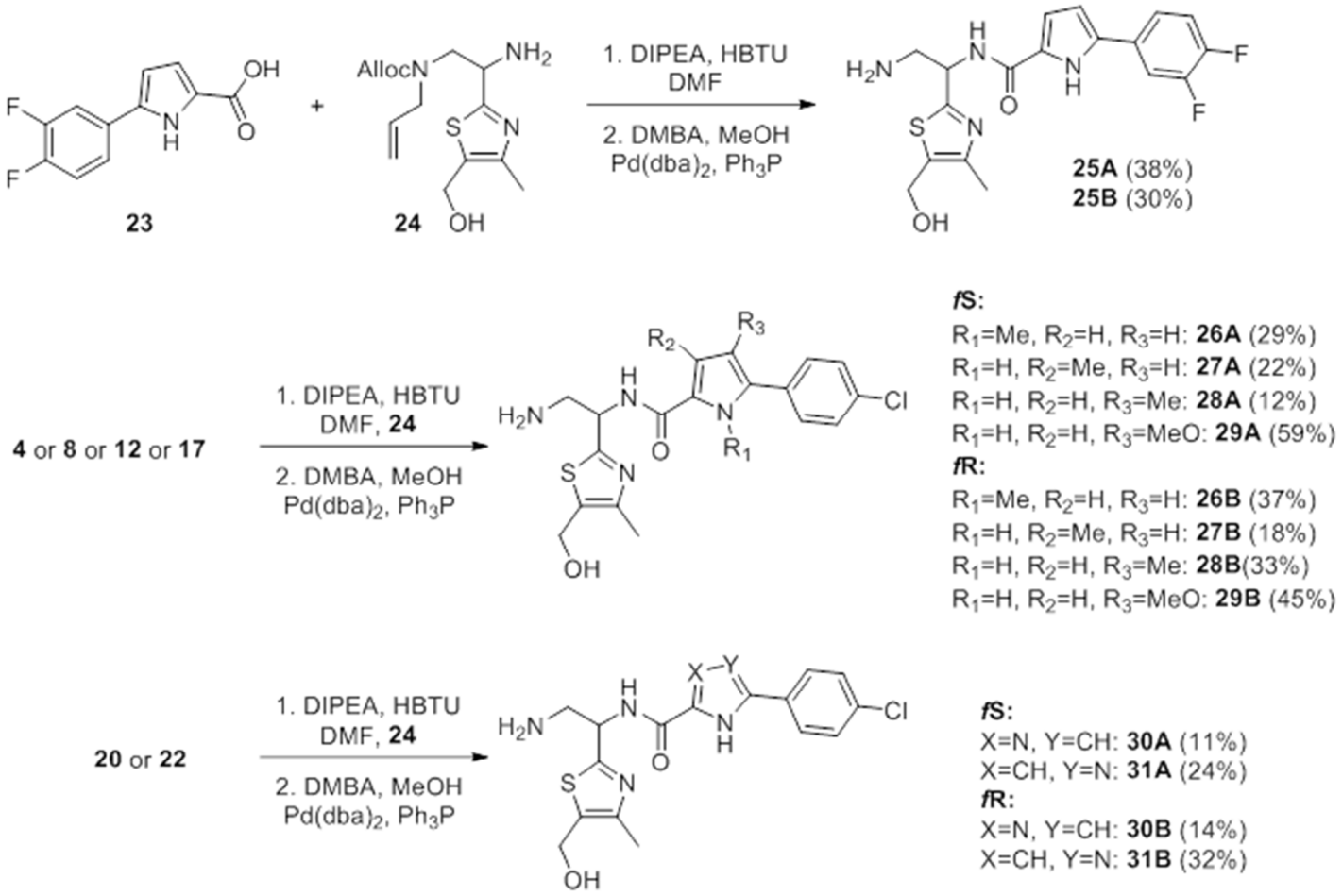

Scheme-2: Coupling-cleavage tandem reactions leading to target compounds **25**-**31**.

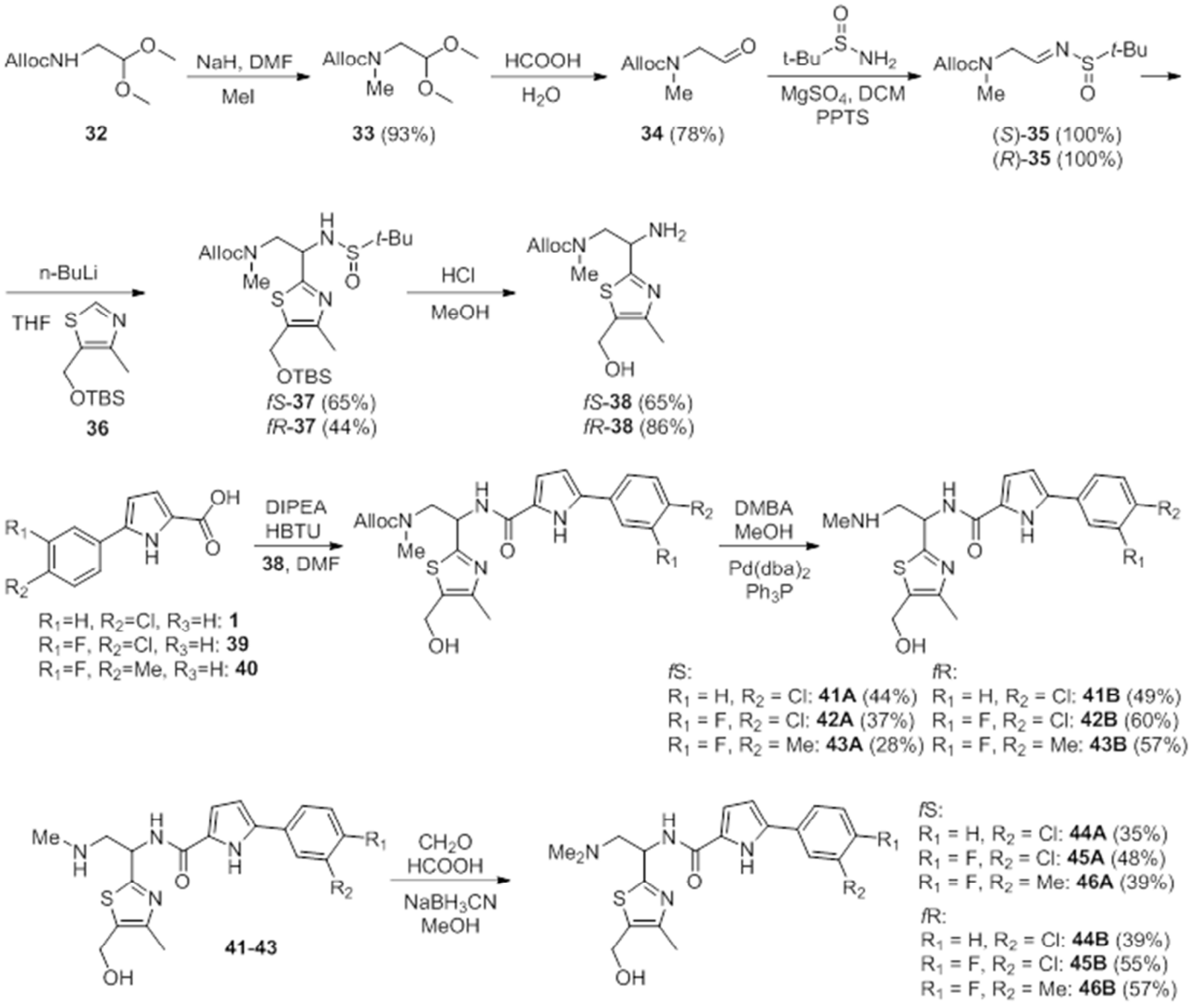

Scheme-3: Synthetic approach leading to target compounds **41**-**46**.

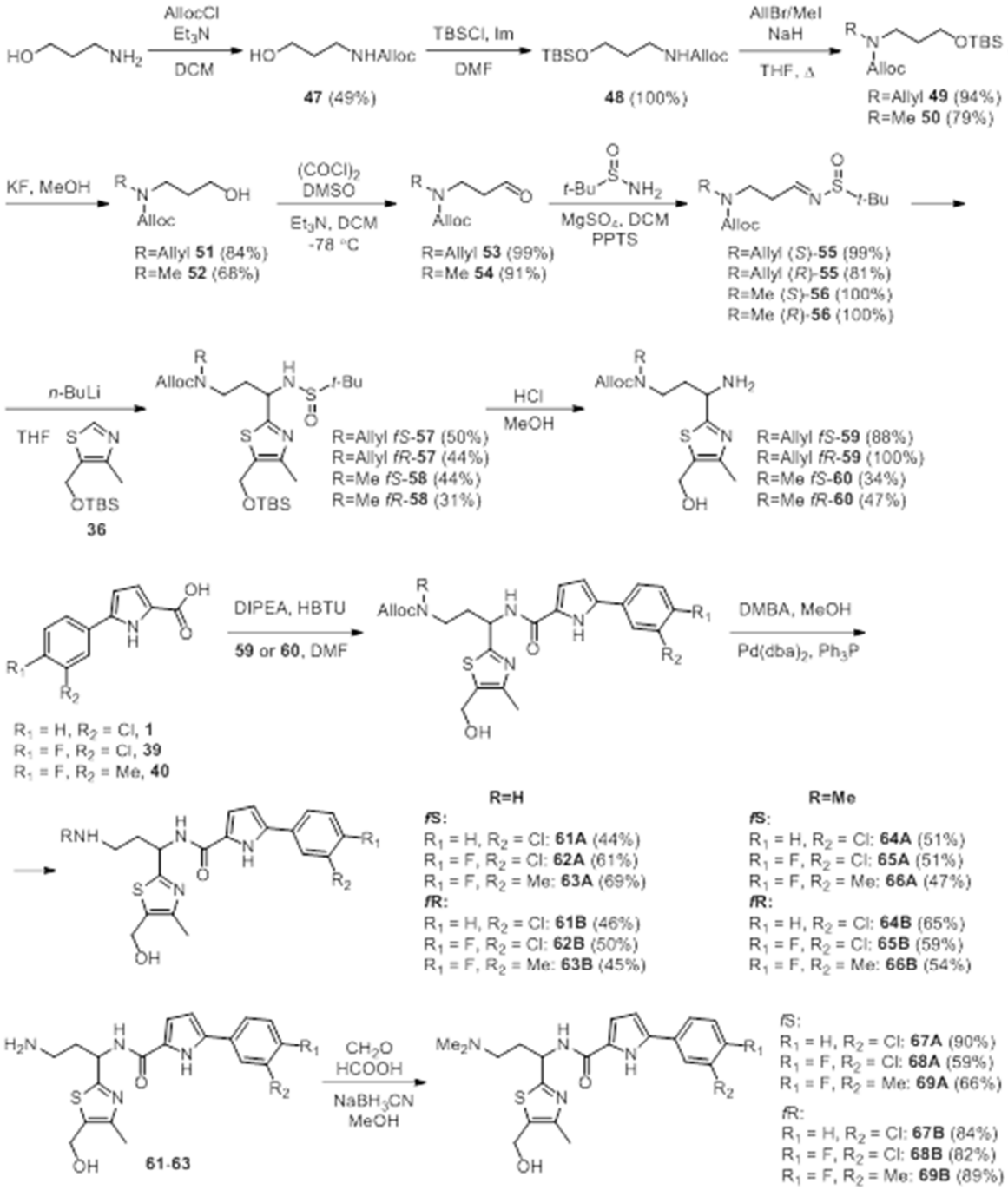

Scheme-4: Synthetic approach leading to target compounds **61-69**.

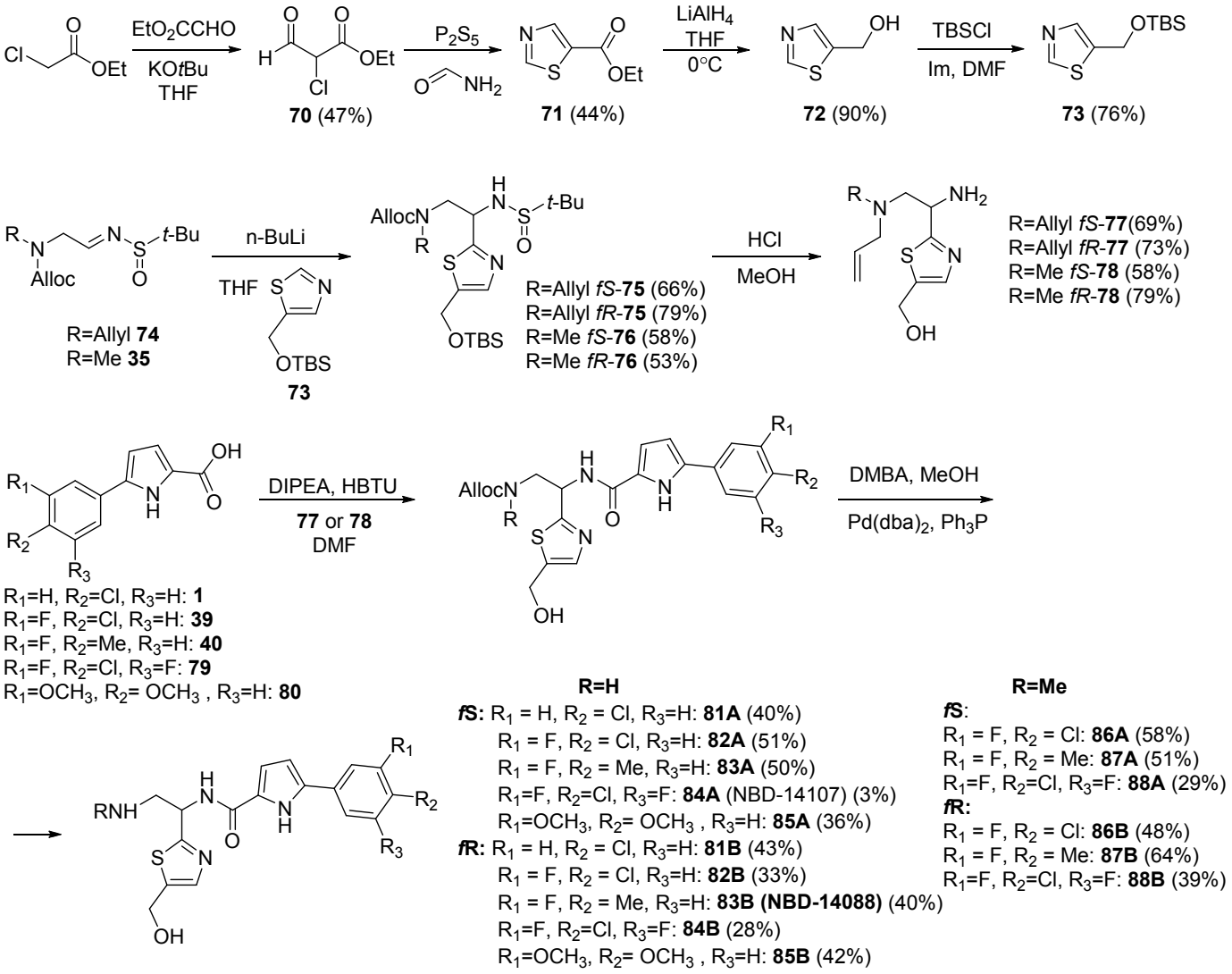

Scheme-5: Synthetic approach leading to target compounds **81**-**88**.

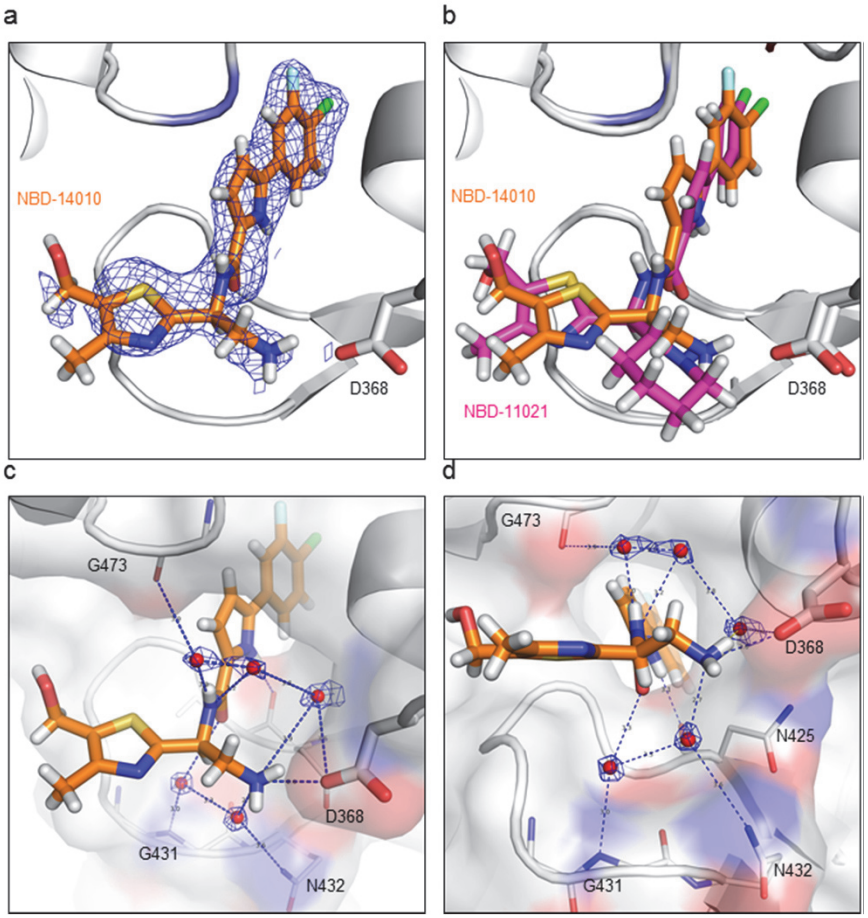
a
NBD-14010
D368
b
NBD-14010
NBD-11021
D368
c
G473
D368
G431
N432
d
G473
D368
N425
G431
N432

Fig-1

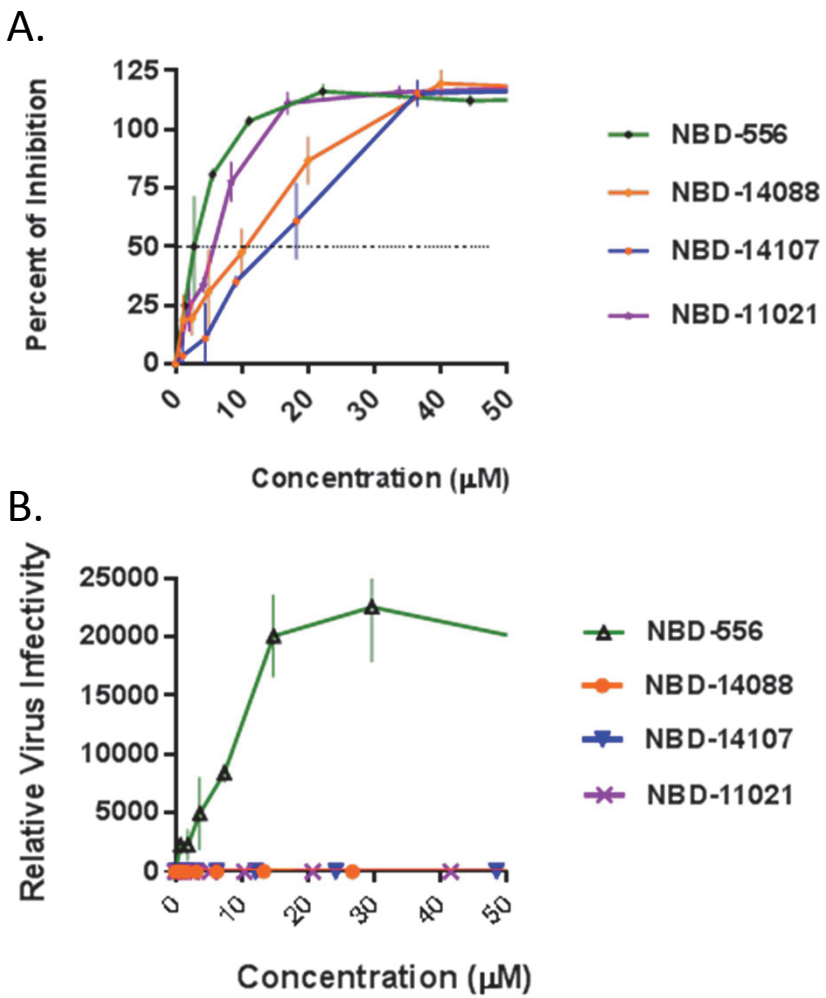
A.
Percent of Inhibition
125
100
75
50
25
0
0
10
20
30
40
50
Concentration (μM)
NBD-556
NBD-14088
NBD-14107
NBD-11021
B.
Relative Virus Infectivity
25000
20000
15000
10000
5000
0
0
10
20
30
40
50
Concentration (μM)
NBD-556
NBD-14088
NBD-14107
NBD-11021

Fig-2

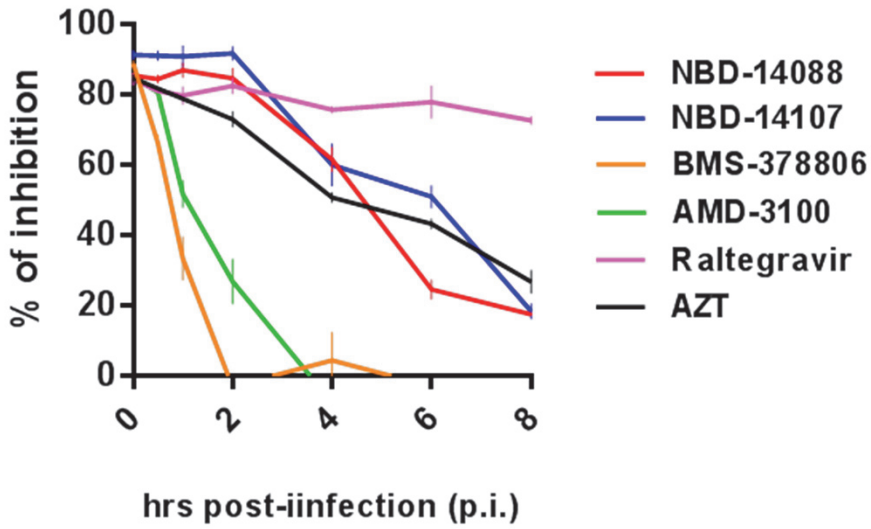
100
80
60
40
20
0
% of inhibition
0
2
4
6
8
hrs post-iinfection (p.i.)
NBD-14088
NBD-14107
BMS-378806
AMD-3100
Raltegravir
AZT

Fig-3

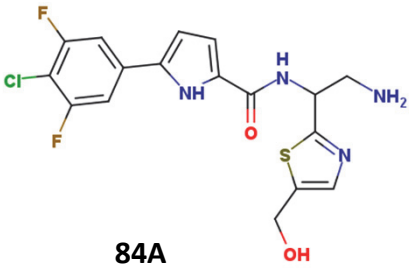

84A

Mean ± SEM (μM) = 0.49±0.02
(against 56 diverse HIV-1 Env-pseudotyped viruses representing clinical isolates of different subtypes)

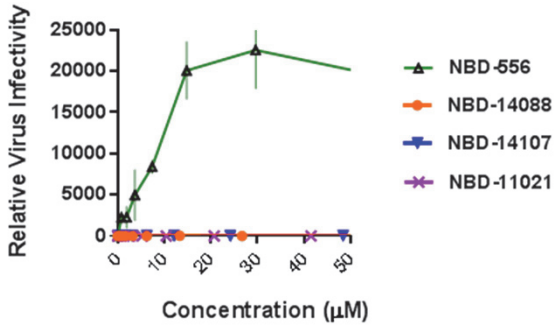

HIV-1 gp120 entry antagonist